

**Development of calcium phosphate based
drug delivery systems for local application of
zoledronic acid**



Doctoral thesis

submitted in fulfilment of the requirements

for the degree of

Doctor in Natural Science

at the

Christian Albrecht University, Kiel, Germany

by

Torben Christian Sørensen

Kiel 2011

Referee:	Prof. Dr. Hartwig Steckel
Co-referee:	Prof. Dr. Rainer Adelung
Date of exam:	November, 22, 2011
Accepted for publication:	November, 22, 2011
	Prof. Dr. Lutz Kipp
	(Decan)

Dedicated to my parents, my brother and my girlfriend.

Lack of a specific mark or a reference to a trademark or a patent does not imply that this work or part of it can be used or copied without copyright permission.

Parts of this doctoral thesis have already been published/ submitted:

Sörensen TC, Arnoldi J, Procter P, Robionek B and Steckel H. Bone substitute materials delivering zoledronic acid: physico-chemical characterisation, drug load and release properties. *Journal of Biomaterials Applications*, submitted and accepted for publication.

Sörensen TC, Arnoldi J, Procter P, Beimel C, Jönsson A, Lennerås M, Emanuelsson L, Palmquist A, Thomsen P, Robionek B and Steckel H. Locally enhanced early bone formation of a zoledronic acid incorporated bone cement plug *in vivo*. *Journal of Biomedical Materials Research (JBMR) Part B: Applied Biomaterials*, submitted.

Table of Contents

1	Introduction and Objectives	1
1.1	Introduction.....	1
1.2	Objectives.....	3
2	Theoretical background.....	4
2.1	Bone	4
2.1.1	Composition	5
2.1.2	Bone cells.....	7
2.1.3	Bone modelling and remodelling.....	8
2.1.4	Fracture healing.....	10
2.1.5	Biochemical markers	14
2.2	Calcium phosphates	17
2.3	Osteoporosis.....	20
2.4	Bisphosphonates.....	22
2.5	Local drug delivery	25
3	Materials	27
3.1	Zoledronic acid (ZOL).....	27
3.2	Bone substitutes	27
4	Methods	29
4.1	BoneSave [®] sieve fractions	29
4.2	Physico-chemical characterisation.....	29
4.2.1	Microscopy.....	29
4.2.2	True density.....	30
4.2.3	Specific surface area	30
4.2.4	Particle size	30
4.2.5	Dynamic vapour sorption (DVS).....	31

4.2.6	pH value of aqueous bone substitute suspensions	31
4.3	HPLC analysis of ZOL	32
4.3.1	Limit of detection (LOD).....	33
4.4	ZOL load and release	34
4.4.1	Drug loading procedure	34
4.4.2	<i>In vitro</i> drug release of ZOL	35
4.4.3	Statistical analysis	36
4.5	Stability	37
4.5.1	Lyophilisation of ZOL	37
4.5.2	ZOL stability tests.....	38
4.6	Cytotoxicity test	39
4.6.1	Cell line	39
4.6.2	Sample preparation	40
4.6.3	MTT assay.....	41
4.6.4	Data analysis	41
4.7	Characterisation of modified HydroSet [®] cement formulations	42
4.7.1	Semi-quantitative wetting of HydroSet [®] powder	42
4.7.2	Characterisation of cement hardness	43
4.7.3	Solubility of ZOL in HydroSet [®] hardening solution	44
4.8	<i>In vivo</i> animal study	45
4.8.1	Implants.....	46
4.8.2	Crushing strength of the HydroSet [®] bone cement plugs	48
4.8.3	Sterility of HydroSet [®] bone cement plugs.....	48
4.8.4	Surgical procedure	50
4.8.5	Implant retrieval and processing.....	52
4.8.6	Quantitative PCR	54
4.8.7	Histology	54
4.8.8	Histomorphometry	55

4.8.9	Statistical analysis	56
5	Results	58
5.1	Physico-chemical characterisation.....	58
5.1.1	Light microscopy/ SEM.....	58
5.1.2	True density and specific surface area.....	61
5.1.3	Particle size	62
5.1.4	Dynamic vapour sorption (DVS).....	62
5.1.5	pH value of aqueous bone substitute suspensions	64
5.2	Limit of detection (LOD).....	65
5.3	Drug load.....	66
5.4	Drug release	71
5.5	ZOL stability test	74
5.5.1	Temperature profile.....	74
5.5.2	Stability at different storage conditions (plastic versus glass)	76
5.5.3	Stability of lyophilisates	79
5.6	Cytotoxicity test.....	83
5.7	Characterisation of modified HydroSet [®] formulations.....	87
5.7.1	Semi-quantitative wetting of HydroSet [®] powder	87
5.7.2	Cement hardness	88
5.7.3	Solubility of ZOL in HydroSet [®] hardening solution	90
5.8	<i>In vivo</i> animal study	91
5.8.1	Sterility of HydroSet [®] bone cement plugs.....	91
5.8.2	Crushing strength	91
5.8.3	Surgeries and bone harvesting	92
5.8.4	SEM analysis of implants	92
5.8.5	Quantitative PCR analysis	93
5.8.6	Histological analysis	95
5.8.7	Histomorphometry	99

6	Discussion	102
6.1	Physico-chemical characterisation.....	102
6.2	Analytics of ZOL	105
6.3	Drug load.....	106
6.4	Drug release	108
6.5	Stability	110
6.6	<i>In vitro</i> cytotoxicity.....	112
6.7	Characterisation of modified HydroSet [®] formulations.....	114
6.8	<i>In vivo</i> animal study	116
7	Conclusion	122
8	Abstract (summary)	123
9	Summary (German version)	125
10	Attachments	128
10.1	List of abbreviations.....	128
10.2	List of utilized substances	131
10.3	Raw data of qPCR analysis.....	132
10.4	Raw data of histomorphometrical analysis	135
10.5	Histological evaluation system	136
11	Figure captions	138
12	Table captions	143
13	References	144

1 Introduction and Objectives

1.1 Introduction

Orthopaedic trauma is a global problem and constitutes a significant source of morbidity and mortality for all ages and both genders [1]. This health detriment is mainly caused by violence or accidental injury and affects every nation in the world [2]. Various forms of traumatic injury lead to long-term consequences for individuals as well as for the society, making up twelve percent of the global disease burden [1, 2]. Trauma-related fractures and healing of bone defects still provide a clinical problem in orthopaedic surgery [3]. Cases with fractures and delayed healing or non-unions may result in a number of surgeries and contribute to increased health care costs [4]. Autologous bone graft that may enhance bone healing processes is not always available in sufficient quantity to enable treatment of these kinds of fractures [5]. The limited amount of graft material and the associated morbidity of the graft harvested procedure are well-known drawbacks of this treatment despite which it represents the current gold standard technique [6]. As an alternative to autologous bone used in fracture treatment, various synthetic materials such as metals, ceramics, glasses, polymers and composites are frequently used either as a bone substitute or as a bone graft extender. In particular, ceramics based on calcium phosphates have a long history of successful orthopaedic applications such as bone void filling and augmentation [7]. These are attractive as they contain calcium which is also present in the mineral phase of bone. Over the last decades, they have been widely used and have proven to have excellent *in vivo* biocompatibility and bone repair abilities when used as synthetic osteoconductive scaffolds [8-12].

In addition to the above mentioned causes for orthopaedic trauma, fractures can also be related to certain musculoskeletal diseases such as osteoporosis. This particular metabolic bone disease is characterized by decreased bone mineral

density. Many orthopaedic patients, predominantly postmenopausal women, are affected by osteoporosis resulting in an increased risk of bone fractures [13]. For the year 2000, nine million new osteoporotic fractures were estimated worldwide [14]. The application of standard implants for fracture fixation of osteoporotic bone is limited due to poor bone quality and fixation failures are more likely to occur [15, 16]. Various drugs and pharmaceutical products have been developed for the treatment and prevention of osteoporosis. Bisphosphonates, a major class of antiporotic drugs, has been shown to be among the most effective inhibitors of bone resorption [17].

During the last decade, numerous studies have established a new field of research focussing on and development of a combination of active bone drugs and medical devices for use in an osteoporotic bone environment. Calcium phosphates have the ability to incorporate several chemical substances on their surfaces, for instance proteins, antibiotics or anti-tumor agents [18-20]. Based on clinical needs, bioceramics may be loaded by adsorption with active agents to offer the potential for innovative drug delivery systems. A candidate bone substitute material must have the ability to incorporate pharmaceuticals in a target load and to release it appropriately to the surrounding bone tissue. Moreover, there is an increasing interest in an additional local pharmacological treatment to generate an added clinical value [20-26]. Many research activities focus on maximizing controlled drug release at specific bone sites and maintaining a prolonged drug concentration level whilst avoiding pharmacological side effects [27].

A combination product which offers an osteoconductive matrix for new bone growth and is also a carrier for local controlled bisphosphonate delivery, could be very attractive in the treatment of osteoporotic fractures. In this, the implantation of bone substitute materials releasing the bisphosphonate zoledronic acid (ZOL) would potentially both, reduce bone resorption and maintain bone mass [28, 29].

1.2 Objectives

There is growing interest in combining the bisphosphonate zoledronic acid (ZOL) with orthopaedic implants with the goal of improving bone quality at the implant-bone interface and reducing the risk of implant migration and failure.

The first objective of the present thesis was to evaluate the feasibility of different calcium phosphate based bioceramics as potential drug carriers. The properties of the materials were tested by using a number of physico-chemical methods. The second aim was to develop a straight forward method for reliably and repeatably combining ZOL with bone substitute materials using a short-term dipping technique which could be promising for clinical application in terms of loading bone substitutes directly prior or during surgery with defined drug content. The third goal was to evaluate the materials with respect to their ZOL loading capacity in a time and concentration dependent manner. The fourth aim was to assess the bone substitutes as release systems for ZOL in an *in vitro* approach. Furthermore, ZOL stability under different storage conditions, cytotoxicity of ZOL with a cell line and a characterisation of modified cement formulations had to be performed to design an implant applicable for an animal model. Dependent on the findings, the final objective was to test the short-term *in vivo* efficacy of a ZOL loaded bone cement plug. For this purpose, a bone defect model in the proximal tibia of rats was used. An *in vivo* study was conducted to gain experience on how to influence bone-implant contact, bone regeneration, and bone area around the implant in cancellous bone. The interpretation of a drug loading and releasing concept using a preshaped bone cement plug was supported by performing quantitative polymerase chain reaction (qPCR) and histological analysis.

The present work is an additional contribution to the knowledge of how ZOL interacts with different forms of calcium phosphate and what effects ZOL could have in an *in vivo* animal model.

2 Theoretical background

2.1 Bone

Bone is a complex and dynamic tissue with several functions such as locomotion of the human body and self maintenance of its intrinsic structure through continuous remodelling [30]. Bones act as an organ responsible for the mineral balance of the body which is controlled by hormones [31]. It acts as a reservoir for calcium and phosphate in the preservation of normal mineral homeostasis [32]. Additionally, bone allows elasticity and rigidity to withstand bending, torsion and combinations of forces without fracturing and provides mechanical support for joints, tendons, and ligaments [33]. Furthermore, bone protects vital organs from damage [34]. A typical structure of bone is shown in Figure 2.1. Bone is divided into cortical and trabecular structures and each of these forms differ in respect of cellular content, metabolic rate and remodelling process [35]. Cortical bone makes up the majority of bone with approximately 80% of skeletal bone mass. It is denser than trabecular bone with a low surface area to volume ratio and is mainly present in the shafts of long bones. It also forms the outer layer of all bones [32]. This type of bone is formed by the Haversian system which consists of osteons, forming concentric lamellae of bone tissue surrounding a central canal containing blood vessels [36]. Approximately 20% of skeletal bone mass consists of trabecular or cancellous bone. It offers porous structures and has a lower density than cortical bone [30]. Cancellous bone is located in the centre of flat bones, vertebrae, and both at the centre and the ends of long bones. This bone structure is characterized by an interconnecting meshwork of defined patterns consisting of a large number of bony trabecular cells combined into a three-dimensional matrix with a large surface area [34, 37, 38]. A high metabolic turnover and concentration of bone cells is specific for trabecular bone [39]. Caused by an increased surface area, the remodelling of trabecular bone proceeds more rapidly compared to cortical bone [30].

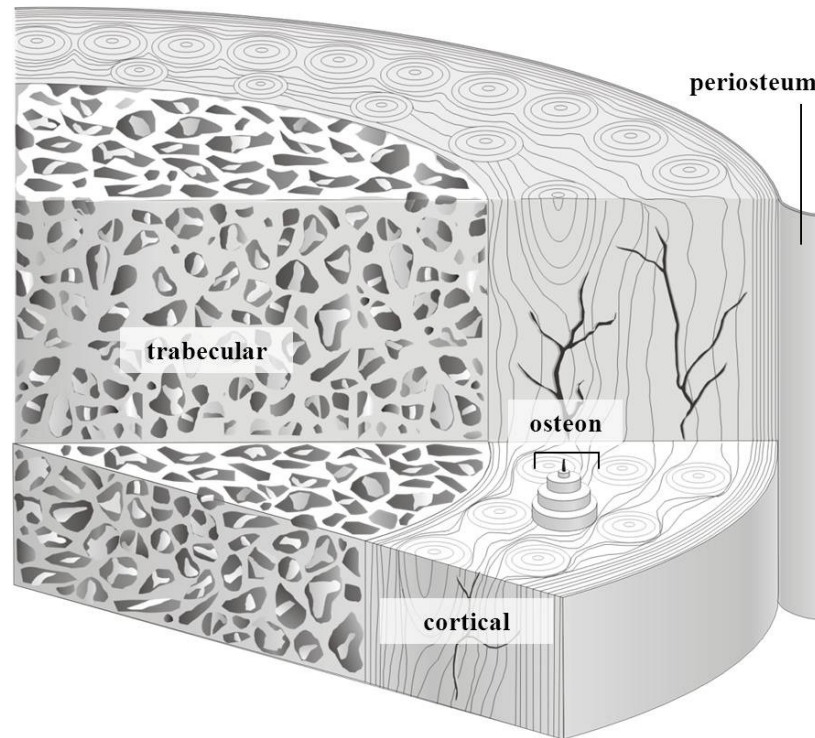


Figure 2.1: Schematic drawing of bone structure modified from Rahn [40].

2.1.1 Composition

Bone is composed of a unique combination of intercellular calcified material (bone matrix) and bone cells (Figure 2.2). Bone matrix is a composite material consisting of organic and inorganic components which is initially deposited by osteoblasts as unmineralized precursor substance (osteoid) [41]. The organic component usually makes up approximately 20% of the wet weight of bone and mainly consists of collagen and other non-collagenous proteins [42]. Collagen fibres are the major structural component of bone matrix, whereby the majority is type I [34]. The distribution of collagen and mineral provides bone with its ability to balance its flexibility and stiffness requirements [43]. The non-collagenous macromolecules are important for controlling the attachment of bone cells to the matrix and regulating cell activity associated with the biomineralization process and remodelling in bone tissue [44]. Some of these substances (e.g. osteocalcin) are specific to bone. Non-specific macromolecules

(e.g. osteopontin, fibronectin and growth factors) are also present in other connective tissues [45]. The inorganic component contributes approximately 70% of the wet weight of bone and serves as a reservoir storing approximately 99% of total body calcium, 85% of phosphorus and 40-60% of body's sodium and magnesium [34]. The mineralized components give strength and rigidity and fulfill the main mechanical support function within the human body. They consist of a mineral hydroxyapatite phase deposited in an organic matrix [34]. The stability of the skeleton to withstand pressure, tension, bending, and torsion, is based upon inclusion of inorganic components in the organic intercellular matrix [39]. The main component is hydroxyapatite, but also fluoroapatite, carbonated apatite, calcium carbonate, and magnesium carbonate are components in the mineral phase of bone [46]. The basic composition of bone is the same for all bones, but the components of the bone types are combined differently to form cortical or trabecular structures.

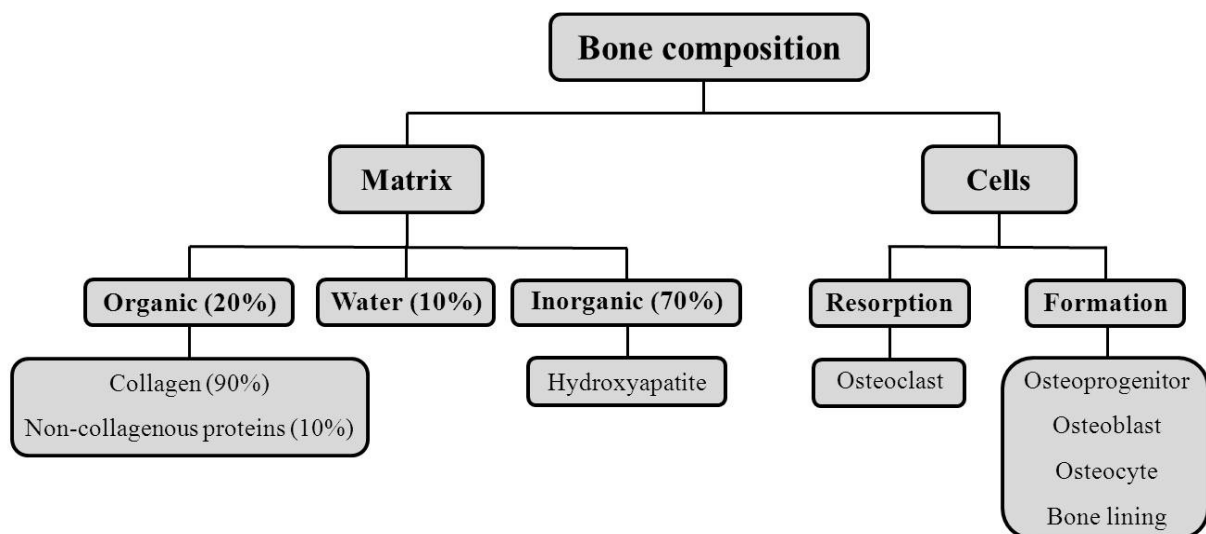


Figure 2.2: Overview of the main bone composition.

2.1.2 Bone cells

In human bone, different cell types can be identified (Figure 2.2). Bone tissue principally contains bone resorption cells (osteoclasts) and bone formation cells (including osteoblasts, osteocytes, bone lining cells and osteoprogenitor cells) [41]. The extracellular materials providing a matrix for these cells are organic material (e.g. collagen), inorganic material (e.g. minerals like calcium and phosphate), and water [34].

Bone resorption processes and resorption of bone substitute materials are mediated by osteoclasts which are differentiated from hematopoietic stem cells of the monocyte-macrophage lineage in the bone marrow [47]. The differentiation is regulated by cytokines and hormones to activate remodelling processes or increase calcium and phosphate concentrations in the blood which is important for calcium and phosphate homeostasis [48]. Osteoclasts are large multinucleated cells and responsible for the absorption and removal of bone [49]. Attached to the bone surface, the osteoclasts create an acidic environment and bone tissue is dissolved by proteinase and enzyme activity to break down bone matrix effectively [50].

Osteoblasts are responsible for bone formation processes of organic matrix and osteogenesis [51]. These cells are differentiated from mesenchymal stem cells. The differentiation is controlled by many cytokines and can be divided into several stages (proliferation, extracellular matrix deposition, matrix maturation and mineralisation) [52]. The osteoblast synthesises and secretes collagen and non-collagenous proteins that comprise the organic matrix of bone and subsequently mineralise the bone matrix [53]. Osteoblasts express high levels of alkaline phosphatase (ALP), a serum marker of bone formation [54]. Some osteoblasts disappear through programmed cell death (apoptosis), whereas others differentiate into flat cells lining the bone surface (bone lining cells) or become osteocytes surrounded by the bone matrix in small lacunae [34, 55].

Both lining cells and osteocytes play an important role in the regulatory process of maintaining bone. Bone lining cells mediate bone turnover by activation of remodelling processes by secreting enzymes [34].

Osteocytes are characterized by long cell processes which form a complex network throughout the bone matrix [56]. These cells are trapped within the bone matrix during the process of bone formation and communicate with osteoblasts and bone lining cells at the bone surface [57]. They express a variety of molecules which make them respond to both, mechanical and hormonal stimuli.

2.1.3 Bone modelling and remodelling

Active bone tissue is able to modulate structures and mass in response to changing requirements. Under physiological conditions, there is a balance between bone-resorbing and bone-forming events. These processes are realized by many cell activities, including bone repair, growth, modelling and remodelling [41]. A higher metabolic bone turnover and remodelling rate take place in cancellous bone (approximately 30% per year) as compared to cortical bone (approximately 3% per year) [39, 58].

Bone modelling involves activation and isolated bone resorption or formation. The process of bone formation and resorption during modelling does not happen at the same location. Modelling primarily occurs during bone growth and usually declines in adults. Stimuli for bone modelling processes in adults are increased mechanical loading, administration of parathyroid hormone (PTH) and specific drugs [31]. Bone modelling is a process to add or remove bone tissue from an existing bone surface to modify bone geometry. It leads to changes in the size and shape of bone. This is achieved by uncoupled actions of osteoblasts and osteoclasts. Remodelling of the human bone matrix is a physiological process of bone reconstruction where parts of bone are replaced by new bone. It occurs permanently and involves coordinated actions of

osteoblasts and osteoclasts. These cells build basic multicellular units (BMUs) which remodel bone by activation, resorption, and formation processes. Bone remodelling is necessary to maintain calcium homeostasis and to repair damage in bone. In the BMU, osteoclastic bone resorption initiates osteoblastic bone formation [59]. The general bone remodelling cycle by a BMU is schematically shown in Figure 2.3. A stimulus activates osteoclastic precursors to differentiate into multinucleated osteoclasts (cutting cone). Osteoclastic cells bind to the bone surface and resorb bone. Bone resorption involves dissolution of crystalline calcium phosphates and degradation of collagen in the extra cellular resorption lacunae with the secretion of acids and enzymes by osteoclasts [50]. Following behind the osteoclasts, osteoblasts deposit layers of osteoid (unmineralized bone matrix). Osteoblasts always follow osteoclasts in BMU. The resorption and formation processes are coupled. The organic components of the matrix are then hydrolysed and osteoblasts are responsible for bone matrix formation and differentiate afterwards into osteocytes and bone lining cells [60].

Many diseases are caused as a result of abnormalities in bone remodelling which compromise the architecture, structure, and mechanical strength leading to clinical symptoms [17]. Consequently, there is a growing interest in defining the molecular mechanism by which bone remodelling is regulated [53].

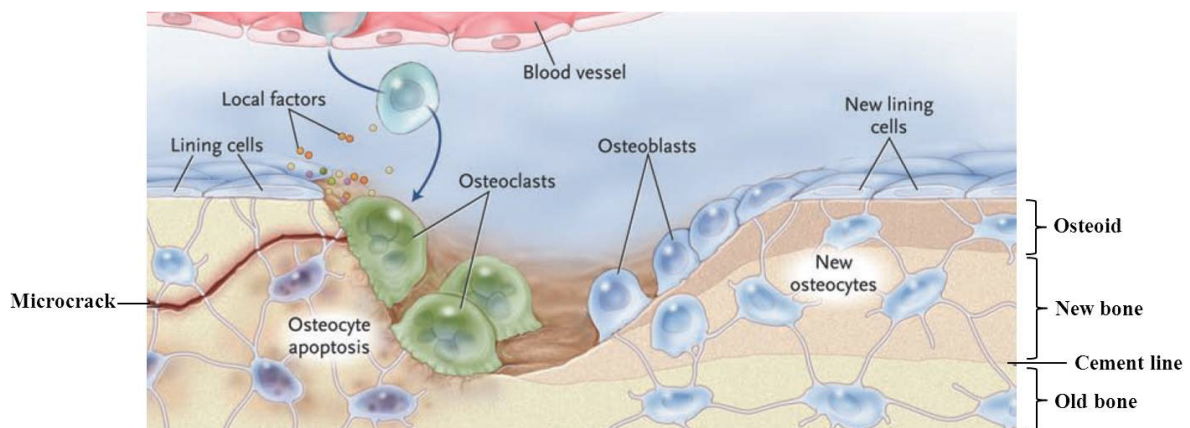


Figure 2.3: Bone remodelling process by a BMU described by Canalis et al. [60].

2.1.4 Fracture healing

A bone fracture is a break in the normal continuity of bone. When a fracture occurs, the bone, periosteum or surrounding tissues, like muscles, nerves or blood vessels, may be damaged or destroyed. The process of fracture healing is a complex cascade of specific events on a cellular and molecular level that ideally ends in complete structural and functional restoration of the involved bone [36]. Many different molecules and cells are involved, including inflammatory cytokines, growth factors, antioxidants, osteoclasts, osteoblasts, hormones, amino acids, and other nutrients [61]. Permanent bone remodelling provides a mechanism for healing and regeneration of damaged bone tissue [62]. This property is initiated in response to injury and healing of bone around and within implants [63]. Multiple factors influence the molecular mechanism that regulates bone tissue formation during bone repair [61]. Bone repair is typically divided into direct or primary and indirect or secondary fracture healing [62].

Primary or direct fracture healing (intramembranous ossification) is described as the basic principle of fracture healing and occurs when fracture surfaces are rigidly held in contact. This type of healing is only possible under absolutely stable conditions and is characterized by the complete absence of a fracture callus [62]. In this situation, intramembranous ossification, bone formation, and the osteoid are directly effected by mesenchymal tissue [36]. Osteoclasts cross fracture sites whereby reestablishing new Haversian systems to form the cutting cone. Therefore, they provide pathways for the penetration of blood vessels [64]. Many fractures heal when micromotion between the fracture surfaces occurs [65]. If the construct is extremely rigid, there is no stimulus for healing. In practice the primary or direct fracture type is the rarest [36].

Secondary or indirect fracture healing (chondral ossification) is characterized by callus formation which is subsequently replaced by lamellar bone. It is found in less rigid, more flexible fixation that allows a certain amount of micromotion in

a wider fracture gap. This type of healing benefits from micromotion [36]. It is a complex process that involves the formation of a bridging callus of cartilage, bone and connective tissue cells, restoring the normal bone structure. In this situation, an interaction between bone forming (osteoblasts), bone resorbing (osteoclasts) cells and the influence of different growth factors, cytokines, and hormones in the formation of fracture callus occurs [62].

Secondary fracture healing is typically characterized by different overlapping stages, such as an early initial inflammatory response (hematoma, inflammation, angiogenesis), a repair phase (cartilaginous callus formation and replacement of callus by lamellar bone), and a late bone remodelling phase [36]. These phases take place in the bone marrow, cortex, periosteum, and external soft tissues and they can overlap in time [62, 66]. A fracture can lead to damage of cortical and cancellous bone, bone marrow, endosteum, periosteum, and adjacent soft tissues. During the inflammatory phase, the hematoma is invaded and replaced by callus. Fracture healing is not homogenous within the callus. A callus consists of fibrovascular tissue in which abundant amounts of collagen fibers and woven bone matrix are laid down. The main zones are the medullary canal, the area between the cortices, the subperiosteal layer, and the surrounding soft tissue [61]. The fibrous callus (soft callus) within the fracture gap (cortical and medullary callus) creates bone by endochondral ossification. Membranous ossification is found in the external callus, far from the fracture site (hard callus). It is a result of direct osteoblast activity which forms both compact and trabecular bone directly without first forming cartilage.

Within the early inflammatory phase a blood clot (hematoma) is formed between the bone ends (Figure 2.4 a). Without an inflammatory process, bone will not heal. An inhibition of the cyclo-oxygenase pathway appears to inhibit bone formation [67]. The hematoma itself is a source of signalling molecules for macrophages and chondroblast precursors which are important for the regulation of cell differentiation and angiogenesis [62, 68]. Inflammatory cells

secrete growth factors and cytokines which have chemotactic effects on other inflammatory cells and osteoblast precursors [69, 70]. The major signalling molecules in the cascade are interleukin 1 (IL-1), interleukin 6 (IL-6) [69], transforming growth factor b (TGF b) [71], insulin-like growth factor (IGF) [72], fibroblast growth factor (FGF) [73], platelet-derived growth factor (PDGF) [74], and bone morphogenetic proteins (BMPs) [67]. Granulocytes, mast cells and monocytes infiltrate locally. In addition, pluripotent stem cells of mesenchymal origin as precursors of osteoblasts migrate into the fracture gap. Within this time period, granulation tissue and new blood vessels rebuild under the influence of growth factors. Fibroblasts, collagen type I, capillaries, and initial mineral deposits are the main components of this granulation tissue and replace the fracture hematoma by fibrocartilaginous callus (Figure 2.4 b). During the reparative phase, the blood clot is replaced by fibrovascular tissue which lays down the collagen fibres and the matrix which will later become mineralised to form the woven bone of the primary callus (Figure 2.4 c) [36]. Proliferation and differentiation of mesenchymal and osteoprogenitor cells into chondroblasts and osteoblasts lead to vascularized granulation tissue and fibrous tissue with the production of extracellular matrix and collagen fibres [75]. Subsequently, these cells begin to form cartilage and woven bone to increase the mechanical stability of the fracture site (chondrogenesis). To promote osteoblastic proliferation, macrophages secrete proteins such as osteocalcin and BMPs. BMUs are formed and break down damaged bone. They are responsible for newly formed woven bone and a process of increased mineralization occurs. The remodelling phase of fracture healing is long-lasting and can take several years (Figure 2.4 d). Through this process, unoriented woven bone is replaced by mature lamellar bone, which is characterized by a dense structure of osteons, i.e. central Haversian canals with concentric layers of surrounding bone. Under ideal circumstances, the original tissue and its function are almost completely restored [36].

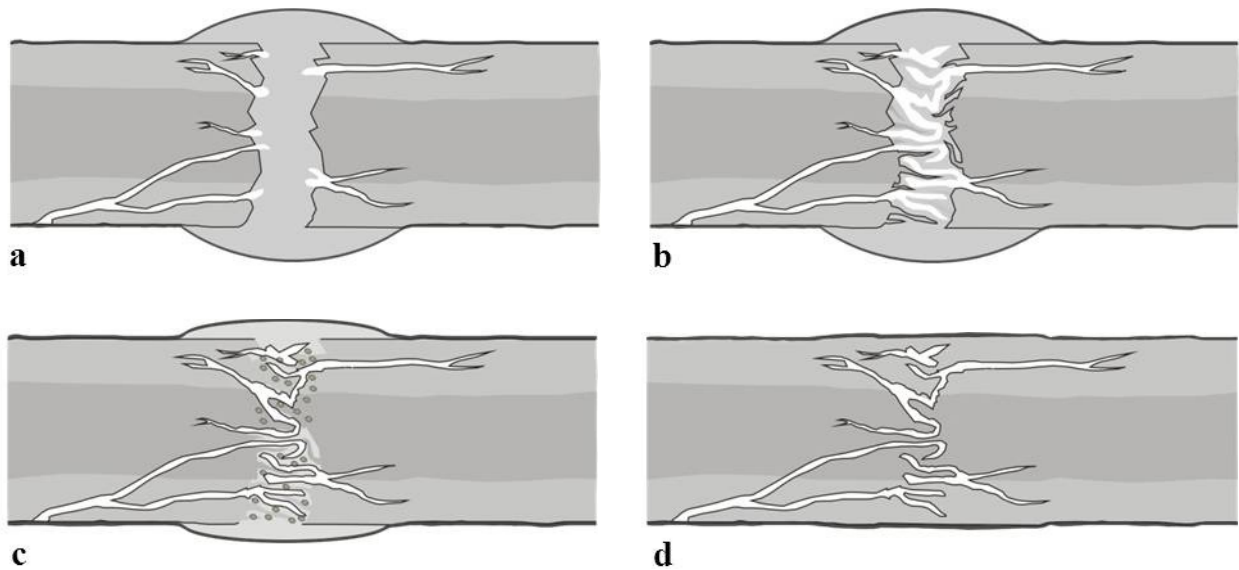


Figure 2.4: Overlapping stages of secondary fracture healing: hematoma formation (a), fibrocartilaginous callus formation (b), bony callus formation (c) and bone remodelling (d).

Differences in fracture healing processes between humans and animals pose a limitation on preclinical research. Fracture healing rates in rats, for example are about twice that in humans [61]. The main cellular and molecular processes of fracture healing in rodents are described by Einhorn [62]. Phillips describes the time period of fracture healing in rats as follows [61]. Briefly, a hematoma is formed in the first hours following a fracture and inflammatory cells are released [69, 76]. Within the first day, mesenchymal stem cells express a number of BMPs which induce angiogenesis, chemotaxis, mitogenesis, cell differentiation, and proliferation. From day two to five, hard callus formation originates in the subperiosteal area. Promoted by micromotion, intramembranous ossification occurs. In the area between the bone ends (soft callus), early cartilage formation starts between days four and seven. Undifferentiated mesenchymal stem cells begin to proliferate by day three. Osteocalcin is expressed in the hard callus from day six to 10. In days 11 to 20, cellular proliferation decreases in the areas of hard callus formation. In the soft callus, the cartilage begins to calcify. From days 21 to 25, there is no more cellular proliferation. The structure in the hard

callus area turned into woven bone. In the soft callus, chondrocytes begin to undergo apoptosis and there is some cellular necrosis. Solid union with woven bone is present by around 35 days, succeeded by remodelling and formation of lamellar bone [61].

2.1.5 Biochemical markers

Bone metabolism can be monitored by using special biochemical markers. The cellular and molecular process of signals triggering bone regeneration events is becoming more and more understood *in vitro*, but the *in vivo* response is still to a certain extent unclear. Early bone reaction to an implant is not yet understood completely although primary stability and long-term performance are thought to be related [50]. Biological processes leading to integration of an implant in bone mainly take place at the tissue-implant interface [77]. However, the cellular and molecular events that occur during normal bone healing processes can be influenced by the presence of a biomaterial. Bone healing processes under different conditions have been widely described in literature and may result in different bone formation. Also, molecular and cellular signalling of bone healing scenarios can be different. Multiple factors influence and control the complex interactions during bone healing. Special precursors and molecules of cytokines, chemokines, integrins and growth factors are temporarily recruited into the circulation [78]. These biochemical markers change rapidly in response to changes in bone formation and resorption and can be monitored by different techniques such as immunohistochemistry, enzyme-linked immunosorbent assay, western blot, microarray analysis, *in situ* hybridisation, and semi-quantitative polymerase-chain reaction [79-84].

Proinflammatory cytokines can indicate processes during the bone healing cascade [85]. Further biochemical markers are usually classified into those associated with bone formation and resorption [86, 87]. Osteogenic cells start to express specific substances during their differentiation within the bone healing

cascade. Early signals of fracture healing in an early stage of bone repair comparing non-fractured with post-fractured rat bones have been identified [88]. Specific markers can indicate changes in bone processes and can exemplarily be used in the monitoring of anti-osteoporotic therapy [89, 90]. The analytic and biologic variability of bone markers can be significant and needs to be considered when they are used [91]. In the present thesis, quantitative PCR together with histological tools were used to explore the bone-implant interface.

2.1.5.1 Proinflammatory cytokines

The major proinflammatory cytokines are tumor-necrosis factor-alpha (TNF- α) and interleukin-1 beta (IL-1 β). They are secreted by hematopoietic immune cells such as macrophages and neutrophils and have a wide range of effects [92]. Locksley et al. described the widespread effects of TNF member (RANKL) and TNF receptor superfamily (OPG) on signalling pathways for cell proliferation, survival, and differentiation and their use in the treatment for many human diseases [93]. Furthermore, the direct effects of TNF- α and IL-1 β on osteoclastogenic differentiation have been largely investigated [94]. IL-1 β is responsible for various biological activities involved in the immune and inflammatory response [95]. Generally, proinflammatory cytokines modulate inflammatory response and have a beneficial effect on regulating bone fracture repair [96]. TNF- α and IL-1 β inhibit the expression of genes for cartilage extracellular matrix and potential functions in injury-induced inflammatory response [96]. The expression of proinflammatory cytokines increases during the initial inflammatory phase after bone injury within the first 24 hours [85].

2.1.5.2 Bone resorption markers

During bone resorption processes, an acidic environment is created by osteoclasts [31]. The released bone resorption markers can be divided into collagenous and non-collagenous molecules. Non-collagenous markers include the enzymes tartrate-resistant acid phosphatase (TRAP) and cathepsin K (CATK) [54]. TRAPs are metalloenzymes that catalyse the hydrolysis of various phosphate esters under acidic conditions. Six isoforms are identified in human tissue. Isoform 5 is expressed in osteoclasts and macrophages [97]. Isoform 5b can be used as a marker of bone resorption and indicates the number of active osteoclasts [98]. In bone, TRAP is found in osteoclasts and in mononuclear cells (osteoclast precursor cells) [99]. Not only in osteoclasts, but also in osteoblasts and osteocytes TRAP is expressed, but the level is much lower [100]. CATK is a member of cysteine protease family and is localized in vacuoles at the ruffled border membrane of osteoclasts [101]. This enzyme has the unique ability to cleave helical and telopeptide regions of collagen type I which is the major type of collagen in bone [102]. The degradation of collagen is a major event during bone resorption and CATK has an important role in osteoclastic activities [102].

2.1.5.3 Bone formation markers

Bone formation markers indicate osteoblastic activity [54]. Two specific and sensitive markers include osteocalcin (OC) and the bone specific alkaline phosphatase (ALP) which reflects different aspects of osteoblastic activity [103-105]. OC is a major non-collagenous extracellular matrix protein with 46-50 amino acids. The protein is an abundant osteoblast-specific non-collagenous protein and is produced during late phases of bone formation [106]. The structure of the protein is characterised by three γ -carboxyglutamic acid residues (Gla) with a high affinity to hydroxyapatite [107]. Osteocalcin is mostly deposited in the extracellular matrix of bone, but a small amount can also be

detected by immunoassay in the blood [108]. ALP is a hydrolase enzyme responsible for removing phosphate groups from many substances. Several ALP isoforms exist and some of them are bone specific. In bone, ALP is primarily expressed on the osteoblast cell surface. The enzyme is a potent inhibitor of mineralisation and important for cleaving inorganic pyrophosphates which promote mineral deposition *in vivo* [109]. Whereas OC represents a late marker during osteogenic differentiations for bone formation, ALP is considered an early differentiation marker [110]. OC and ALP gene expressions are already used in rat studies to indicate bone formation processes [35, 111].

2.2 Calcium phosphates

Calcium phosphate-like bone substitute materials have a long history of successful orthopaedic applications such as bone void filling and augmentation [7]. Many patients are treated with a bone substitute material to repair a bone defect resulting from an injury or a disease. Bone substitute materials based on calcium phosphates are of particular interest for these clinical applications.

They have been demonstrated to be effective in a number of bone healing applications. Bone substitutes are proven to have an excellent *in vivo* biocompatibility and bone repair properties for example stimulating tissue regeneration [8-12]. Biomaterials play an important role in reconstructive orthopaedic surgery and it is necessary to understand the biological effects of these materials for their optimal application [112].

Bioceramic materials most commonly in recent times have been based on hydroxyapatite and beta-tricalcium phosphate and these offer a similar structure to the human mineral bone phase. The large range of calcium phosphate formulations available can mainly be divided into three subgroups: sintered hydroxyapatites, solid tricalcium phosphates, and calcium phosphate cements [7]. Hydroxyapatite is the main inorganic component of human bones and widely used as the main component of an implantable medical device [113].

Sintered hydroxyapatites are often used as preformed matrices with an interconnecting pore system to allow bone ingrowth [21]. Furthermore, the degradation rate of water-insoluble hydroxyapatite formulations is very slow [114, 115]. Solid β -tricalcium phosphates are often used as a porous osteoconductive bone graft substitute. An advantage of β -tricalcium phosphate is a reduced dissolution time when compared to sintered hydroxyapatite and calcium phosphate cements. A disadvantage is the limited mechanical strength. Commercially available β -tricalcium phosphate products are preformed granules, blocks, or wedges [7]. Calcium phosphate cements usually consist of calcium phosphate powders that are mixed with a liquid water or phosphate solution to obtain an injectable paste. After implantation, the compound hardens *in situ* with almost no exothermal reaction [7]. The cement is mouldable which ensures perfect fit at the implant site. Remodelling in bone substitutes is slow and incomplete, but by adding more and larger pores, like in ultraporous β -tricalcium phosphate, complete or nearly complete resorption can be achieved [7]. Different surface structure and shape of commercially available biominerals are a result of their manufacturing process. Critical parameters are sintering temperature and time [116]. All these bioceramics promote the formation of new bone by their osteoconductive properties during the natural mineralisation process [8-12]. Calcium phosphates act as synthetic osteoconductive matrices after implantation in bone. When placed in a stable configuration adjacent to bone, osteoid will be formed directly on the surface of the calcium phosphate with no soft tissue interposed [7]. Such biomaterials are frequently used for bone void filling to replace bone loss [117]. A bone void filling leads subsequently to a bone regeneration and repair [118].

In the clinical use of bone void fillers based on calcium phosphates, there is an increasing interest in an additional local pharmacological treatment to generate further benefits [20-23]. Many investigations have been conducted to maximize controlled drug release to specific bone sites to maintain a prolonged drug

concentration level and avoid pharmacological side effects [27]. Calcium phosphates are able to adsorb several chemical substances on their surfaces, such as proteins, antibiotics or chemotherapeutic agents [18-20]. The adsorptive affinity of these materials to active pharmaceuticals can be used for the development of innovative drug delivery systems. A potential bone substitute material must have the ability to incorporate pharmaceuticals at a target load and to deliver it to the surrounding bone tissue if it is intended to be used as a drug carrier. Offering an osteoconductive matrix for new bone growth and being a carrier for local and controlled bisphosphonate delivery, a combination product is very attractive for the treatment of bone diseases. Maintenance of bone density and reduction of bone resorption can theoretically be enhanced after implantation of bone substitute materials releasing bisphosphonates [28].

Several parameters can influence both, drug loading and release properties. A careful physico-chemical characterisation of bone substitute materials is, therefore, necessary to evaluate the feasibility of being optimal candidates for an innovative local drug delivery system. A short-term dipping technique for drug loading could be promising for a clinical application in terms of loading bone substitutes directly prior or during surgery with well-defined drug content. In the present study, a sintered body, differently sized granules, and powders were selected as bone substitute materials to investigate the major influencing factors. The choice of bone substitute materials represents three common forms of materials: solid, granular and an injectable paste that sets *in situ*. Whilst there is a lot of literature on drug delivery through implantable devices, there still is much to be learned about how to do this safely and effectively. At the time of writing, there is no product (combining a calcium phosphate with a bisphosphonate) yet available for clinical application that is approved for use in either Europe or United States of America. It is known that a company called Graftys has initiated a clinical trial in which a calcium phosphate cement is used to deliver a bisphosphonate [119].

2.3 Osteoporosis

The previously described bone processes do not refer to metabolic and disease-related changes in bone structure. In addition to the above mentioned healthy conditions, bone structures can also be modified by bone diseases such as osteoporosis. Many orthopaedic patients are affected by osteoporosis resulting in an increased risk of bone fractures [13]. For the year 2000, nine million new osteoporotic fractures were estimated world-wide [14]. Osteoporosis is a metabolic disease affecting bone which is an important issue within the geriatric population primarily affecting women [120]. The disease pattern is characterized by a decreased bone mineral density (BMD) and microarchitectural deterioration of bone tissue (Figure 2.5). The mechanical strength of bone is strongly determined by its mass [17]. It is also shown that increased bone turnover correlates with an increased fracture risk [121]. This relationship has been seen in therapeutic trials with bisphosphonates, in which increased bone density and decreased bone turnover have correlated with reduced fracture risk [122]. Osteoporotic bone leads to a consequent increase in bone fragility and susceptibility to fracture [123]. Studies have shown a close correlation between low BMD and increased fracture risk [124, 125]. Bone architecture is not only affected in cancellous bone (thinning and loss of trabeculae) but also in cortical bone (thinning of the cortex and increase in intercortical porosity). In healthy bone, osteoclasts and osteoblasts constantly adjust the bone density balance. If the number of osteoclasts is higher than the number of osteoblasts, the bone density decreases. In osteoporosis, the amount of active osteoclasts and remodelling units are elevated and shift the balance in favour of resorption [13]. Furthermore, the osteoblasts are less active and fail to completely restock the resorption lacunae. This results in incremental porous structures of bones. With aging, less bone is formed by osteoblasts than removed by osteoclasts [13]. Estrogen deficiency increases osteoclasts' while simultaneously decreasing osteoblasts' life span. This results in an increased rate of bone remodelling

during the menopause which increases the risk of osteoporosis in postmenopausal patients [13]. The aim of medical osteoporosis treatment is to maintain or increase BMD and reduce exceeding bone turnover [126]. Many pharmacological treatments are available to affect bone loss [127]. This can be achieved by inhibiting bone resorption or by stimulating osteoblasts to induce bone formation. In first line therapy for treatment and prevention of osteoporosis, bisphosphonates have been shown to be one of the most effective inhibitors of bone resorption [17].

The use of conventional implants in fracture fixation of osteoporotic bone is limited as fixation failures are more likely to occur as a consequence of the weak bone structure [15, 16]. Current research that focus on implant fixation in weak bone structure includes optimized implant-bone interfaces such as hydroxyapatite coating or biodegradable welded implants [128-130]. Osteoporotic fractures and their adequate fixation are an important future challenge in traumatology.

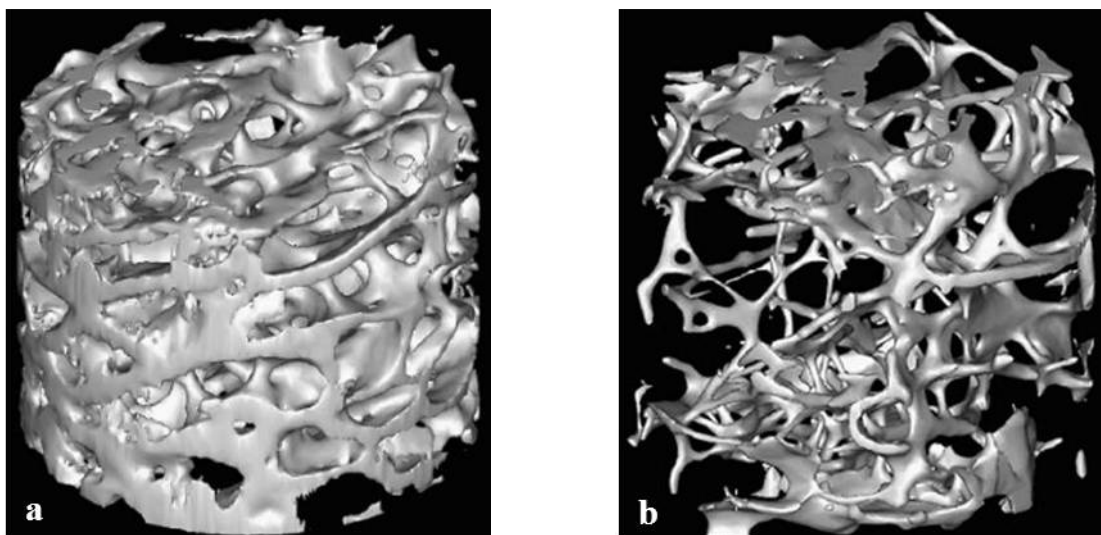


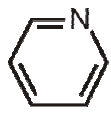
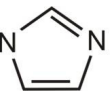
Figure 2.5: Trabecular bone architecture of normal (a) and osteoporotic cancellous bone (b) described by Moritz et al. [131].

2.4 Bisphosphonates

During the last decades, bisphosphonates have extensively been developed as drugs for the treatment and prevention of bone diseases [132]. Nowadays, there is preclinical evidence that bisphosphonates have antitumor activity and are appropriate for the treatment of metabolic bone diseases [133]. Bisphosphonates are drugs that influence the quality of bone in patients suffering from osteoporosis. The mechanisms underlying their effects are still not fully understood. Bisphosphonates have been used widely in the treatment of disorders associated with excessive bone resorption. They are effective inhibitors of bone resorption and one of the most effective agents available for the treatment and prevention of osteoporosis [134]. This property leads to their use in the treatment of other metabolic bone diseases in which abnormal bone resorption occurs such as Paget's disease of bone, fibrous dysplasia, and metastatic cancer of bone [135]. Bisphosphonates are stable analogues of inorganic pyrophosphate (P-O-P), an endogenous regulator of calcium metabolism preventing ectopic calcification [136]. The bridging oxygen has been replaced by carbon. They are compounds characterized by two C-P bonds. The metabolic stable P-C-P structure allows a great number of chemical variations. The two lateral chains on the carbon can be changed or the phosphate groups can be esterized [132]. Nevertheless, every bisphosphonate has its own chemical, physicochemical, and biological characteristics which implies that it is not possible to extrapolate from the results of one compound to others with respect to its actions [132]. Caused by a stable carbon structure, bisphosphonates are resistant against hydrolysis under acidic influence as described for osteoclastic environments. The half-life of bisphosphonates in the circulation are short, and they adsorb rapidly into bone because of their high affinity for calcium and hydroxyapatite and bind directly to mineralized bone [137]. There are two main generations of bisphosphonates. Non-nitrogen-containing (e.g.

etidronate (Didronel[®]) and clodronate (Ostac[®]) and nitrogen-containing bisphosphonates (e.g. pamidronate (Aredia[®]), alendronate (Fosamax[®]), risedronate (Actonel[®]), ibandronate (Bondronat[®]) and zoledronate (Zometa[®])) have different molecular structure modifications (Table 2.1). Russell et al. described their different molecular actions [138].

Table 2.1: Chemical structures of major bisphosphonates and their relative potency to inhibit bone resorption in rats modified from Fleisch [132].

<i>Basic bisphosphonate structure</i>				
$ \begin{array}{ccccccc} & & \text{O} & & \text{R}_1 & & \text{O} \\ & & \parallel & & & & \parallel \\ \text{HO} & - & \text{P} & - & \text{C} & - & \text{P} & - & \text{OH} \\ & & & & & & & & \\ & & \text{OH} & & \text{R}_2 & & \text{OH} & & \end{array} $				
Agent	R₁	R₂	Rel. potency	Brand name
Etidonate	-OH	-CH ₃	~ 1x	Didronel [®]
Clodronate	-Cl	-Cl	~ 10x	Ostac [®]
Pamidronate	-OH	-(CH ₂) ₂ -NH ₂	~ 100x	Aredia [®]
Alendronate	-OH	-(CH ₂) ₃ -NH ₂	>100 - <1000x	Fosamax [®]
Risedronate	-OH	-CH ₂ - 	>1000 - <10000x	Actonel [®]
Ibandronate	-OH	-CH ₂ -CH ₂ -N(CH ₃)(CH ₂) ₄ -CH ₃	>1000 - <10000x	Bondronat [®]
Zoledronate	-OH	-CH ₂ - 	>10000x	Zometa [®]

The highest potency of bisphosphonates to inhibit bone resorption in rats is demonstrated by ZOL which is a member of the most recent generation of bisphosphonates [132]. ZOL is a very potent N-containing bisphosphonate which may decrease the resorption of newly formed bone in rats [139].

Furthermore, ZOL inhibits osteoclastic activity and regulates cell proliferation, differentiation, and gene expression in osteoblasts [134]. ZOL pharmacologically acts in the mevalonate pathway (Figure 2.6). ZOL inhibits the farnesyl diphosphate synthase (FPPS) which is responsible for the synthesis of farnesyl diphosphate (FPP) and its downstream metabolite geranylgeranyl diphosphate (GGP) [140]. FPP and GGP trigger the modification of small GTPases which are important for the regulation of osteoclasts functions [141].

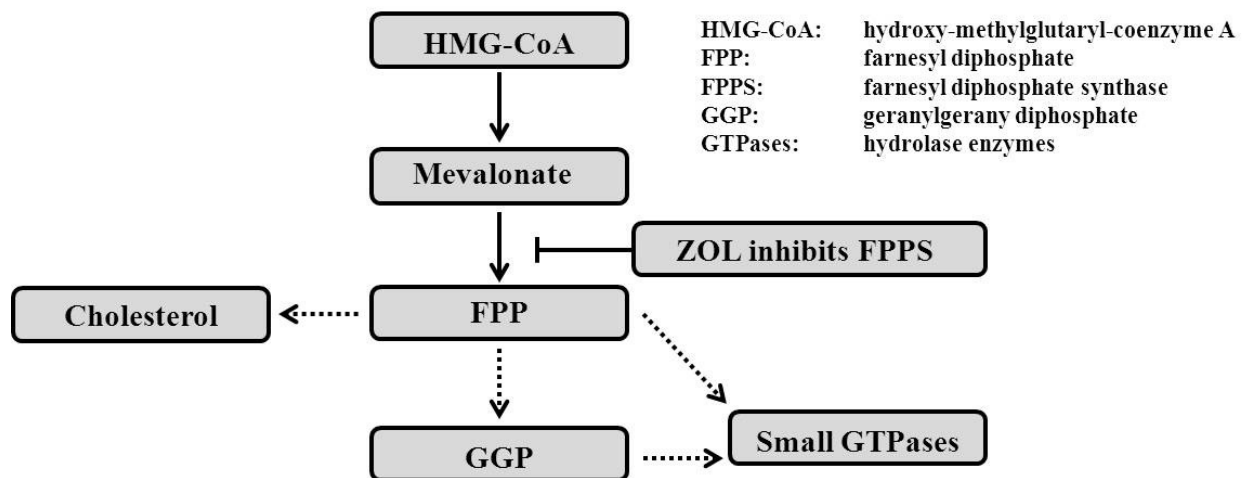


Figure 2.6: Simplified pharmacological action of ZOL in the mevalonate pathway.

The efficacy and safety of a yearly infusion of five milligram ZOL have been investigated in placebo-controlled, multicenter, international trials for the treatment of osteoporosis and the reduction of fracture risk [142, 143]. A side-effect associated with the use of bisphosphonates is bisphosphonate-related osteonecrosis of the jaw, but the pathogenesis of this effect is still mostly unclear [144-146]. Up to date, there is no evidence of a specific association between osteonecrosis of the jaw and ZOL in the doses used for treatment of osteoporosis in postmenopausal women [147]. It has also been suggested that there are risks of femoral fracture, however, the risk here is considered small in relation to the benefit [148]. There is growing interest in using these drugs in combination with orthopaedic implants with the goal of improving the quality of

bone at the implant-bone interface and reducing the risk of implant migration and failure. Bisphosphonates are occasionally the most commonly used osteoporosis treatment, but there are other therapies that impact on bone loss. Current alternatives to bisphosphonates are selective estrogen receptor modulators (SERMs), parathyroid hormone (PTH), strontium ranelate, and calcitonin. Calcium and vitamin D are also associated with osteoporosis treatment. They are usually taken at the same time as other drugs [127]. Nevertheless, it is mainly bisphosphonates that have been evaluated in the role of combination with orthopaedic implants for the purpose of improving bony support or fixation. One factor that might explain this focus is the affinity for calcium salts and these form the basis for most bone substitutes and implant coatings in common use today.

2.5 Local drug delivery

The site of pharmacological action of a drug can mainly be divided into systemic and local [149]. A systemic drug therapy refers mainly to a treatment that affects the whole body or that acts specifically on systems that involve the entire body (e.g. cardiovascular, respiratory, gastrointestinal, or nervous systems). A local drug therapy is mainly limited to a treatment that affects a certain location in the body. The aim of every drug therapy is to maximize the therapeutic effect of the drug and minimize drug-related site effects. This can be mainly achieved by delivering the drug locally at the site of pharmacological action [150]. Not all conventional systemic applications have an adequate biological availability. By systemic administration routes often only small drug amounts reach the target tissue. Furthermore, drugs could also accumulate locally. The general objective of local applications is to release a desired drug concentration level for long periods of time without reaching a toxic level [151, 152]. Defining a locally delivered dose for beneficial biological effects frequently provides a lot of challenges. Nevertheless, the use of combination

implants as drug carriers in orthopaedic surgery could have an added value for bone tissue [130]. A local drug application generates many benefits as lower pharmacological side effects compared to systemic application due to lower dosages, better control of bioavailability and toxicity, and a longer duration of drug delivery at the site of pharmacological action [153]. Furthermore, a drug-loaded implant provides the possibility to combine the controlled and local drug delivery with systemic therapy strategies. However, a careful testing of drug-loaded implants has to be undertaken to prove the added clinical value.

Different techniques are available to combine bisphosphonates with an implant [154]. The carrier systems used are mainly calcium phosphate coatings [129, 155], polylactic-glycolic acid polymer coatings [156], and cross-linked fibrinogen layers which are linked to metals via silanes [157, 158]. In the present thesis, different calcium phosphate based drug delivery systems were chosen for a local application of ZOL. Calcium phosphates are proven materials already approved for implantation as a bone substitute whilst fibrinogen and polylactic-glycolic acid are well known per se but as a coating have many unknowns [7].

3 Materials

3.1 Zoledronic acid (ZOL)

ZOL (1-hydroxy-2-[(1-H-imidazole-1-yl)ethylidene]1-bisphosphonate) was obtained from Alexis Biochemicals (Lausen, Switzerland) and used as active pharmaceutical agent. ZOL is a white, crystalline powder. The water used in the investigations was of double-distilled quality.

3.2 Bone substitutes

The selected bone substitute materials varied in manufacturing processes, shapes and compositions. These were also selected as they correspond to the main bone substitute implant forms available today.

- 1) A LagFix[®] cylinder (Stryker Trauma GmbH, Schönkirchen, Germany)

This is a hollow tube structure made up of sintered hydroxyapatite granules. It is designed for use in augmenting lagscrew fixation in fractures of the proximal femur.

- 2) BoneSave[®] granules (Stryker Howmedica Osteonics, Limerick, Ireland)

These are granules that contain calcium phosphate in the form of 80% tricalcium phosphate and 20% hydroxyapatite. They are available in two different sizes of 2-4 mm and 4-6 mm. These granules are indicated for the filling of bone voids that are non load bearing and not intrinsic to the stability of the bony structure.

- 3) HydroSet[®] (Stryker Leibinger GmbH, Freiburg, Germany)

This is an injectable self-setting calcium phosphate cement that is provided in a self contained surgical set containing a liquid-filled syringe and a powder. The liquid contains sodium hydrogen phosphate, polyvinylpyrrolidone (PVP) and water. The powder used in the present

investigations contains dicalcium phosphate dihydrate and tetracalcium phosphate as well as trisodium citrate dihydrate. The cement is indicated for non load bearing bone void filling, and in the European Union is additionally approved for augmenting screws.

4 Methods

4.1 BoneSave[®] sieve fractions

To achieve BoneSave[®] fractions in the desired particle size range, 4-6 mm BoneSave[®] granules were ground with a mortar and a pestle followed by sieving on a Retsch Sieve Tower, Type Vibro (Retsch, Haan, Germany) using sieves 500, 355, 90 and 63 PhEur.

4.2 Physico-chemical characterisation

A sufficient investigation of the physico-chemical characterisation of bone substitute materials was necessary to assess their potential as drug carriers. Several parameters influence both, drug loading and release properties. Accordingly, the physico-chemical properties of the materials were characterized by using a number of investigative methods.

4.2.1 Microscopy

Surface structures were assessed by a digital light microscope (Keyence VHX-500K, Keyence Deutschland GmbH, Neu-Isenburg, Germany). Visualisation of particle size and morphology was achieved by scanning electron microscopy (SEM). Scanning electron micrographs at different magnifications were taken using a Carl Zeiss DSM 940 scanning electron microscope (Carl Zeiss AG, Oberkochen, Germany). A piece of bone material was fixed on an aluminium stub with conductive double-sided adhesive tape (Leit-Tabs, Plano GmbH, Wetzlar, Germany) and sputter-coated with gold in an argon atmosphere (50 Pa) at 50 mA for 65 seconds (Sputter coater, Bal-Tec AG, Vaduz, Liechtenstein).

4.2.2 True density

Determination of true density was performed with a helium pycnometer from Pycnomatic ATC (Porotec GmbH, Hofheim/Taunus, Germany). Results are shown in Table 5.1. All measurements were carried out in triplicate.

4.2.3 Specific surface area

The specific surface area of the bioceramic samples was determined with a BET gas adsorption method. Degassing of the samples was completed for one hour under vacuum at 40°C prior to analyzing the samples with a Gemini 2360 BET surface area analyzer (Micromeritics, Norcross, USA) using nitrogen as measuring gas. The BET multipoint method was used to calculate the specific surface area (Table 5.1). All measurements were carried out in triplicate.

4.2.4 Particle size

The volume based particle size distribution of HydroSet[®] powder was measured with a Sympatec HELOS laser diffractometer (Sympatec GmbH, Clausthal Zellerfeld, Germany) in dry powder form after dispersing with compressed air (2 bar). The particle size distribution is characterized by the x_{50} value, giving the percentage undersize. Values presented are the average of at least three determinations.

4.2.5 Dynamic vapour sorption (DVS)

Dynamic vapour sorption experiments were carried out with a DVS 1 (Surface Measurement Systems Ltd., London, UK) using a gravimetric approach to determine the water sorption kinetics of the different bioceramics. Approximately 55 mg of each bone substitute material was weighed onto a Cahn microbalance and dried in a dry nitrogen flow at almost 0.0% relative humidity (RH) until equilibrium; dry mass was used for the calculation of water uptake. The drying step was followed by increasing stepwise the RH in 10% increments until equilibrium moisture uptake was achieved up to a RH of 90%. Then, again the sample was stepwise dried in 10% steps to a RH of 0.0%, followed by a second cycle using the same protocol.

4.2.6 pH value of aqueous bone substitute suspensions

2 g of HydroSet[®] powder, BoneSave[®] 2-4 mm and LagFix[®] cylinder were added to 10 mL water to determine the pH value. This was done after 1, 6 and 24 hours with a pH 540 GLP glass electrode (Weilheim, Germany). After each measurement the pH value was adjusted to the initial pH value of 7.2 with nitric acid. The samples were shaken on a laboratory shaker (150 min⁻¹).

4.3 HPLC analysis of ZOL

The quantification of ZOL was carried out with high pressure liquid chromatography (HPLC) for determination of drug content and release kinetics. The mobile phase was a mixture of methanol (10%, v/v) and 5 mmol sodium hydrogen phosphate buffer (90%, v/v) that contains 6 mmol tetrabutylammonium hydrogen sulphate as ion-pair for ZOL at a pH of 2.6. A flow rate of 0.8 mL/min and a wavelength of 208 nm were utilised for the HPLC (Waters Corp. Milford, MA, USA) analysis. The instrument consisted of an RP-18 column (LiChroChart 125-4, LiChroSpher 100 RP-18, 5 μ m) with a pre-column (LiChroChart 4-4, LiChroSpher 100 RP-18, 5 μ m, both obtained from Merck, Darmstadt, Germany) as stationary phase, a high precision pump (Waters 600E Multisolvent Delivery System), an autosampler (Waters Inline Degasser AF and a Waters 717 plus autosampler), and a Waters UV detector (Waters 996 Photodiode array detector). Data analysis was performed using the Waters Empower 1154 software. A volume of 100 μ L was injected.

In addition, three-dimensional HPLC scans were generated. As shown in Figure 4.1, these plots provide a three-dimensional visualization of the data. The data was plotted on three axes; the x-axis represents time (minutes), the y-axis represents absorbance units (intensity), and the z-axis represents wavelength (nm). This enables the detection of all detectable components in the sample and can, for instance, be used for stability evaluations.

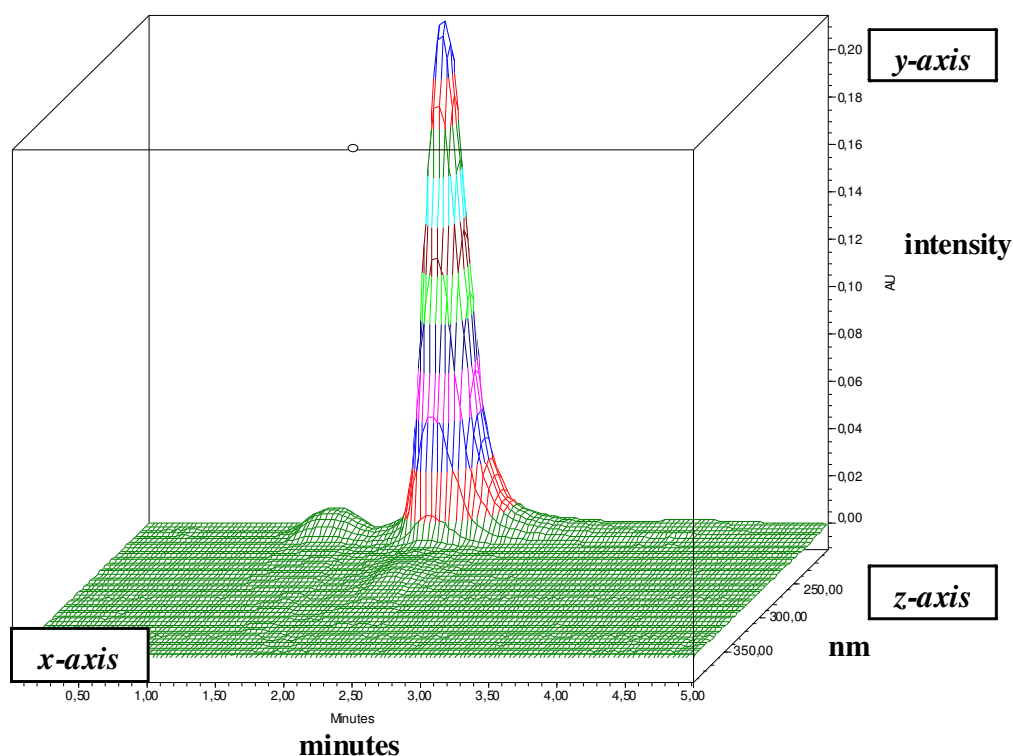


Figure 4.1: Three-dimensional HPLC plot of ZOL dissolved in water.

4.3.1 Limit of detection (LOD)

The LOD is the lowest concentration in a sample that can be detected, but not necessarily quantified, under the stated experimental conditions. The LOD is important for the assays of dosages containing low drug levels, especially for the *in vitro* release kinetics presented. The parameter LOD was determined on the basis of signal to noise ratio (3:1). Additionally, LOD was calculated by the method which is based on the standard deviation (SD) of the response and the slope (SI) of the calibration curve using the following general equation [159]:

$$\text{LOD} = 3.3 \times (\text{SD}/\text{SI}).$$

The LOD was confirmed by analyzing a number of samples near this value. Furthermore three-dimensional scans were used for visual evaluation. Due to a difficult analytic and low ZOL release rates, LOD was used as the lowest level to quantify drug release samples *in vitro*.

4.4 ZOL load and release

4.4.1 Drug loading procedure

Incorporation of ZOL into the different bone substitute materials was carried out by dipping the biomaterials in aqueous ZOL solutions. Drug loading experiments were performed in a time and concentration dependent manner. The biomaterials were dipped for 5, 15 and 30 minutes in 5 mL of variable aqueous ZOL solutions (2.25×10^{-6} , 2.25×10^{-5} , 2.25×10^{-4} , and 2.25×10^{-3} mol/L) on a laboratory shaker (150 min^{-1}).

For drug loading experiments, a LagFix[®] cylinder (740 mg) and for all BoneSave[®] experiments 300 mg of each material were used. The sample weight of HydroSet[®] powder was 200 mg. Furthermore, placebo plugs of the animal study were also used for drug loading experiments. After dipping, the materials were removed from the drug solution. The remaining amount of ZOL in the supernatant at the end of the loading procedure was determined by HPLC. The difference to the initial amount of ZOL present in the solution was assumed as the drug adsorbed onto the biomaterials. All ZOL loading experiments were done in triplicate to confirm reproducibility of the loading procedure.

The samples for analysing the drug release rates were prepared as follows: for HydroSet[®], BoneSave[®] 63-90 μm and BoneSave[®] 355-500 μm powder a special technique for determination of drug release kinetics was developed. 200 mg HydroSet[®], BoneSave[®] 63-90 μm or BoneSave[®] 355-500 μm powder, respectively, was transferred into 5 mL of a 2.25×10^{-4} mol concentrated ZOL solution in a centrifugation tube. After two minutes shaking, the suspension was centrifuged for three minutes. After these five minutes the ZOL loading solution was removed for analysis by HPLC and the powder was dried for two hours at 60°C . LagFix[®] cylinder was loaded by dipping 15 minutes in 5 mL of a 2.25×10^{-4} mol aqueous ZOL solution as described previously. 350 mg

BoneSave[®] 2-4 mm granules were loaded by dipping 22 hours in 5 mL 2.25×10^{-4} molar aqueous ZOL solution.

4.4.2 *In vitro* drug release of ZOL

For the drug release tests, a LagFix[®] cylinder (740 mg) loaded with $77.76 \pm 1.06 \mu\text{g}$ ZOL, 200 mg BoneSave[®] 63-90 μm fraction loaded with $132.64 \pm 2.22 \mu\text{g}$, 200 mg BoneSave[®] 355-500 μm fraction loaded with $44.12 \pm 2.47 \mu\text{g}$, 350 mg BoneSave[®] 2-4 mm granules loaded with $160.28 \pm 2.07 \mu\text{g}$ and 200 mg HydroSet[®] powder loaded with $91.04 \pm 1.82 \mu\text{g}$ were used. Additionally, the described drug loaded placebo plugs and verum implants were used for evaluation of *in vitro* release kinetics.

The *in vitro* drug release studies were performed by incubating the drug loaded bone substitute material in 3 mL of water at room temperature and horizontal shaking. The dissolution medium of drug loaded plugs was reduced to 1 mL. In intervals of 5, 15 and 30 minutes, the dissolution medium was collected for analysis and completely replaced with fresh water. The ZOL content was assayed by HPLC at each time point. For BoneSave[®] 355-500 μm , BoneSave[®] 63-90 μm and HydroSet[®] powders 3 minutes for centrifugation of the suspension was included in each test occasion. All *in vitro* release tests were carried out in triplicate.

4.4.3 Statistical analysis

For statistical comparison of drug load and release experiments, data of each material group and dipping time points were summarized ($n = 9$). After summarizing the valid data points, all relevant descriptive parameters were identified to assess central position and variation of the data. Normality of all continuous variables was assessed with the Shapiro-Wilk Test. Due to the small sample sizes in each group ($n = 9$) the prediction of a normal distribution is imprecise, regardless of the Shapiro-Wilk Test outcome. Therefore, the unpaired Mann-Whitney Test was selected for comparison. Also Monte Carlo Simulation was used to raise precision of test outcome. The level of significance for all tests was set to 95% ($p < 0.05$ was significant). All calculations were performed with the software PASW Statistics Version 18.0.2 (SPSS).

4.5 Stability

Drug stability is an essential assessment to determine the quality and efficacy of different ZOL formulations. In order to ensure adequate drug stability, a stability test of ZOL under different storage conditions was performed. For the dipping technique used, ZOL was dissolved in water. Therefore, it was necessary to gain information about drug stability in an aqueous solution over a defined period of time when stored in different materials. The temperature dependent stability of ZOL stored in glass or plastic was tested. Furthermore, the stability of different ZOL lyophilisates was evaluated. The concentration of ZOL at various conditions was monitored over time by HPLC.

4.5.1 Lyophilisation of ZOL

The ZOL solutions were produced by first dissolving different amounts of mannitol (Roquette Frères, Lestrem, France), trehalose-dihydrate (Fluka AG, Buchs, Switzerland) or sucrose (Merck KGaA, Darmstadt, Germany) followed by ZOL in double distilled water under constant stirring. The solutions prepared, resulted in a ZOL concentration of 100 µg/mL and a carrier amount of 5 to 20 mg/mL. Freeze-drying of the solutions was carried out using an Alpha 1-4 laboratory-scale freeze-dryer (Christ GmbH, Osterode, Germany). 1.0 mL-aliquots of the solutions were filled into 2R-Vials, partially stoppered and cooled to below minus 27°C. Then, primary drying was started for 24 hours. Afterwards, secondary drying at elevated temperatures took place for another 24 hours to remove the unfrozen water. After completion of the lyophilization cycle, samples were stoppered under nitrogen atmosphere and then removed from the freeze-dryer.

4.5.2 ZOL stability tests

The first test series was performed to evaluate the temperature influence to ZOL stability when stored in glass over a time period of 180 days. A 2.25×10^{-4} mol/L ZOL solution was prepared and samples of 1 mL were stored in HPLC glass vials (Waters, Milford, USA), protected from light, for defined time points, under four different temperature conditions (2-8°C, 25°C, 40°C and 60°C) in a drying chamber (Heraeus, Hanau, Germany). The 2.25×10^{-4} mol/L ZOL stock solution was measured directly after preparation and served as reference.

For a second test series, a 2.25×10^{-4} mol/L ZOL solution was stored in glass or plastic vials for a time period of 55 days. 1 mL of ZOL solution was added to HPLC glass vials and HPLC plastic vials (Waters, Milford, USA). The samples were stored under two different temperature conditions (2-8°C and 25°C). 1 mL water was added to the freeze-dried sample for stability testing of different lyophilisate formulations. The lyophilisates were stored in glass vials at room temperature. At defined time points, all samples were measured by the described HPLC method for determination of the ZOL concentration. Additionally, three-dimensional plots were calculated for visualisation of sample changes. Triplicate HPLC determinations were performed at each time point. Furthermore, visual examination of the samples was performed in normal laboratory light. The samples were examined for precipitation, colour and clarity.

4.6 Cytotoxicity test

An *in vitro* cytotoxicity test was performed to evaluate the toxicity of ZOL. Such *in vitro* studies are helpful to screen the toxicity of new and established excipients used in special formulations prior to preclinical assessment in an animal study [160]. Cell cultures can be used as *in vitro* model for toxicity test in a living system [161].

4.6.1 Cell line

In the present study, a Calu-3 cell line was used for toxicity tests of ZOL according to the method described by Scherließ [161]. The Calu-3 (HTB-55) cells were obtained from the American Type Culture Collection (ATCC, Manassas, VA, USA). Passage numbers 42–50 have been used for all toxicity tests. The cells are an adherent cell line derived from a bronchial adenocarcinoma (25 years old male Caucasian). The cells form a monolayer culture and can be cultivated in flasks, 96-well-plates and on membrane inserts [161]. Briefly, the cells were cultivated in minimal essential medium (MEM) with Earle's salts supplemented with 10% fetal bovine serum, 1% Penicillin-Streptomycin, 1% non-essential amino acids and 1% sodium pyruvate (all from Biochrom AG, Berlin, Germany) in plastic culture flasks at 37°C in an atmosphere of air humidified supplemented with 5% CO₂. For the test, the cells were seeded in 96 well plates to allow numerous and simultaneous sample determinations.

4.6.2 Sample preparation

The *in vitro* toxicity of ZOL was tested under three different aqueous conditions. Within the first test series, 1.59 mg ZOL was dissolved in 1.5 mL water. For preparation of eight further samples the stock solution (1060 µg/mL) was diluted with water resulting in 530, 265, 132.5, 66.25, 33.13, 16.56, 8.28, and 4.14 µg/mL. For the second test, 9.93 mg ZOL was dissolved in 10 mL water. For preparation of eight further samples the stock solution (993 µg/mL) was diluted with water resulting in 496.5, 248.25, 124.13, 62.06, 31.03, 15.52, 7.76, and 3.88 µg/mL. After sample preparation, the osmolarity was adjusted with sodium chloride to a value between 290–310 mosmol. The osmolarity was determined with an Osmomat 030-D (Gonotec GmbH, Berlin, Germany). The pH values were not adjusted. In the third test series, 9.36 mg ZOL was dissolved in 10 mL buffer (defined mixture of water, sodium phosphate and citric acid) to assure a pH of 6.8 (pH 540 GLP (Weilheim, Germany)). For preparation of eight further samples the stock solution (936 µg/mL) was diluted with buffer resulting in 468, 234, 117, 58.5, 29.25, 14.63, 7.31, and 3.66 µg/mL. Afterwards, the iso-osmolarity (290-298 mosmol) was adjusted with sodium chloride. For evaluating the toxicity of HydroSet[®] verum and placebo plugs, defined samples from *in vitro* release tests were determined. For this, two plugs of each implant type were incubated in 3 mL water at room temperature under horizontal shaking (150 min⁻¹). After a time interval of three hours and five days the osmolarity of the dissolution medium was adjusted to 290–300 mosmol and used for *in vitro* cytotoxicity tests.

4.6.3 MTT assay

The toxicity of ZOL was evaluated using an MTT assay described by Scherließ [161]. The test is based on the inhibition of mitochondrial succinate dehydrogenase, involving the reduction of yellow MTT under tetrazolium ring cleavage to a water-insoluble purple-blue formazan product. First, the medium was removed from the cells, 200 μ L of the prepared samples were pipetted to each well (quadruple determination) and were incubated at 37°C for four hours. Afterwards, the samples were removed and 25 μ L MTT solution (5 mg/mL in HBSS+HEPES) were added to each well and incubated for two hours. Subsequently, all cells were lysed with 100 μ L lysis solution (5% SDS in DMF:water 50:50, pH 4.7) per well. A solution of 5 mM SDS (sodium dodecyl sulphate) in HBSS+HEPES was used as positive control (0% viability). Negative control (100% viability) was HBSS+HEPES. Detection and quantification of the formazan was performed by a multiwell plate reader (Thermo Spectra III Reader with software easyWINfitting, V6.0a, Tecan, Austria) at 570 nm (reference wavelength 690 nm).

4.6.4 Data analysis

For data analysis the optical density was measured accounting for the number of living cells. The relative cellular viability was calculated from the adsorbance values as a percent of the negative control. All adsorptions were converted to viability results individually. The mean value of four determinations was then taken for further calculations and analysis.

4.7 Characterisation of modified HydroSet[®] cement formulations

For the animal study, a ZOL-loaded implant based on the HydroSet[®] cement had to be developed. A characterisation of modified HydroSet[®] cement formulations was required to evaluate the most practical loading procedure for ZOL-loaded implants without influencing the cement hardness. In this section, the additional amount of water for complete wetting of HydroSet[®] powder was evaluated to ensure homogenous drug distribution. Furthermore, the influence of different drug loading procedures on the cement hardness had to be determined. Finally, the solubility of ZOL in the HydroSet[®] hardening solution was tested to evaluate the feasibility of directly solving ZOL in the hardening solution.

4.7.1 Semi-quantitative wetting of HydroSet[®] powder

To achieve homogenous drug distribution the powder has to be fully surrounded by water. A wetting study was performed to find out how much additional water is required to completely wet HydroSet[®] powder. Therefore, 2 cm³ HydroSet[®] powder was placed in the standard mixing container at room temperature. The initial conditions were used as dry mass for the calculation of water uptake. 5% additional water was stepwise added to the powder with a micropipette. The suspension was homogeneously mixed after each addition of water. The wetting status was macroscopically evaluated and calculated by the needed percentage amount of water for a fully surrounded distribution of water. These measurements were done in triplicate.

4.7.2 Characterisation of cement hardness

Hardness measurements of different cement formulations were conducted by using a Zwicki Z2.5/TN1S testing machine (Zwick GmbH & Co. KG, Ulm, Germany). A special experimental setup for sample placement and nail penetration into the formulations was developed (Figure 4.2). The different samples were placed in the sample holder (\varnothing 1.7 cm). The formulation penetration resistance was measured by moving the nail indenter into contact with the bone cement formulation placed in a sample holder. The measurement began with a contact force of 0.04 N with a test speed of 0.2 mm/s and ended at a penetration of 2.5 mm into the formulation. During compression the force-penetration profiles could be followed on a computer screen and were recorded by testXpert[®] software (version 10.0, Zwick GmbH & Co. KG, Ulm, Germany). The tests were performed at room temperature (21°C). Each formulation was measured at a time interval of 3, 6, 9, 12, 15, and 18 minutes. All time points of each formulation were determined in the same sample holder. Therefore, the sample holder had to turn 60° prior each measurement. For cement hardness tests four different formulations were used and prepared as follows:

Each formulation was mixed in the regular HydroSet[®] mixing container and quantitatively transferred to the sample holder. The first sample was a mixture of 1.5 cm³ HydroSet[®] powder and 1.5 mL hardening solution. The second sample were prepared by mixing 1.5 cm³ HydroSet[®] powder, 1.5 mL hardening solution and 50 μ L ZOL solution (3.18 mg/mL). The third formulation contained 1.5 cm³ HydroSet[®] powder, 1.5 mL hardening solution and 475 μ L water. For the fourth sample, 1.5 cm³ HydroSet[®] powder was dipped in 5 mL water for 5 minutes. The powder was dried for 24 hours at 55°C and then mixed with 1.5 mL hardening solution.

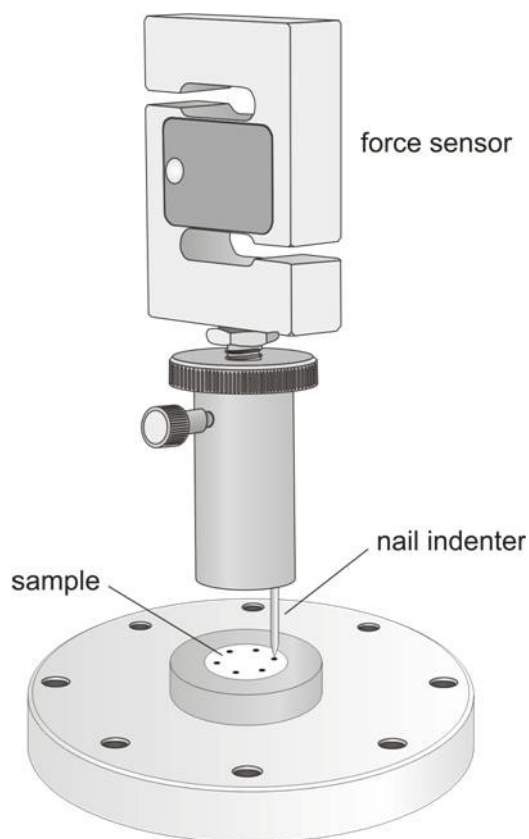


Figure 4.2: Experimental setup for the determination of cement hardness.

4.7.3 Solubility of ZOL in HydroSet[®] hardening solution

A semi-quantitative solubility of ZOL was determined in normal HydroSet[®] hardening solution at room temperature. Defined amounts of ZOL were given to 500 μL hardening solution. The solubility was macroscopically determined after 30 minutes equilibration on a laboratory shaker (150 min^{-1}). The results are shown in Table 5.2.

4.8 *In vivo* animal study

A proximal tibia bone defect rat model was used for testing the short-term *in vivo* efficacy of a ZOL loaded bone cement plug.

Male Sprague-Dawley rats were bred at the local animal care facility (EBM, Gothenburg University, Sweden) and housed in accordance with guidelines of the Animal Committee of the University of Gothenburg. The animal experiments were approved by the University of Gothenburg Local Ethical Committee for Laboratory Animals (Dnr 301/09). Surgeries, keeping and accommodation of the rats were carried out at EBM facility in Gothenburg (Sweden). A pilot study with three rats was performed, intended to verify surgical and post-operative procedures. Gene expression analysis was conducted at TATAA Biocenter AB (Gothenburg, Sweden). Histological preparation and analysis were performed at the Institute of Biomaterials and Cell Therapy (IBCT, Gothenburg, Sweden) [162]. An additional qualitative and semi-quantitative analysis of histological slides was performed by Biomatech (Chasse sur Rhône, France) [163]. The animal study was supported and funded by Stryker Trauma GmbH (Schönkirchen, Germany).

4.8.1 Implants

Moulded bone cement plugs were used for implantation (cylindrical head: \varnothing 3.5 mm, 1.3 mm depth; cylindric body: \varnothing 2.4 mm, 3.0 mm depth; volume: 14.5 mm^3 (head) + 14.7 mm^3 (body) = 29.2 mm^3). At the bottom the plugs were rounded (Figure 4.3 a).

The basic bone substitute material for the moulded plugs was HydroSet[®]. Moulding of HydroSet[®] plugs that were both loaded with and without ZOL was performed under aseptic conditions. The procedures were carried out under laminar airflow in a ventilated and disinfected box. Equipment to be used during manufacturing was either disinfected with isopropanol 70% or by heat sterilisation or autoclaving, depending on what was appropriate for the respective material. ZOL was used in a concentration intended to result in a drug load of 50 μg per implant (verum). HydroSet[®] plugs without ZOL served as controls (placebo). For the preparation of the ZOL solution, the drug was added directly to the sterile HydroSet[®] hardening solution, followed by sterile filtration (0.2 μm). The sterile hardening solution was added to HydroSet[®] powder (powder was propounded in the normal mixing container of HydroSet[®]). After mixing both compounds with the HydroSet[®] spatula for 30–45 seconds the mixture was loaded into a sterile two-piece-moulding system (Figure 4.3 b). For a homogeneous distribution of the still free-flowing cement mixture the cement was mixed with the help of a stainless steel nail. After the hardening process the drug loaded and non-loaded HydroSet[®] plugs were removed from the moulds, transferred into PE bags (Stericlin[®]) which were heat-sealed to allow transport without the risk of contamination (Figure 4.3 c) and labeled according to good preclinical practice requirements.

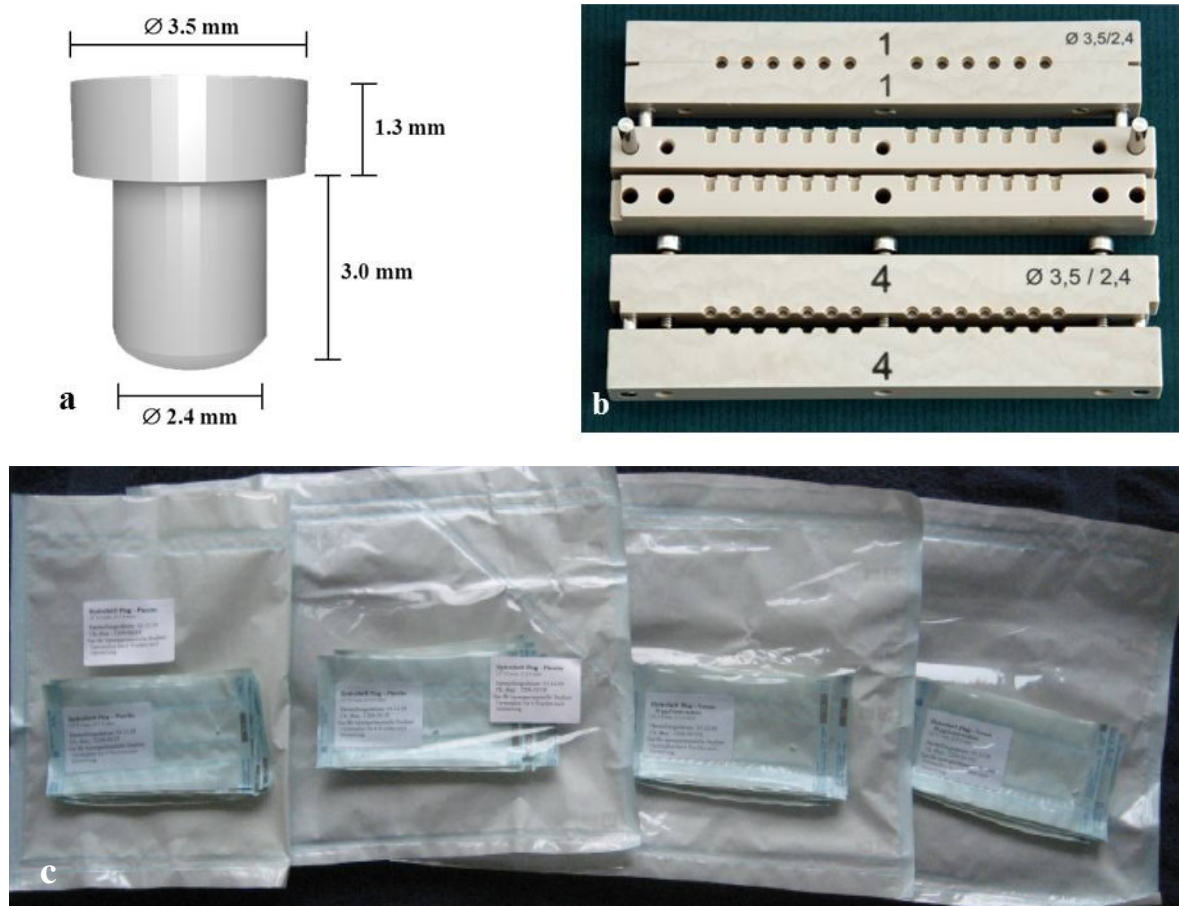


Figure 4.3: Geometric shape of the HydroSet[®] plug (a), the corresponding two-piece moulding systems for manufacturing (b) and packaging of sterile implants (c).

4.8.2 Crushing strength of the HydroSet[®] bone cement plugs

The crushing strength of the HydroSet[®] bone cement plugs was investigated using a Pharmatest PTB 300 (Pharmatest GmbH, Germany). Determination of crushing strength of verum and placebo plugs was performed in triplicate one week after plug manufacture. Wetted verum and placebo plugs were tested in addition. Accordingly, the plugs were stored in 1 mL water for one minute and tested immediately after removal. The test principle is shown in Figure 4.4.

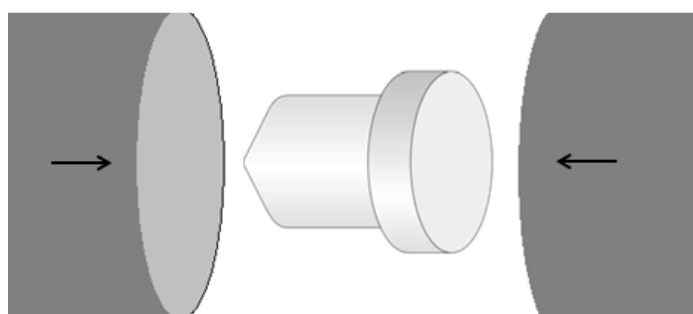


Figure 4.4: Principle of crushing strength test for HydroSet[®] bone cement plug.

4.8.3 Sterility of HydroSet[®] bone cement plugs

A product intended for use in an *in vivo* study has to pass the PhEur sterility test. The test was performed by membrane filtration using a Steritest II pump and a presterilised disposable system consisting of two filtration vessels with membranes, connecting tubes and needle by Millipore (Billerica, MA USA). The system was attached to the pump, required to filter the samples and to transfer the test media onto the membranes. The procedure took place under aseptic conditions in a laminar air flow cabin (class 2) surrounded by a cleanroom, standard B (determined at rest). A schematic drawing of sterility test principle is shown in Figure 4.5. Implant samples (4-6 plugs per test, according to batch size) were rinsed in a sterile bottle with 50 mL sterile sodium chloride peptone broth buffered, containing 0.01% polysorbate 80, by shaking for

5 minutes. A portion of about 10 mL of sterile saline was transferred to the membranes and was filtrated. Subsequently, the whole volume of the test fluid used for rinsing the samples was transferred to the membranes followed by filtration. Thereafter, the membranes were rinsed again using 100 mL of sterile saline. The vessels were closed at the bottom and filled with the thioglycollate (thio bouillon) test media and fluid soybean casein digest medium (CASO bouillon) (Figure 4.5). The incoming tubes were cut through and closed by sterile clamps. The containers with the test media were incubated for 14 days, thioglycollate medium at 34°C and soybean casein digest at 22.5°C. During incubation, the test media were visually controlled daily for any sign of turbidity development representing microbial growth. A sample of each batch produced for the animal study was tested for sterility as described above (test frequency).

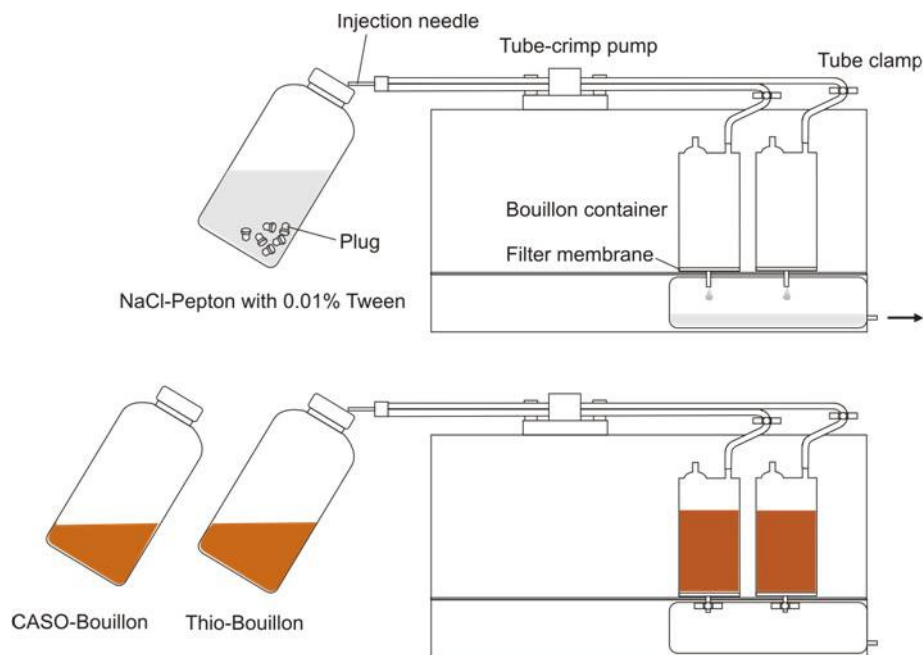


Figure 4.5: Schematic drawing of sterility test principle.

4.8.4 Surgical procedure

Thirty-six male Sprague-Dawley rats (380-390 g, 10-11 weeks old) were divided into four experimental groups. A total of eight rats for each time point (one and three weeks) were designated for the PCR analysis ($n = 8$) and ten rats were designated for histological analysis. Each animal was intended to receive one test (verum) and one control (placebo) implant.

Animals were fed on a standard pellet diet, received water *ad libitum* and were housed under standard conditions. For surgery, rats underwent anesthesia using a Univentor 400 anesthesia unit (Univentor, Zejtun, Malta) under isoflurane (Isoba[®] Vet, Schering-Plough, Uxbridge, England) inhalation (4% with an air flow of 650 mL/min). Anesthesia was maintained by continuous administration of isoflurane (2.7% with an air flow of 450 mL/min) using a mask. Preoperatively, analgesic treatment (Temgesic 0.03 mg/kg, Reckitt & Coleman, Hull, Great Britain) was administered subcutaneously. After shaving and cleaning (5 mg/mL chlorhexidine in 70% ethanol), the medial aspect of the proximal tibial metaphysis was exposed through a 5–6 mm longitudinal skin incision, followed by skin and periosteum reflection with blunt instrument dorsally to the physis. The cortex was opened using a \varnothing 2.1 mm dental drill, followed by performing a \varnothing 2.5 mm and 3.0 mm deep drill defect, 3–6 mm from the proximal physis (Figure 4.6 a-c). After rinsing with saline solution, in a bilateral approach, one test or control implant was inserted in each tibia (Figure 4.6 d). Implantation was blinded and randomized for placebo and verum implants.

Subcutaneously, the wound was closed with resorbable polyglactin sutures (5-0, Vicryl, Ethicon, Johnson & Johnson, Brussels, Belgium) and, finally, the skin using Monocryl 4-0 (Ethicon) which is shown in Figure 4.6 e-f. Animals were monitored until complete recovery and afterwards returned to their cages. The animals recovered within a few minutes of surgery due to the controlled

anaesthetic dose. Each rat received analgesic treatment postoperatively (Temgesic 0.03 mg/kg, Reckitt & Coleman, Hull, Great Britain) twice a day for a period of 48 hours.

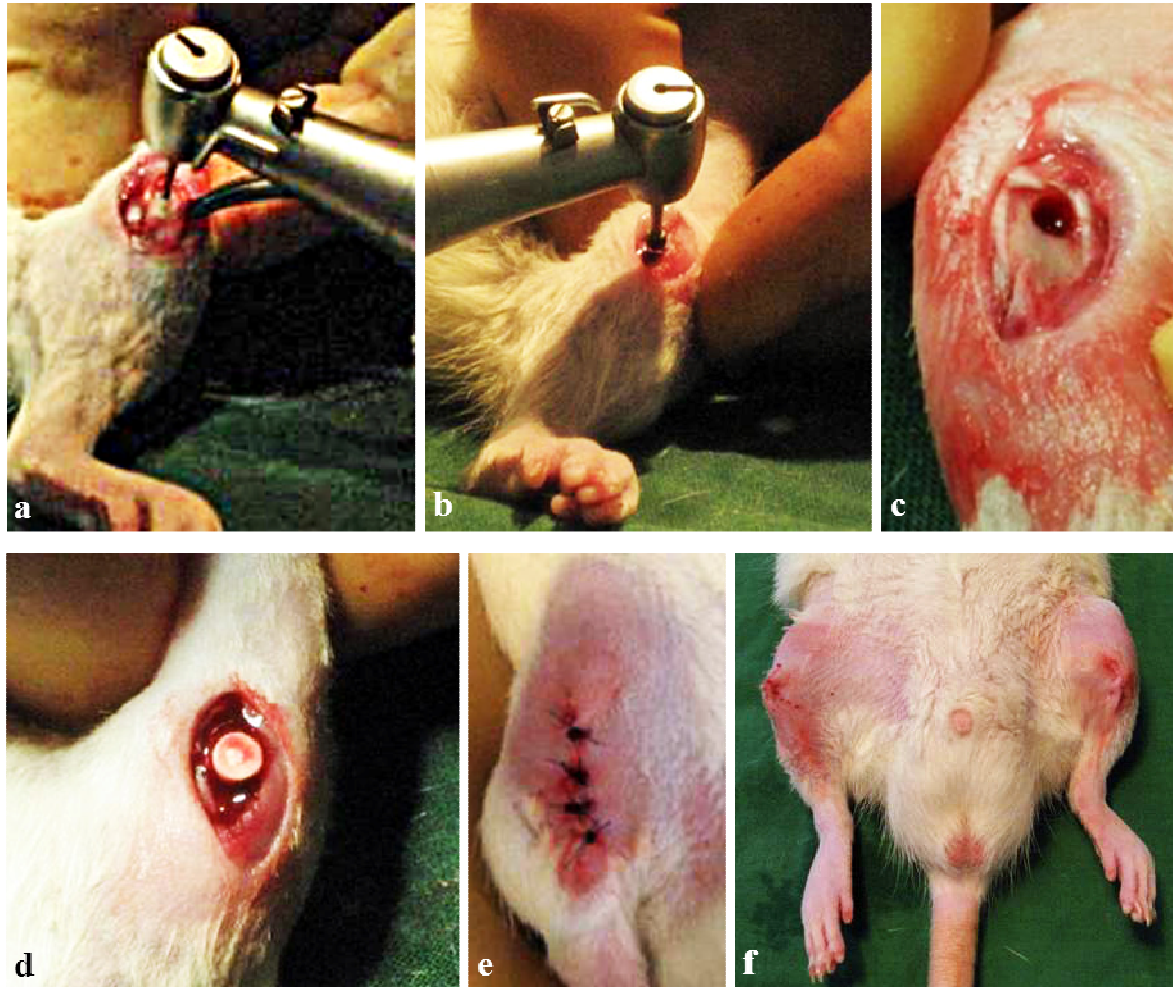


Figure 4.6: Drilling procedure: 2.1 mm \varnothing dental drill (cortex opening) (a), 2.5 mm \varnothing dental drill (b), bone defect (c), final implant position (d), wound closure (e) and after surgery (f).

4.8.5 Implant retrieval and processing

The retrieval procedure was performed after one and three weeks. The rats were euthanized by intraperitoneal application of sodium pentobarbital (60 mg/mL; ATL Apoteket Production & Laboratories, Kungens Kurva, Sweden).

For qPCR analysis, a trephine with an internal diameter of 3.6 mm was chosen to harvest the implant-tissue blocks. (Figure 4.7 a and c). This diameter allowed cutting around the outer diameter of the implant. The biopsy was immediately immersed in RNA Later solution (Quiagen GmbH, Hilden, Germany) and stored at 4°C until analysis. The sample was then homogenized, followed by RNA extraction and purification. Prior to qPCR analysis with the designed primers, the RNA was reverse transcribed to cDNA [164].

The implant-tissue blocks for histology and histomorphometry were harvested en bloc by transverse sawing, and immediately transferred into formalin (Figure 4.7 b). After dehydration in a graded series of ethanol, resin infiltration and embedding, ground-sections were prepared by sawing and grinding until a final thickness of 15-20 µm was obtained [165]. The ground-sections were stained by toluidine blue followed by light microscopical evaluation (Nikon Eclipse E600, Japan). The measurements were performed using an image software analysis (Easy Image Measurement 2000, Tekno Optik AB, Sweden) with x10 eyepiece at 10x magnification while magnification up to 40x was used for visualization during measurements.

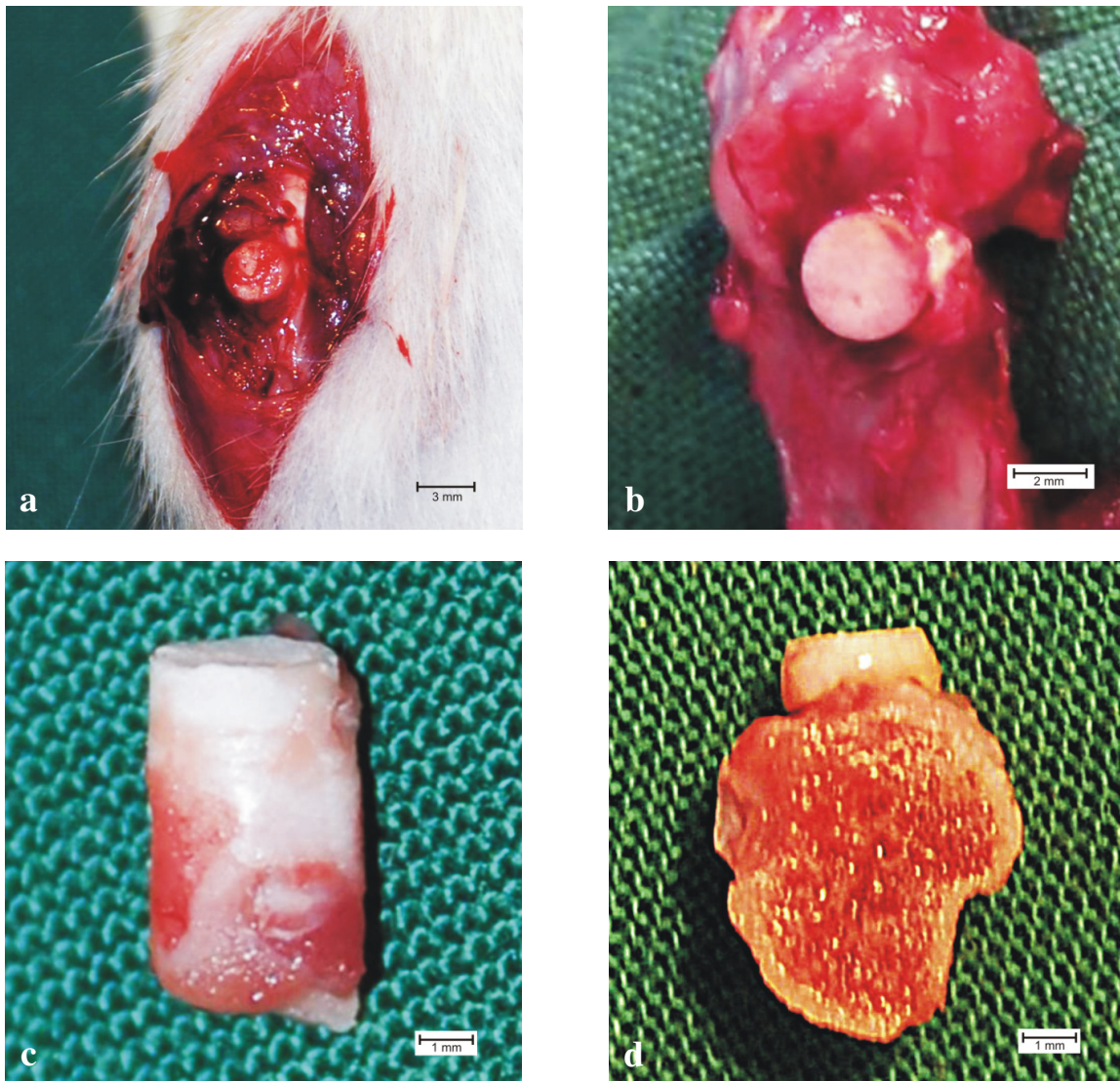


Figure 4.7: Plug before dissection (a), medial aspect of the tibia before trephine drilling (b), trephine drilled sample for qPCR (c) and sample for histology (d).

4.8.6 Quantitative PCR

Quantitative PCR was performed to determine the level of gene expression in cells, harvested out of the peri-implant tissue. The gene panel was composed of reference genes (18S RNA and glyceraldehyde-3-phosphate dehydrogenase (GAPDH)), genes for bone formation (OC and ALP), bone resorption (TRAP and CATK) and inflammatory markers (TNF- α and IL1- β). Statistics were performed for both, normalized data and non-normalized data. The quantities of target genes were normalized using the expression of 18S RNA. The normalized relative quantities were calculated using the delta Ct method and 90% PCR efficiency ($k \cdot 1.9^{\Delta Ct}$) [166].

4.8.7 Histology

The histological sections were prepared for qualitative evaluation and observed under light microscopy (Nikon Eclipse E80i, Japan) equipped with x2, x4, x10, x20 and x40 objectives.

Additional qualitative and semi-quantitative analyses of the local effects were performed according to the evaluation scheme, mentioned in the attachment E of the ISO 10993-6 standard. The parameters evaluated included cellular events during the inflammatory reaction (polymorphonuclear cells, lymphocytes, plasma cells, macrophages, giant cells/ osteoclastic cells), signs of necrosis, fibroplasia, fibrosis, fatty infiltrate, osteolysis, cell or tissue degeneration, as well as amount of fibrin, level of encapsulation and material degradation. Bone regeneration performance was qualitatively and semi-quantitatively assessed by analyzing signs of osteointegration, woven bone, osteoblastic cells, osteoconduction, bone density, neovessels, bone marrow signs, and bone remodelling. All parameters were assessed using a score with a 0-4 grading scale (0: absent, 1: slight, 2: moderate, 3: marked, 4: severe) as defined in Table 10.6 and Table 10.7. The cell type response and performance parameters

are selected based on ISO 10993-6 and previously published systems [167, 168].

4.8.8 Histomorphometry

Blinded histomorphometric analysis was conducted by ground-section technology using light optical microscopy. The parameters being assessed were bone-implant contact (BIC) along the implant surface perimeter and bone area (BA) adjacent to the implant surface as well as at a distance from the surface.

As shown in Figure 4.8, the bone-implant contact (BIC) and bone area (BA) were divided into different areas (800 μm) and zones (800x250 μm) along the implant, representing the cortical level, endosteal level and the marrow compartment. For bone-implant contact (BIC), the relation of the perimeter of direct bone to plug contact (length of bone contacting the implant surface) and the entire perimeter of the implant (total length of the implant surface) was taken into account. For bone area (BA), the area occupied by bone was determined according to the areas close to the implant (0-250 μm) and at a distance (250-500 μm) (Figure 4.8). The statistical analysis was performed for total bone-implant contact (mean value for A, B, area 1, 2 and 3 for both proximal and distal side and D) and mean bone areas (mean values of area 1, 2 and 3 for both proximal and distal side).

One implant of each type from a single rat of the one week group was used for performing x-ray analysis (data not included) and thus was not considered in the quantitative evaluation. Finally, the sample size was $n = 9$ for the one week group and $n = 10$ for the three week group.

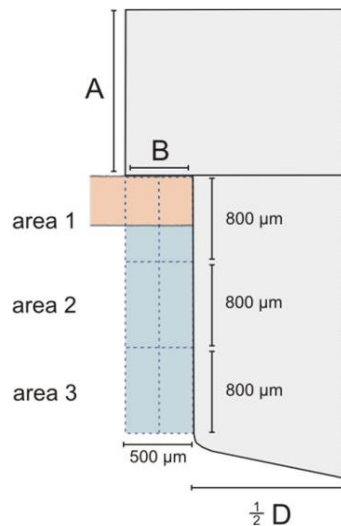


Figure 4.8: Schematic drawing of histomorphometric evaluation areas.

4.8.9 Statistical analysis

After summarizing valid data points, all relevant descriptive parameters were identified to assess central position and variation of the data. Normality of all continuous variables was assessed with the Shapiro-Wilk Test [169]. Due to the small sample sizes in each group ($n = 8-10$) the prediction of a normal distribution is imprecise, regardless of the Shapiro-Wilk Test outcome. Therefore, the paired non-parametric Wilcoxon Rank Test and the unpaired Mann-Whitney Test were selected for comparison [170, 171]. Also Monte Carlo Simulation was used to raise precision of test outcome [172]. The level of significance for all tests was set to 95% ($p < 0.05$ was significant). All calculations were performed with the software PASW Statistics Version 18.0.2 (SPSS). For comparison and to avoid biological variations, qPCR data were normalized. Normalization of the values to 18S was performed for each target gene sample. Therefore, the relative quantity value was divided by the value derived from 18S control sequence in the corresponding target gene.

For graphical visualization and comparison box- and whisker plots were chosen for all variables (placebo and verum) and time points (one or three weeks). The box corresponds to the range in which the middle half (50%) of the data are

included (Figure 4.9). The median is shown as a line in the box. Furthermore, the lower quartile (25%) marks the onset of the box and the upper quartile (75%) the end of the box. The whiskers mark the minimum (0%) and the maximum data value (100%) of the data that are not outliers. Values deviating more than 1.5 times the interquartile distance from the median were considered as outliers and marked as circles. Values shown in the graphs of $p < 0.05$ were considered significant and values of $p < 0.01$ highly significant. Statistically significant differences between the implant types (placebo and verum) and time points (one and three weeks) are labeled in the diagram by a line and the corresponding p-value.

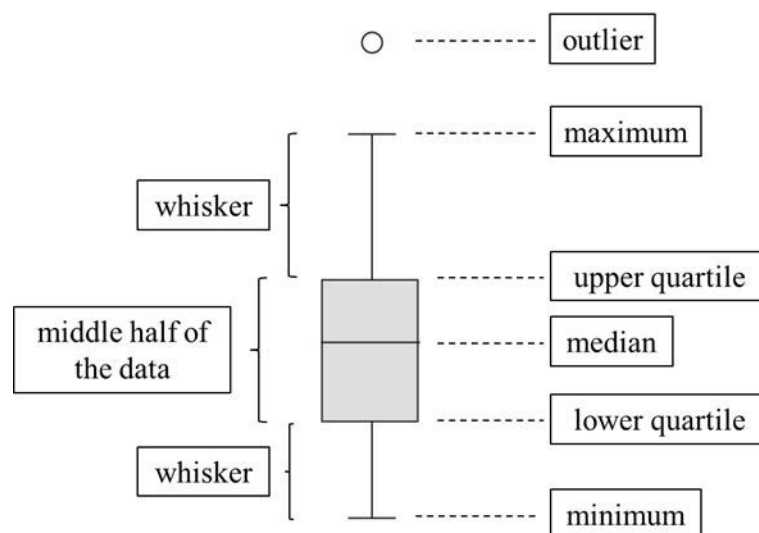


Figure 4.9: Information from a box- and whisker plot.

5 Results

5.1 Physico-chemical characterisation

5.1.1 Light microscopy/ SEM

The visualisation of microstructures by light microscopy and SEM gave qualitative information about the three different bioceramic structures. The LagFix[®] cylinder, BoneSave[®] material and HydroSet[®] powder varied in porosity, pore structure, pore- and crystal size and pore size distribution which are mainly caused by the different manufacturing processes (Figure 5.1 and Figure 5.2). As shown in Figure 5.1, all the ceramics have non-interconnecting pores whilst the individual materials differ substantially with respect to the type of pores. LagFix[®] cylinder showed a few macro- and micropores without any interconnectivity. Only BoneSave[®] granules in both sizes of 2-4 mm and 4-6 mm demonstrated a pore size range from 10 μm (Figure 5.2 b) to 300 μm (Figure 5.1 c). The pictures show macro- and microporosity of BoneSave[®] granules. For the smaller-sized BoneSave[®] fractions (Figure 5.1 d-f), the macroporosity is partly destroyed by the grinding process. The surface structures and microporosity of big and small sized BoneSave[®] granules are very similar (Figure 5.1 c-f). HydroSet[®] powder does not show pores and structure at all due to the small particle size. The SEM pictures illustrate the construction principle of the different materials and demonstrated how closely and homogeneously fused the hydroxyapatite crystals are (Figure 5.2 a-c).

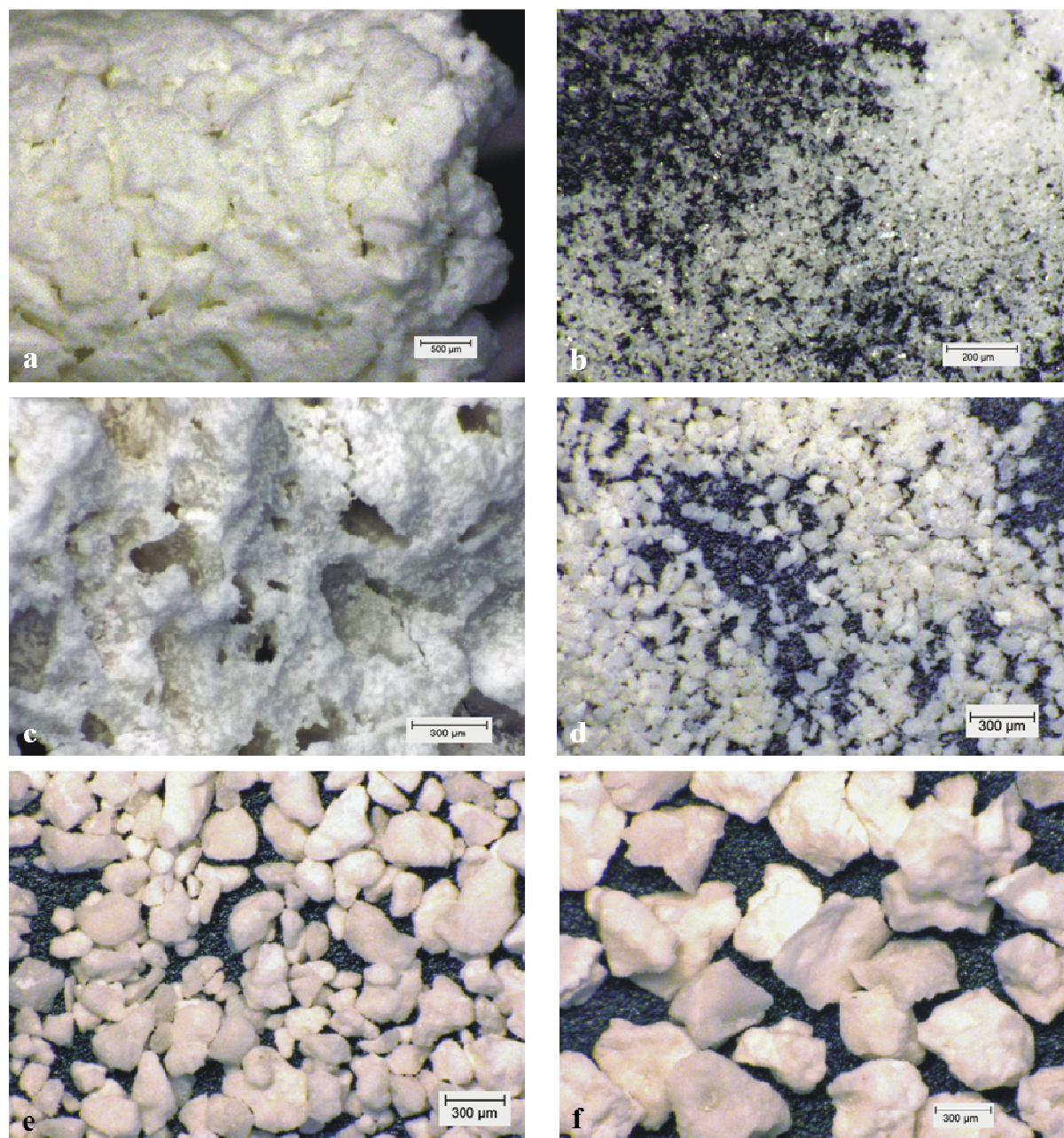


Figure 5.1: Light microscopy of LagFix[®] cylinder (a), HydroSet[®] powder (b) and different sizes of granules: BoneSave[®] 2-4 mm (c), BoneSave[®] 63-90 μm (d), BoneSave[®] 90-355 μm (e) and BoneSave[®] 355-500 μm (f).

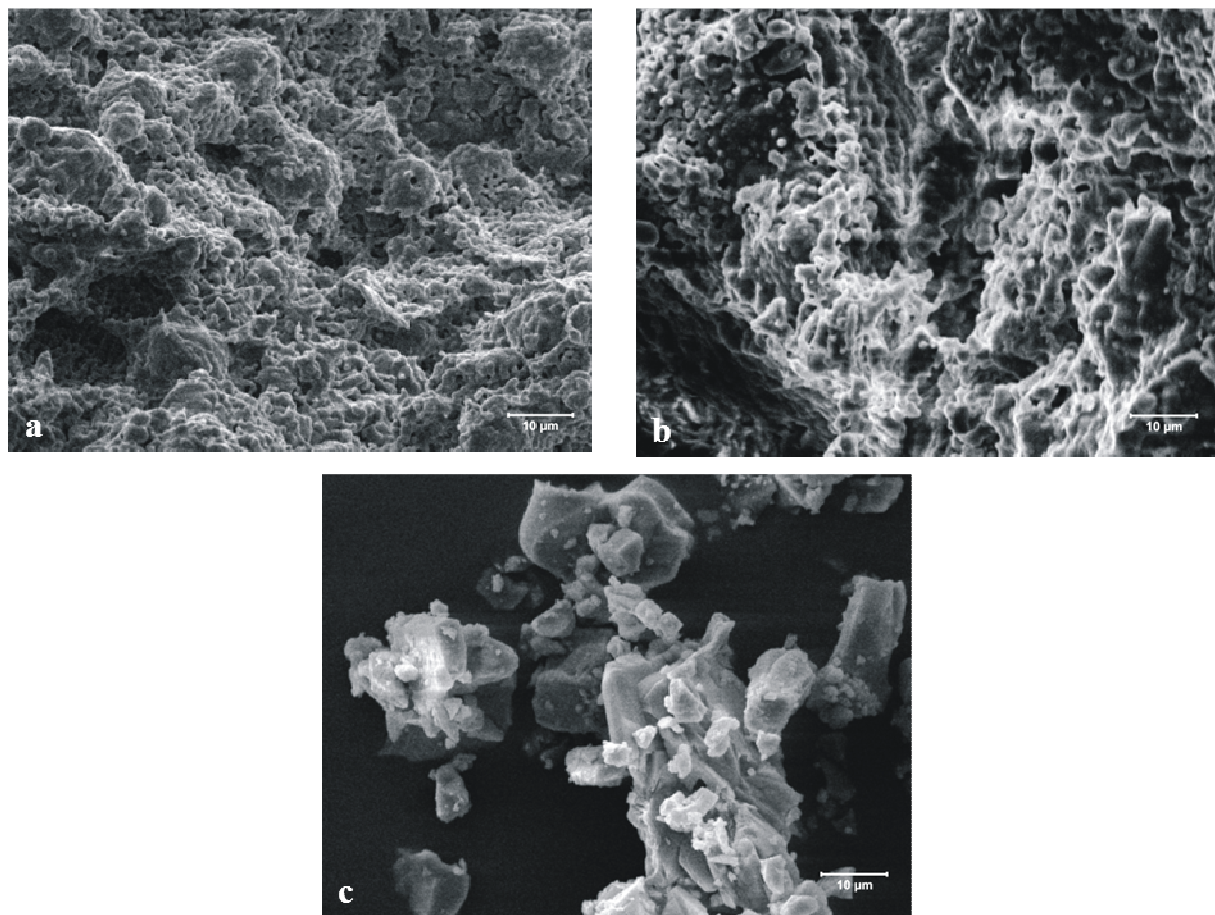


Figure 5.2: Scanning electron microscopy (SEM) of LagFix[®] cylinder (a), BoneSave[®] granules (b) and HydroSet[®] powder (c).

5.1.2 True density and specific surface area

Another important parameter for the characterisation was the determination of the true density and the specific surface area (Table 5.1). The true density of the three different bioceramics resulted in a range of 2.65 to 3.24 g/cm³. LagFix[®] cylinder had a low surface area of less 0.1 m²/g. BoneSave[®] granules demonstrated a particle size dependent specific surface area. A low carrier particle size (63-90 µm) resulted in the highest specific surface area of 0.74 m²/g which decreases exponentially to 0.14 m²/g for BoneSave[®] 4-6 mm (Table 5.1). HydroSet[®] powder had a surface area of 0.45 m²/g. The light microscopic and SEM photographs (Figure 5.1 and Figure 5.2) confirmed that the small specific surface area of the bioceramics used compared to natural bone mineral is caused by sintering and the disappearance of micro- and macropores.

Table 5.1: True density and specific surface area of different bone substitute materials (n = 3; errors = standard deviation).

Bone substitute	True density (g/cm³)	Specific surface area (m²/g)
LagFix [®] cylinder	3.24 ± 0.02	< 0.1
BoneSave [®] 63-90 µm	3.11 ± 0.02	0.74 ± 0.07
BoneSave [®] 90-355 µm		0.58 ± 0.01
BoneSave [®] 355-500 µm		0.44 ± 0.01
BoneSave [®] 2000-4000 µm		0.27 ± 0.01
BoneSave [®] 4000-6000 µm		0.14 ± 0.03
HydroSet [®] powder (x ₅₀ = 21.0 ± 0.4 µm)	2.65 ± 0.01	0.45 ± 0.01

5.1.3 Particle size

As shown in Figure 5.3, the particle size distribution of HydroSet[®] powder measured in compressed air exhibited an x_{50} of $21 \pm 0.4 \mu\text{m}$.

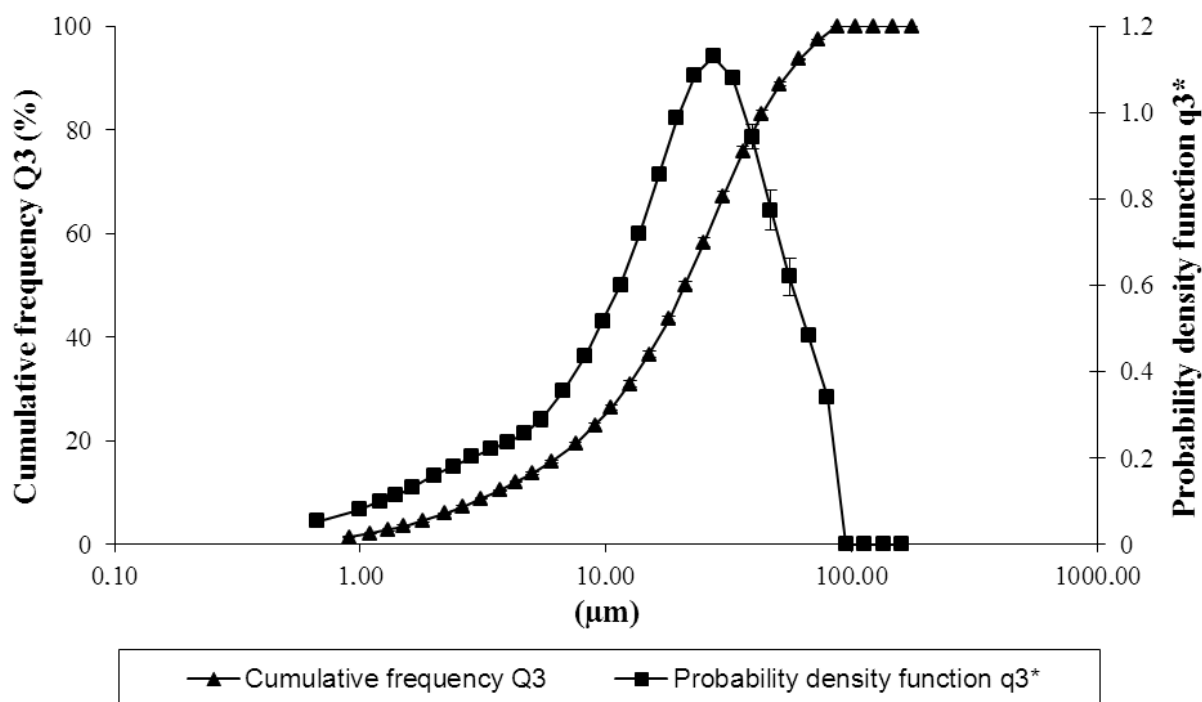


Figure 5.3: Particle size distribution of HydroSet[®] powder.

5.1.4 Dynamic vapour sorption (DVS)

Water sorption kinetics was investigated by using DVS and gave information about the potential of a drug adsorption by dipping in an aqueous drug solution. LagFix[®] cylinder and BoneSave[®] granules had a low water uptake of less than 0.03% during the whole humidity program (Figure 5.4 a and b). HydroSet[®] powder showed a water uptake up to 3% during the program. An increase in water uptake at 90% relative humidity was measured. The powder also showed higher water desorption than adsorption (Figure 5.4 c).

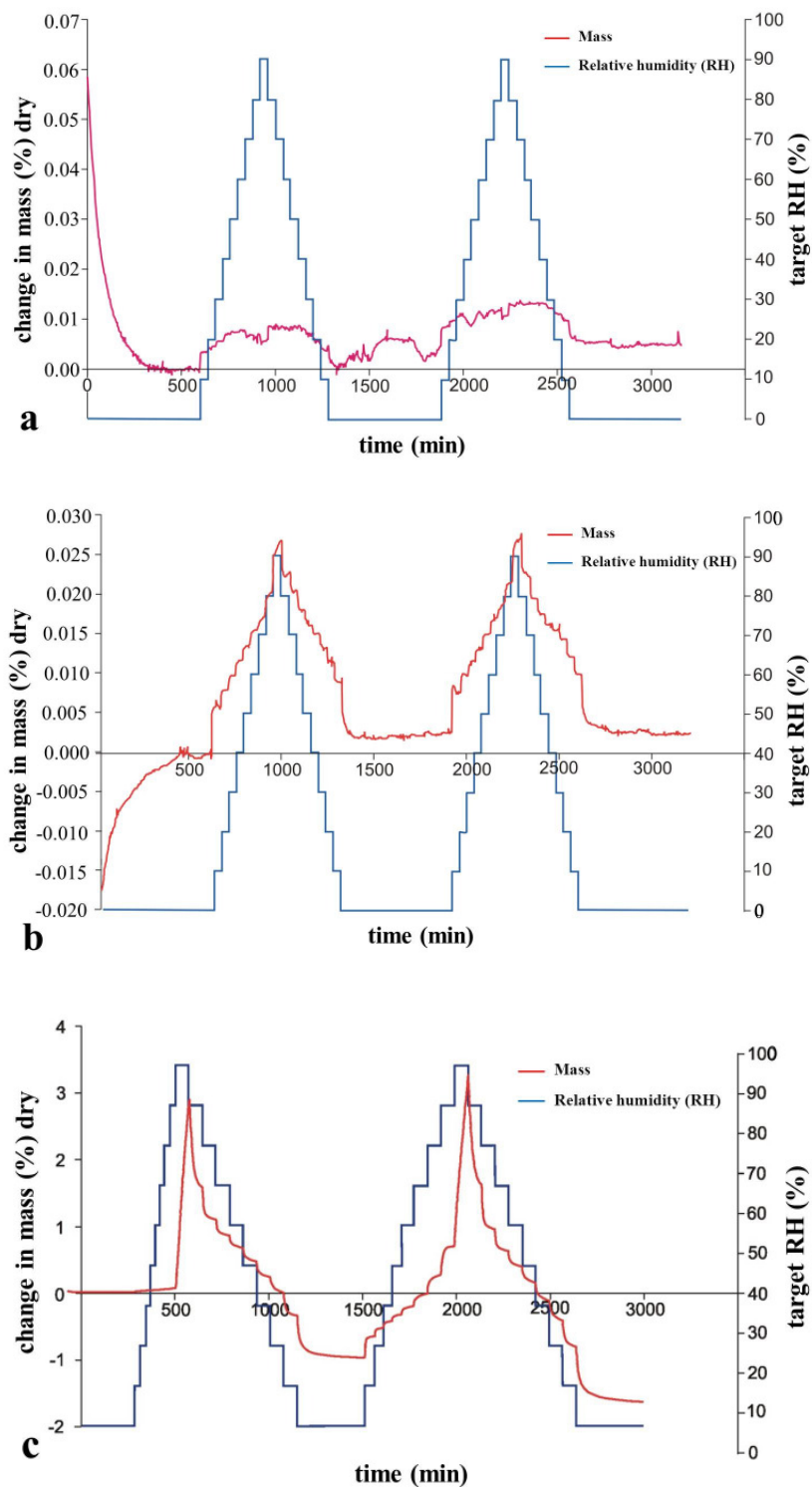


Figure 5.4: DVS kinetics of LagFix[®] cylinder (a), BoneSave[®] granules (b) and HydroSet[®] powder (c).

5.1.5 pH value of aqueous bone substitute suspensions

The results of pH value determination are shown in Figure 5.5. The initial pH value was adjusted to 7.2 for all materials tested. HydroSet[®] powder resulted in a pH value of 8.70 ± 0.16 after one hour. After adjusting the initial pH value, HydroSet[®] powder was measured to have a pH value of 7.45 ± 0.05 after six hours and a pH value of 7.46 ± 0.05 after 24 hours. The highest pH value of 9.64 ± 0.22 was measured for BoneSave[®] 2-4 mm after one hour. After six and 24 hours, the pH value resulted in 9.44 ± 0.20 and 8.56 ± 0.17 . LagFix[®] cylinder demonstrated the lowest pH values. A pH value of 7.49 ± 0.21 after one hour, a value of 7.44 ± 0.24 after six hours, and a pH value of 7.26 ± 0.19 after 24 hours were measured.

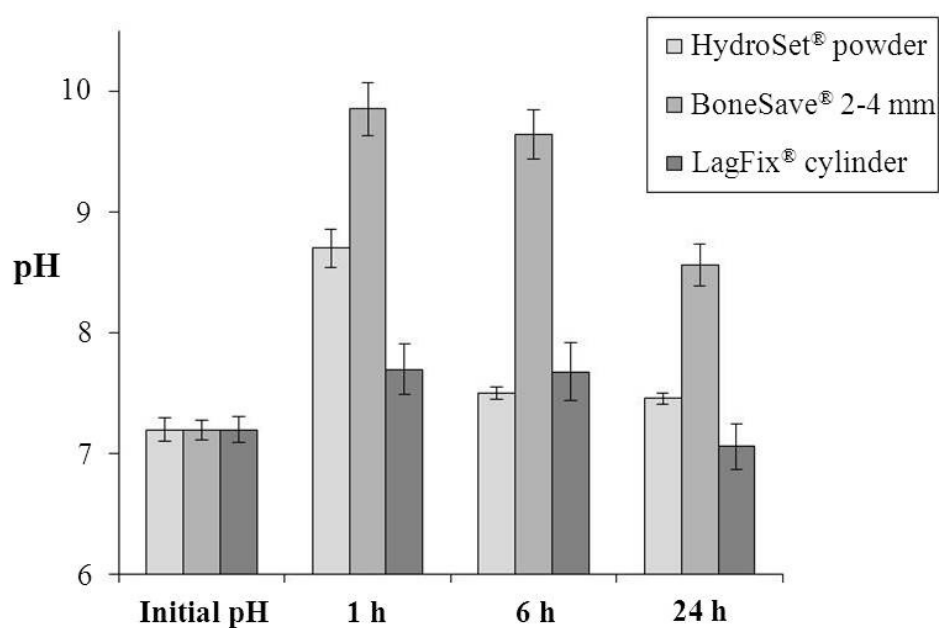


Figure 5.5: pH value of bone substitute materials after different time periods ($n = 3$; error bars = standard deviation).

5.2 Limit of detection (LOD)

The LOD of ZOL with the HPLC was found to be $1.3 \pm 0.1 \mu\text{g/mL}$. In order to visualize different drug concentrations around the calculated LOD, additionally three-dimensional plots are shown in Figure 5.6. The plots visualize ZOL detection at drug concentrations of 8.44 and $4.22 \mu\text{g/mL}$ (Figure 5.6 a and b) and scans near the evaluated LOD of 2.11 and $1.05 \mu\text{g/mL}$ (Figure 5.6 c and d).

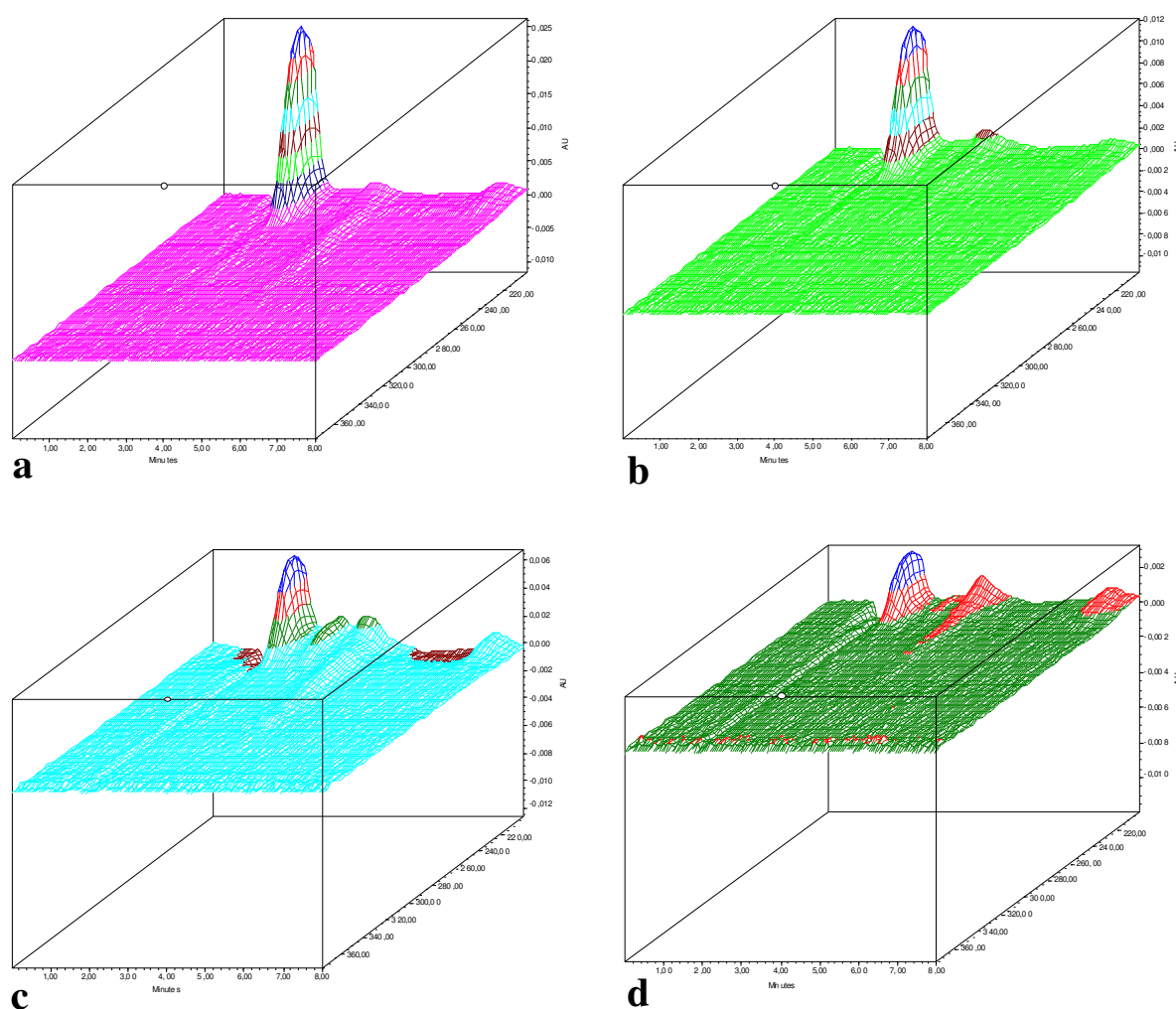


Figure 5.6: Three-dimensional plots of different concentrated ZOL solutions: $8.44 \mu\text{g/mL}$ (a), $4.22 \mu\text{g/mL}$ (b), $2.11 \mu\text{g/mL}$ (c), $1.05 \mu\text{g/mL}$ (d).

5.3 Drug load

The objective of drug loading experiments was to evaluate the influence of drug concentration and the dipping time on the resulting drug adsorption.

In Figure 5.7 the time dependent ZOL adsorption per mg of the corresponding bone substitute after dipping in 5 mL of a 2.25×10^{-4} molar ZOL solution is shown. The experimental setup gave information about the potential of a controlled short-term loading. After 5 minutes dipping a ZOL incorporation of $0.06 \mu\text{g}$ per mg was measured for the LagFix[®] cylinder. The ZOL adsorption of the LagFix[®] cylinder increased in a time dependent manner. The total drug load after 15 minutes was found to be $0.11 \mu\text{g}$ and $0.12 \mu\text{g}$ after 30 minutes per mg material, respectively. The BoneSave[®] material demonstrated both, a time and particle size dependent ZOL adsorption. The BoneSave[®] 4-6 mm granules showed the lowest drug adsorption of the used BoneSave[®] fractions of $0.04 \mu\text{g}/\text{mg}$ after 5 minutes and $0.05 \mu\text{g}/\text{mg}$ after 30 minutes dipping. BoneSave[®] 2-4 mm granules were loaded with $0.12 \mu\text{g}/\text{mg}$ after 5 minutes, increasing to $0.14 \mu\text{g}/\text{mg}$ after 15 minutes and $0.16 \mu\text{g}/\text{mg}$ after 30 minutes dipping. For the three sieve fractions of BoneSave[®] material, an increased ZOL incorporation for lower particle sizes was measured. BoneSave[®] 355-500 μm was loaded in a range of 0.15 to $0.24 \mu\text{g}$ ZOL per mg material during the 30 minutes dipping experiment. A loading of $0.28 \mu\text{g}/\text{mg}$ after 5 minutes and $0.37 \mu\text{g}/\text{mg}$ after 30 minutes dipping was measured for the BoneSave[®] 90-355 μm fraction. BoneSave[®] 63-90 μm fraction showed the highest drug load of all used materials. The material was loaded with $0.57 \mu\text{g}$ after 5 minutes, increased to $0.59 \mu\text{g}$ after 15 minutes and $0.64 \mu\text{g}$ after 30 minutes per mg material. HydroSet[®] powder resulted in $0.45 \mu\text{g}/\text{mg}$ loading after 5 minutes, $0.50 \mu\text{g}/\text{mg}$ after 15 minutes and $0.52 \mu\text{g}/\text{mg}$ after 30 minutes. No change in surface structures was detected after the dipping procedure.

Statistical analysis demonstrated significant differences between all material groups in the experimental setup presented. Selected statistically significant differences are shown in Figure 5.7. Under test conditions, BoneSave® 63-90 µm demonstrated significantly higher drug loading compared to all other materials tested.

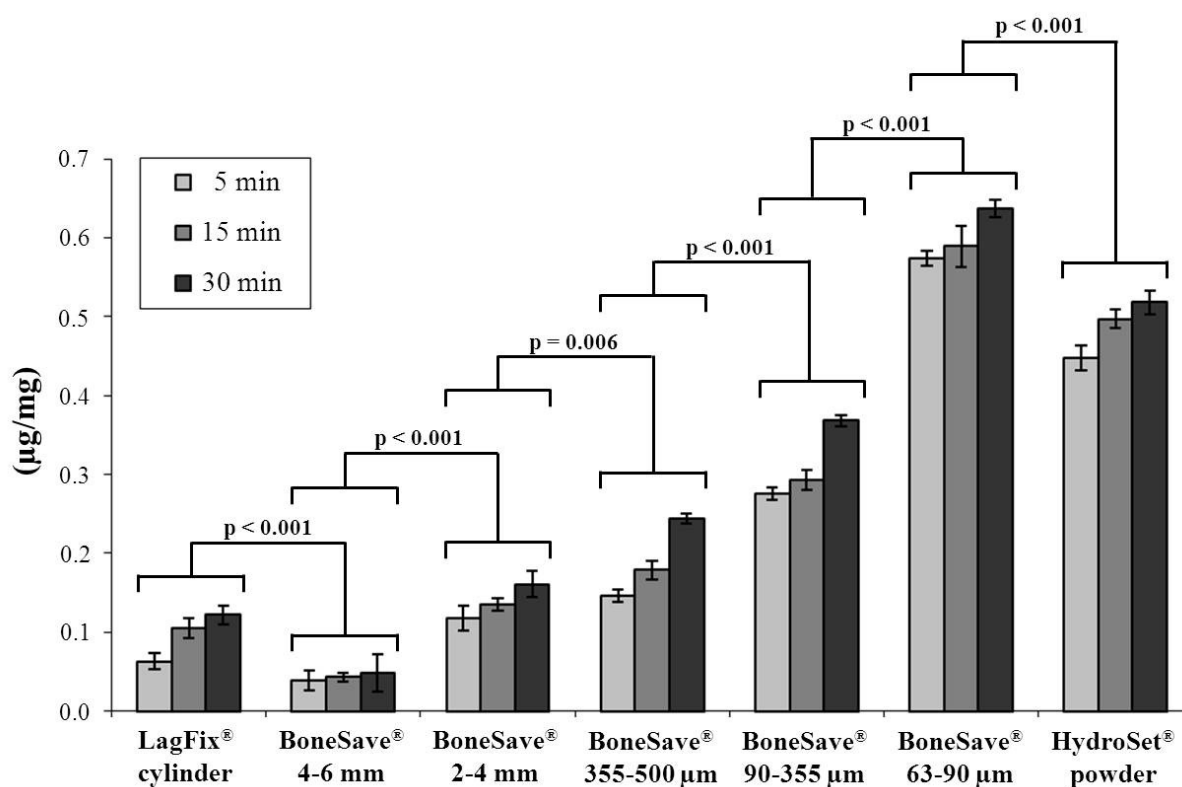


Figure 5.7: Time dependent ZOL load ($\mu\text{g}/\text{mg}$) onto bone substitutes after dipping in 5 mL of a 2.25×10^{-4} molar ZOL solution ($n = 3$; error bars = standard deviation). Selected statistically significant differences between the material types are labeled in the diagram by a line and the corresponding p -value ($n = 9$).

Figure 5.8 demonstrates the time and concentration dependent ZOL adsorption per mg HydroSet[®] powder by dipping in differently concentrated ZOL solutions. HydroSet[®] powder was loaded with 1.48 μg ZOL per mg material by dipping 5 minutes in 5 mL of a 2.25×10^{-3} molar concentrated ZOL solution. After 15 minutes an increased loading of 1.69 μg per mg and after 30 minutes a loading of 1.86 $\mu\text{g}/\text{mg}$ was determined. By dipping HydroSet[®] powder 5 minutes in 5 mL 2.25×10^{-4} molar concentrated ZOL solution, a loading of 0.45 μg per mg was measured. The values increased after 15 minutes (0.50 $\mu\text{g}/\text{mg}$) and 30 minutes (0.52 $\mu\text{g}/\text{mg}$). A controlled and reproducible drug load in a time and concentration dependent manner of HydroSet[®] powder was also shown to be feasible.

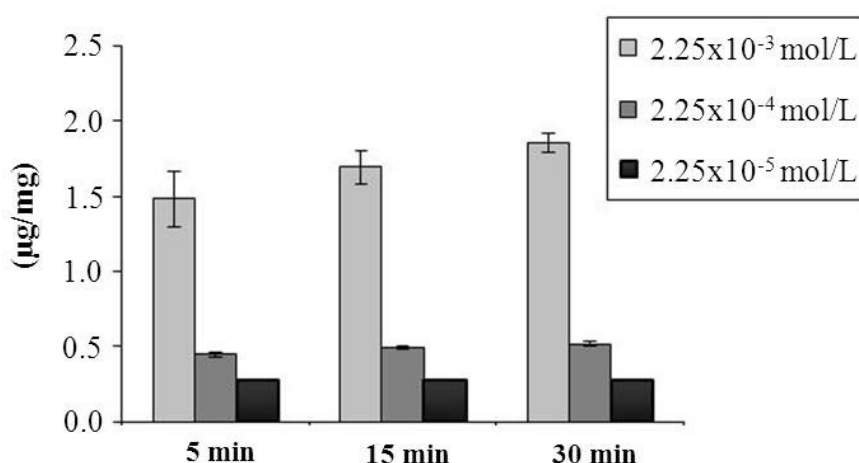


Figure 5.8: Time and concentration dependent ZOL adsorption ($\mu\text{g}/\text{mg}$) to HydroSet[®] powder after dipping in 5 mL aqueous solution of different ZOL concentrations ($n = 3$; error bars = standard deviation).

Furthermore, loading efficiency ($\mu\text{g}/\text{mg}$) versus surface area (cm^2) of 300 mg BoneSave[®] fractions was calculated and is shown in Figure 5.9. The calculations for different BoneSave[®] fractions allow suggestion of the dependency of the surface area and the amount of drug load. The total surface area (cm^2) of 300 mg of each BoneSave[®] fraction was calculated with BET data (Table 5.1) and related to drug loading results (Figure 5.7). Generally, a higher surface area resulted in a higher ZOL loading. The lowest ZOL loading of 0.039–0.048 $\mu\text{g}/\text{mg}$ by dipping 5 to 30 minutes could be calculated for a BoneSave[®] surface area of 4200 cm^2 . A surface area of 8100 cm^2 incorporated ZOL in a range of 0.118–0.161 $\mu\text{g}/\text{mg}$ during dipping time. A further increase in ZOL loading was calculated for surface areas of 13200 and 17400 cm^2 , resulting in 0.146–0.244 $\mu\text{g}/\text{mg}$ and 0.275–0.368 $\mu\text{g}/\text{mg}$, respectively. The highest drug load of 0.574–0.637 $\mu\text{g}/\text{mg}$ was demonstrated for the highest surface area of 22200 cm^2 .

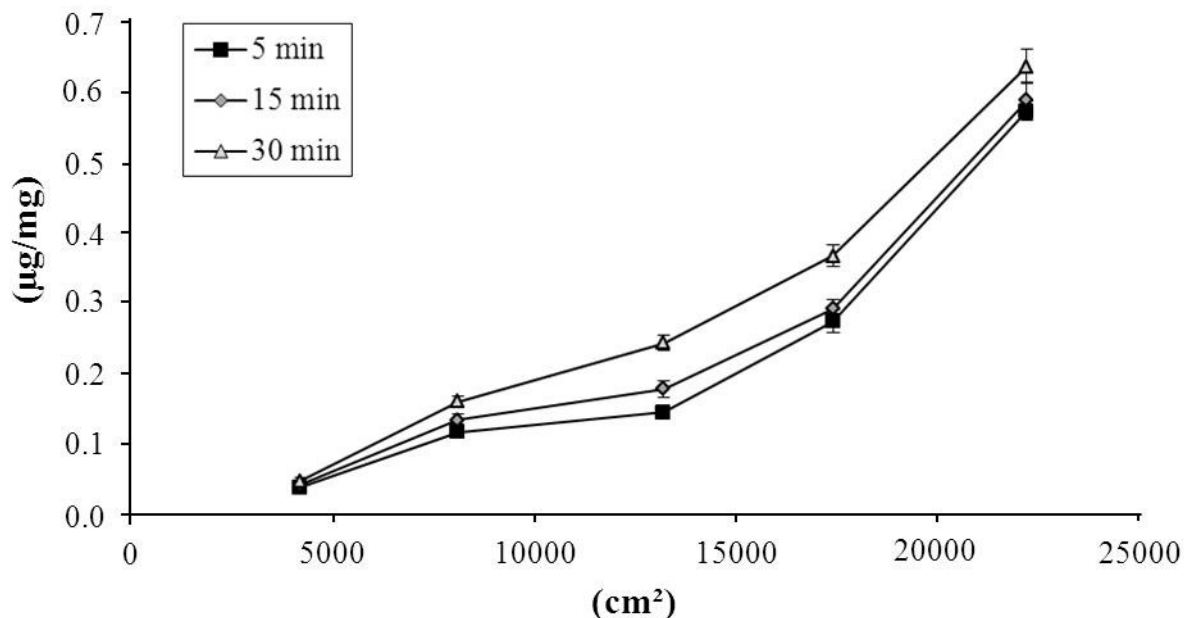


Figure 5.9: Loading efficiency ($\mu\text{g}/\text{mg}$) versus surface area (cm^2) of 300 mg BoneSave[®] fractions ($n = 3$; error bars = standard deviation).

Finally, HydroSet[®] placebo plugs which were used for the animal study were tested within drug loading experiments. Therefore, in each case three placebo plugs were dipped in a time and concentration dependent manner in 5 mL aqueous solution of different ZOL concentrations. The results of total ZOL adsorption (μg) to each placebo plug are shown in Figure 5.10.

Under test conditions, a placebo plug was loaded with $12.69 \pm 0.65 \mu\text{g}$ ZOL after dipping in 5 mL of a 2.25×10^{-3} molar concentrated ZOL solution for 5 minutes. The drug load increased to $17.71 \pm 0.83 \mu\text{g}$ after 15 minutes and to $23.57 \pm 1.64 \mu\text{g}$ after 30 minutes dipping. By dipping in 5 mL of a 2.25×10^{-4} molar concentrated ZOL solution, the drug load was found to be in a range of 5.18–14.06 μg in the tested time period. Lowest drug load in a range of 3.21–9.42 μg was measured for the lowest concentrated ZOL dipping solution (2.25×10^{-4} molar) for the different dipping time points. The weight of a single placebo plug was $35.08 \pm 0.58 \text{ mg}$. In comparison to drug load per mg HydroSet[®] powder (Figure 5.8), ZOL load per mg bone cement plug was less at all dipping times and drug concentrations.

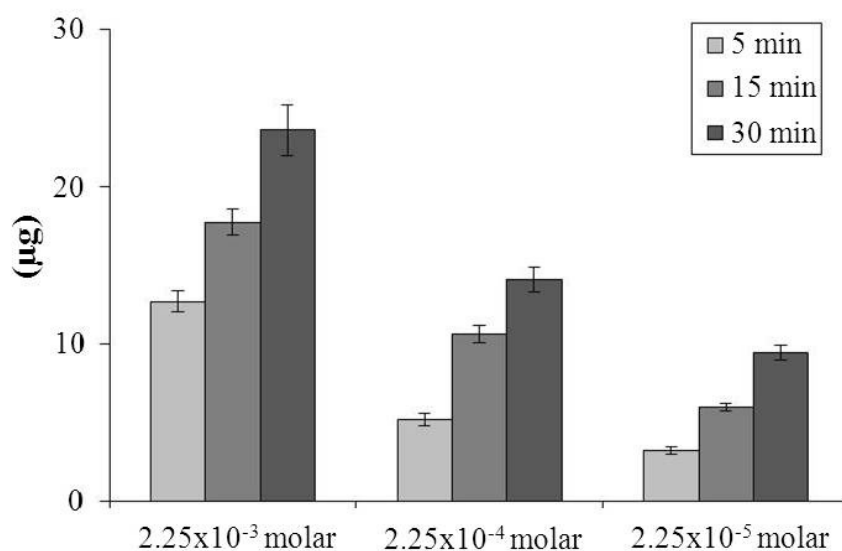


Figure 5.10: Time and concentration dependent ZOL adsorption (μg) to a placebo plug after dipping in 5 mL aqueous solution of different ZOL concentrations ($n = 3$; error bars = standard deviation).

5.4 Drug release

Besides drug adsorption, the ZOL release from the loaded bone substitutes was evaluated. The release profiles (ZOL release in μg per mg material) of five of the loaded formulations are shown in Figure 5.11. Generally the release of ZOL was greatest during the first 30 minutes for all materials when compared to later test occasions where the drug release per time rapidly decreased. The release rates at later test occasions in the release studies of the materials were mainly limited by the detection limit of ZOL. Data for release rates less than the LOD could not be quantified and are not shown. In addition, the levels of released ZOL did not correlate with the drug amount adsorbed to the different ceramics within the experimental time.

The total ZOL release from LagFix[®] cylinder was 0.02 $\mu\text{g}/\text{mg}$ during the first 30 minutes and indicated the lowest release rates of ZOL in the materials used. A slightly higher release rate was observed for BoneSave[®] 2-4 mm granules which demonstrated a release of 0.04 $\mu\text{g}/\text{mg}$ after 30 minutes *in vitro*. The total ZOL release of BoneSave[®] 355-500 mm was increased compared to BoneSave[®] 2-4 mm granules and LagFix[®] cylinder, respectively 0.07 $\mu\text{g}/\text{mg}$ versus 0.04 $\mu\text{g}/\text{mg}$ and 0.02 $\mu\text{g}/\text{mg}$. The highest drug release rate for the BoneSave[®] materials was seen for the BoneSave[®] 63-90 μm fraction and resulted in 0.14 $\mu\text{g}/\text{mg}$ after 30 minutes. Finally, the ZOL release from HydroSet[®] powder was 0.18 $\mu\text{g}/\text{mg}$ after 30 minutes.

Statistical analysis demonstrated significant differences between all material groups in the presented experimental setup. Selected statistically significant differences are shown in Figure 5.11. Under test conditions, HydroSet[®] powder demonstrated the highest drug release profile compared to all other tested materials.

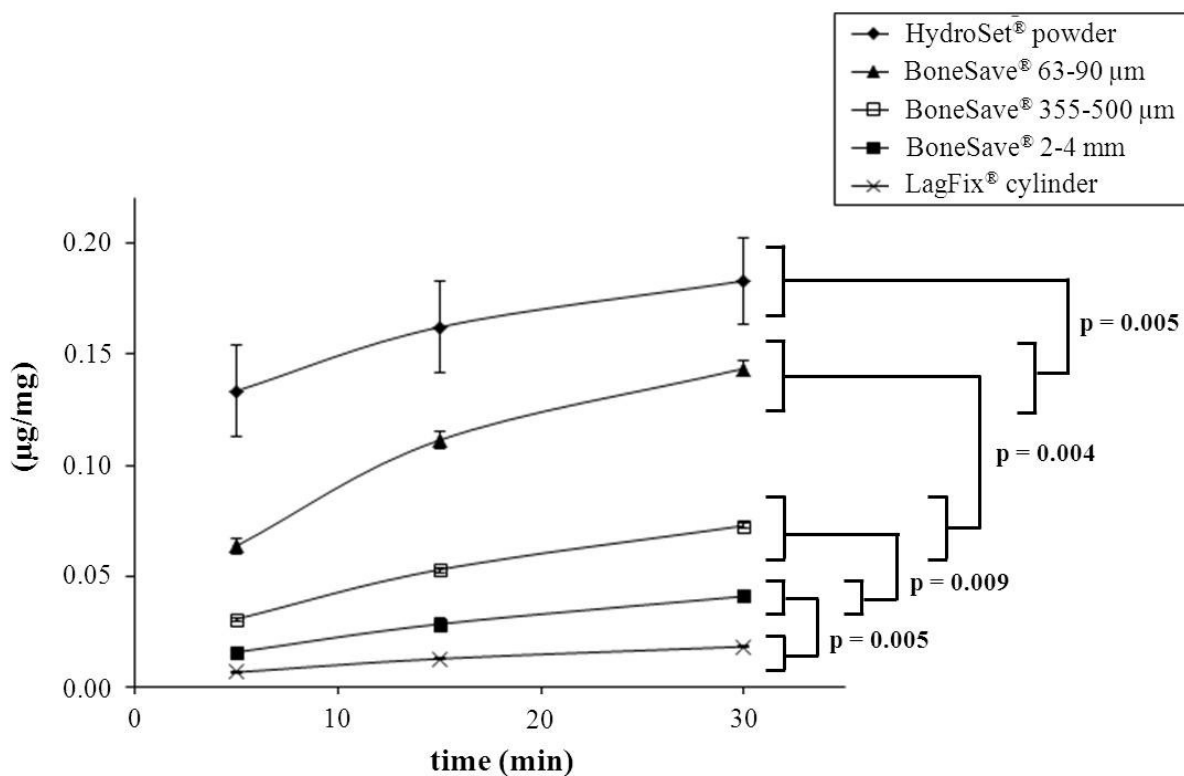


Figure 5.11: Cumulative ZOL release ($\mu\text{g}/\text{mg}$) from HydroSet[®] powder, BoneSave[®] 63-90 μm , BoneSave[®] 355-500 μm , BoneSave[®] 2-4 mm, and LagFix[®] cylinder ($n = 3$; error bars = standard deviation). Selected statistically significant differences between the release profiles of the material types are labeled in the diagram by a line and the corresponding p -value ($n = 9$).

In addition, the cumulative ZOL release per unit surface area ($\mu\text{g}/\text{cm}^2$) was calculated. As shown in Figure 5.12, the ZOL release per unit surface area for the BoneSave[®] materials was less than $0.01 \mu\text{g}/\text{cm}^2$ after 5 minutes. The values increased to 0.01 – $0.02 \mu\text{g}/\text{cm}^2$ after 15 minutes and to $0.02 \mu\text{g}/\text{cm}^2$ after 30 minutes. The values for BoneSave[®] 63-90 μm were higher compared to BoneSave[®] 355-500 μm and BoneSave[®] 2-4 mm. Furthermore, HydroSet[®] powder showed a ZOL release of $0.03 \mu\text{g}/\text{cm}^2$ after 5 minutes. After 15 and 30 minutes HydroSet[®] had a cumulative drug release of $0.04 \mu\text{g}/\text{cm}^2$.

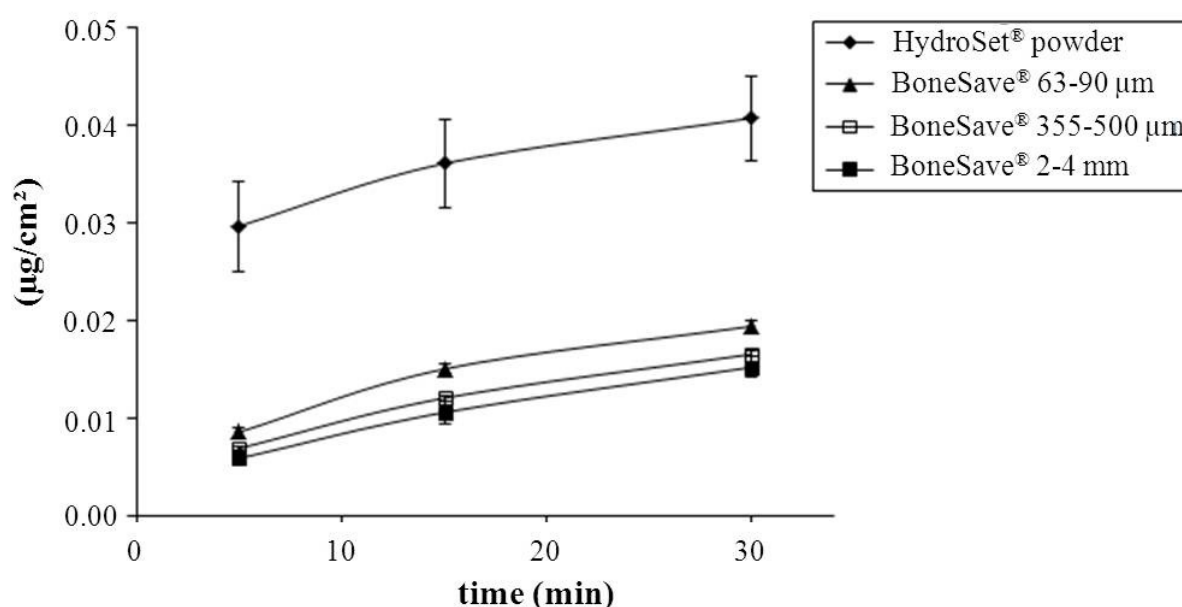


Figure 5.12: Cumulative ZOL release per surface area ($\mu\text{g}/\text{cm}^2$) from HydroSet[®] powder, BoneSave[®] 63-90 μm , BoneSave[®] 355-500 μm , and BoneSave[®] 2-4 mm ($n = 3$; error bars = standard deviation).

Finally, the drug release of verum plugs and drug-loaded placebo plugs was tested. All release rates from these plug formulations were less than the evaluated LOD of the described HPLC method and could not be quantified.

5.5 ZOL stability test

At each sampling time, there was no evidence of precipitation. Visual examination of all tested vials showed them to be clear and without any change of colour.

5.5.1 Temperature profile

The results of ZOL stability in a temperature dependent manner are shown in Figure 5.13. A ZOL content of more than 98% up to 15 days was measured at a storage temperature of 2-8°C. The drug content decreased to $95.91 \pm 2.0\%$ after 42 days. The ZOL content decreased to $88.40 \pm 3.1\%$ after 180 days storage. At storage temperature of 25°C, the ZOL content was $95.07 \pm 2.9\%$ after 15 days. At day 42, the ZOL amount was measured to be $90.57 \pm 3.3\%$. Finally, a ZOL content of $81.85 \pm 5.5\%$ was determined after 180 days. At a storage condition of 40°C, the ZOL content was $91.43 \pm 4.2\%$ after 15 days. A decrease to $85.69 \pm 4.2\%$ was observed at day 42. After 180 days storage at 40°C, the ZOL content was $72.57 \pm 6.8\%$. At a storage temperature of 60°C, the ZOL content was $86.90 \pm 4.3\%$ after 15 days. A decrease to $65.39 \pm 6.8\%$ was measured at day 42. The ZOL content further decreased to $5.93 \pm 5.2\%$ after 180 days.

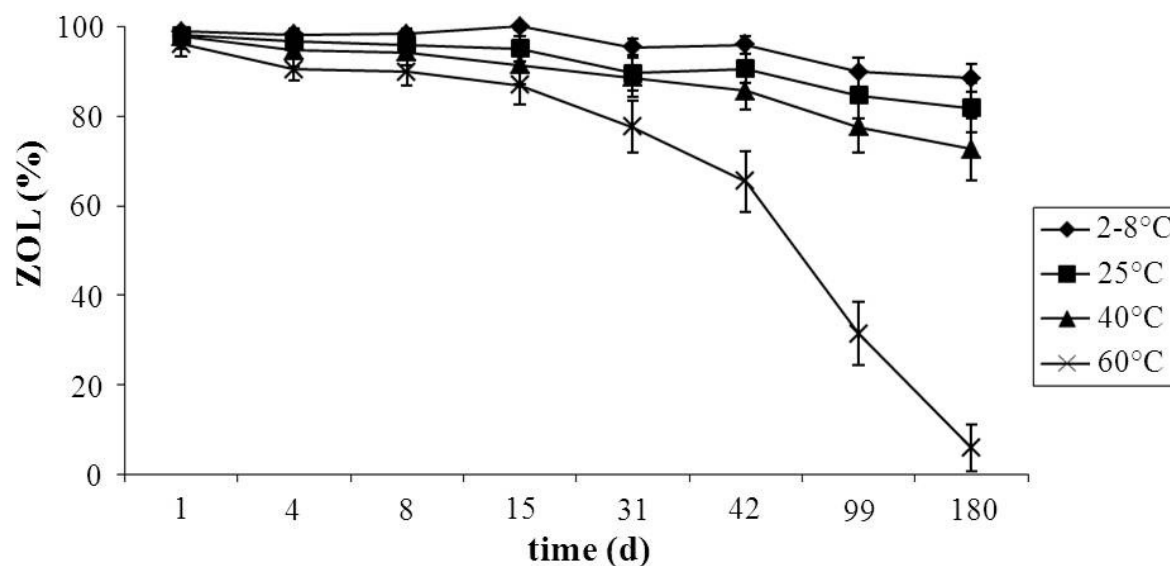


Figure 5.13: Temperature profile of ZOL stability ($n = 3$; error bars = standard deviation).

To confirm and visualize sample changes in the data, three-dimensional scans were generated and evaluated. The highest degradation was seen at a storage temperature of 60°C. Selected three-dimensional scans showing these sample changes at 60°C in a time-dependent manner are presented in Figure 5.14.

In Figure 5.14 a, the three-dimensional scan of a 2.25×10^{-4} molar ZOL solution at day zero is shown. The peak intensity was approximately at 0.20 adsorption units (AU) under test conditions. After 15 days storage at 60°C, the peak intensity decreased to 0.14 AU (Figure 5.14 b). The peak geometry was similar to the peak measured at day zero. The peak intensity decreased further to 0.12 AU at day 42 (Figure 5.14 c). Additionally, the small peak prior to the main ZOL peak slightly increased. After 99 days storage, the peak intensity was about 0.055 AU (Figure 5.14 d). The convergence of both peak intensities is clearly seen.

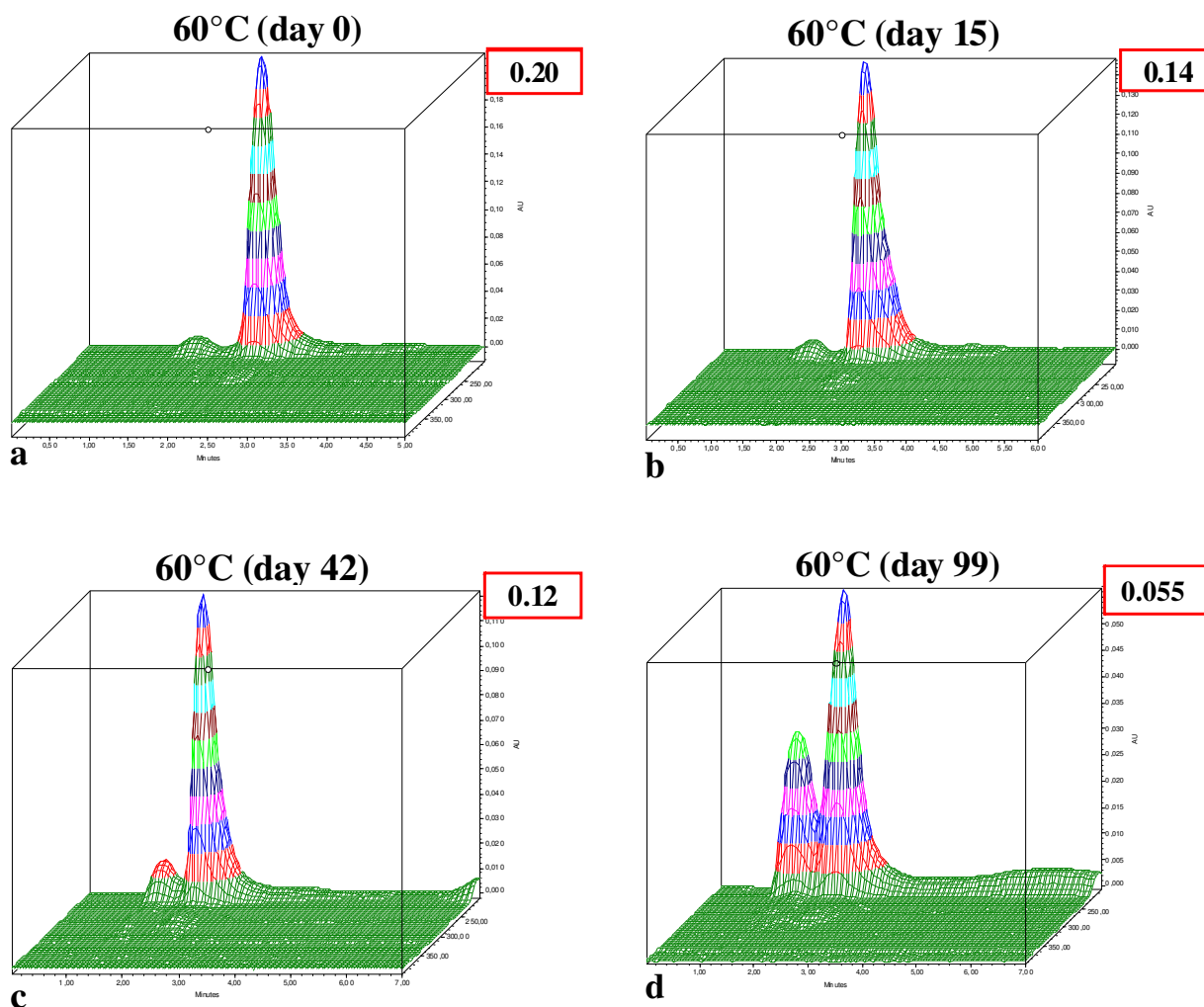


Figure 5.14: Three-dimensional evaluation of time-dependent ZOL stability at a storage temperature of 60°C.

5.5.2 Stability at different storage conditions (plastic versus glass)

To evaluate the influence of the storage material, plastic storage containers were compared to glass containers. The stability results at different storage conditions (plastic and glass) are summarized in Figure 5.15.

During storage in plastic, a ZOL content of more than 99% was demonstrated when stored for 55 days at 2-8°C and 25°C. Compared to storage in plastic, ZOL demonstrated less stability when stored in glass. After 19 days storage at 2-8°C in glass, the drug content decreased to $97.74 \pm 1.8\%$. Under the same test conditions, a drug concentration of $95.63 \pm 2.1\%$ was determined after 55 days

storage. At a storage temperature of 25°C in glass, drug assay decreased to $95.94 \pm 2.2\%$ after 19 days and to $90.20 \pm 2.6\%$ after 55 days.

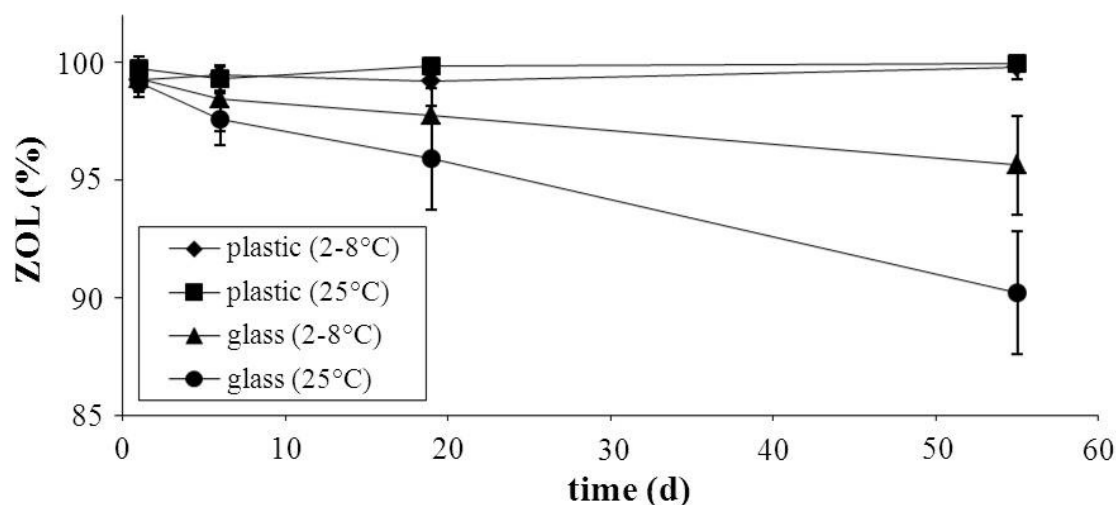


Figure 5.15: ZOL stability stored in glass and plastic at different temperatures ($n = 3$; error bars = standard deviation).

In Figure 5.16, two-dimensional HPLC scans of the same concentrated ZOL solution are shown when stored in different materials (plastic and glass). The ZOL chromatogram (when stored in plastic) showed the drug peak with a peak area of 5.35×10^6 area units (Figure 5.16 a). No other peaks are visible in this chromatogram. The same ZOL concentration resulted in a different chromatogram when stored in glass (Figure 5.16 b). In addition to the main peak at a retention time of about 3 minutes, another peak was discovered at a lower retention time. The main peak with the greater intensity had an area of 5.04×10^6 area units. The small peak had an area of 2.9×10^5 area units. Overall, both peaks had a total peak area of 5.33×10^6 area units. This total peak area corresponded to almost the total peak area of the main ZOL peak when stored in plastic.

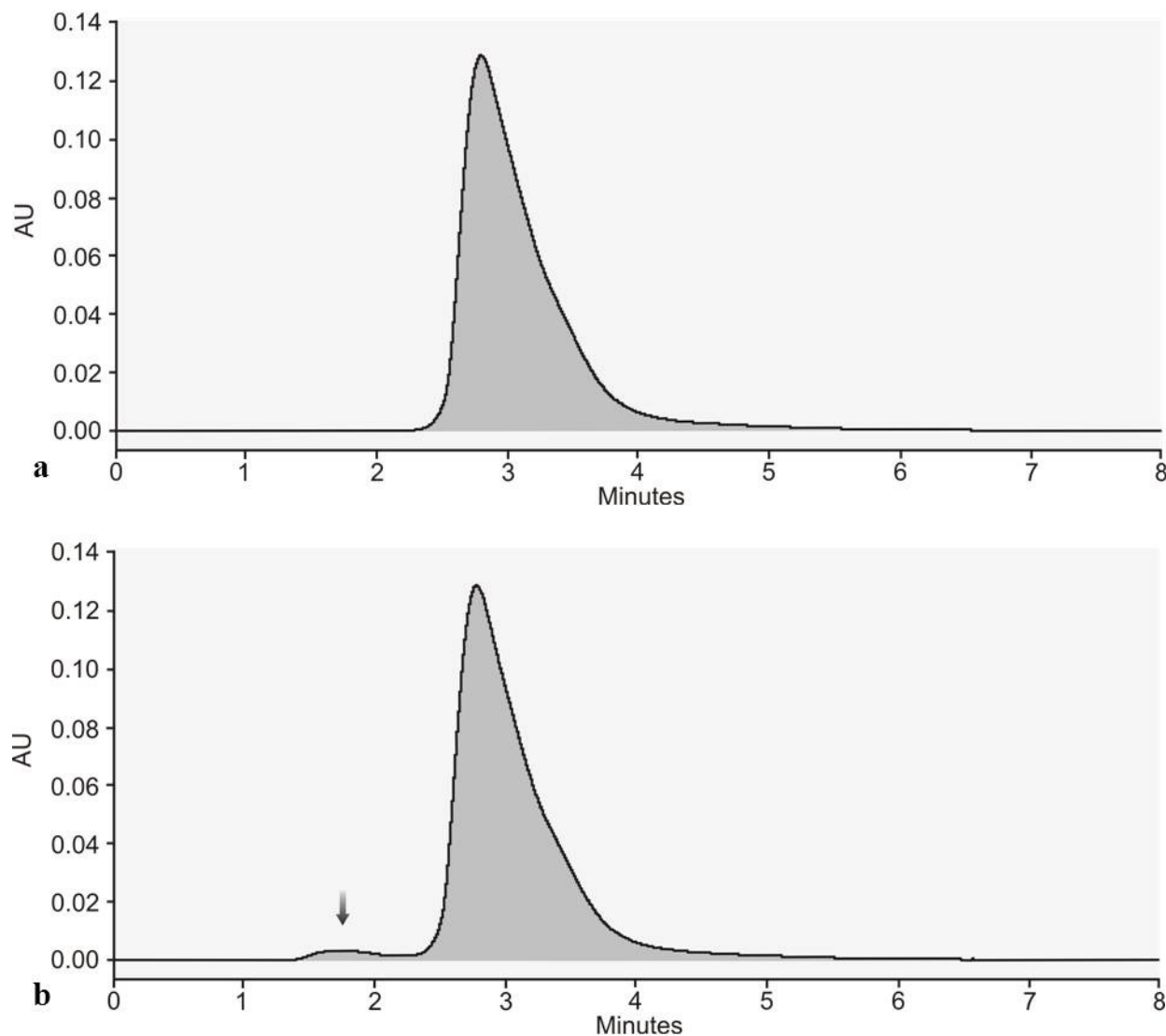


Figure 5.16: 2.25×10^{-4} mol/L concentrated ZOL solution stored in a plastic vial (a) and a glass vial (b)

The differences in the chromatograms of different storage conditions were additionally visualized by three-dimensional HPLC plots (Figure 5.17). The additional peak can clearly be seen in the ZOL sample stored in glass (Figure 5.17 b).

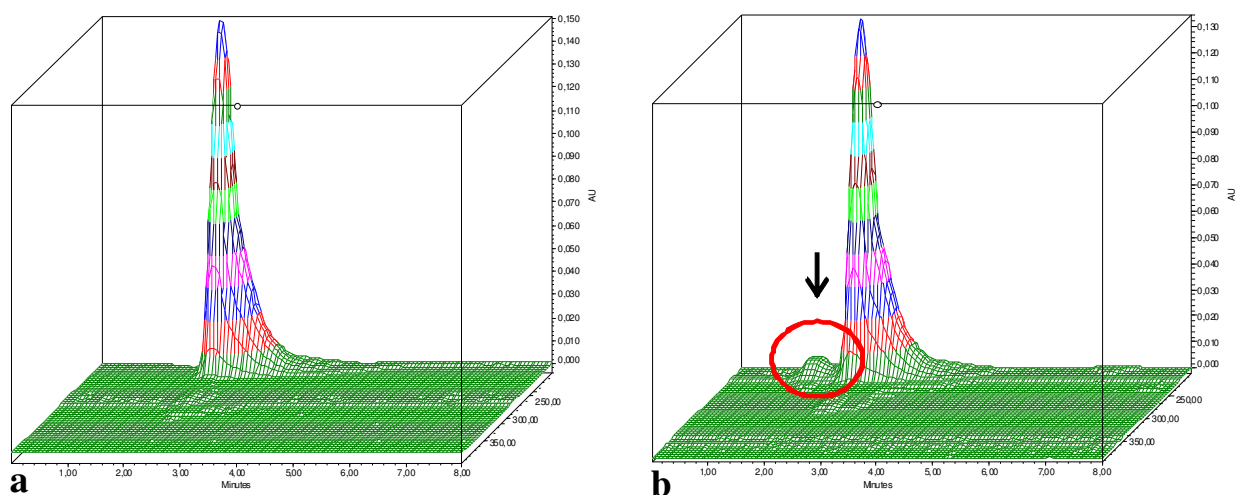


Figure 5.17: Three-dimensional plots of a 2.25×10^{-4} mol/L concentrated ZOL solution stored for one day at 40°C in plastic (a) and glass (b).

5.5.3 Stability of lyophilisates

A light microscopy picture of the lyophilisate structure containing $100 \mu\text{g}$ ZOL and 20 mg mannitol is shown in Figure 5.18. The picture demonstrates the lyophilisate structure after 223 days storage at room temperature. The process parameters selected resulted in a stable structure with mannitol as a carrier excipient which remained intact even after several months of storage at room temperature.

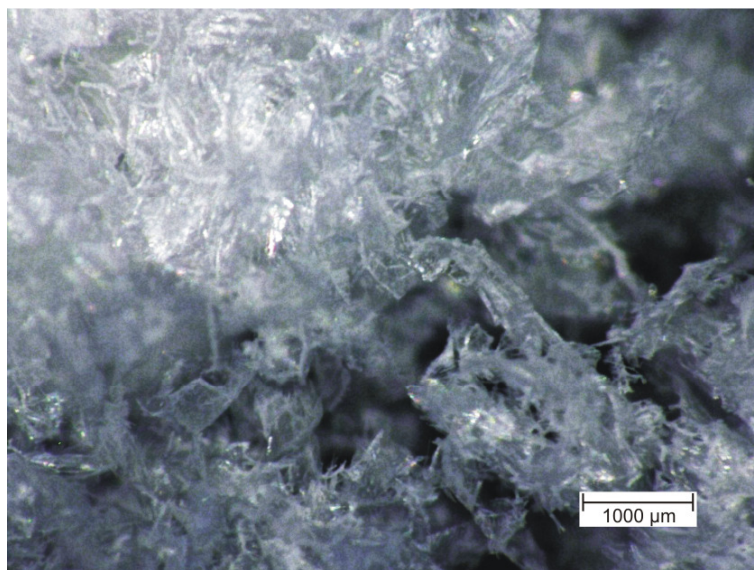


Figure 5.18: Light microscopy picture of a lyophilisate containing 20 mg mannitol and 100 µg ZOL.

In Figure 5.19, a photograph of the different lyophilisate formulations is shown. All mannitol formulations result in a stable network (1-4). The formulations with trehalose (5) or sucrose (6) as carrier for ZOL resulted directly after manufacturing in lyophilisates that are partially or completely collapsed.



Figure 5.19: Photograph of different lyophilisates containing 100 µg ZOL and 5 mg (1), 10 mg (2), 15 mg (3), 20 mg (4) mannitol, 15 mg trehalose (5) or 15 mg sucrose (6).

The stability results of different lyophilisate formulations are shown in Figure 5.20. The data demonstrated stability with more than 98% drug content of all formulations during a storage period of 223 days at room temperature.

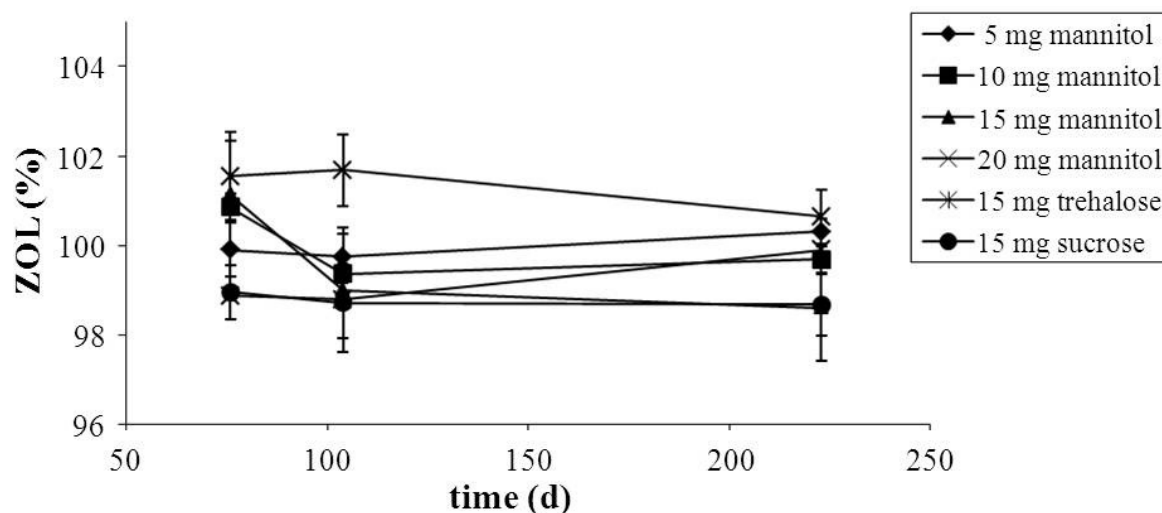


Figure 5.20: Stability of different ZOL lyophilisates ($n = 3$; error bars = standard deviation).

Furthermore, three-dimensional HPLC scans were used to demonstrate an exact determination of ZOL in the lyophilisate formulations with the established HPLC method. The different lyophilisates immediately dissolved in water. In Figure 5.21, the three-dimensional plots of the different mannitol lyophilisates dissolved in water are shown. The ZOL peak appeared at a retention time of about 3 minutes with the same intensity in every formulation. The ZOL peak showed a higher intensity in every shown mannitol formulation compared to the mannitol peak at a lower retention time. The increasing amounts of mannitol in the different formulations can clearly be detected.

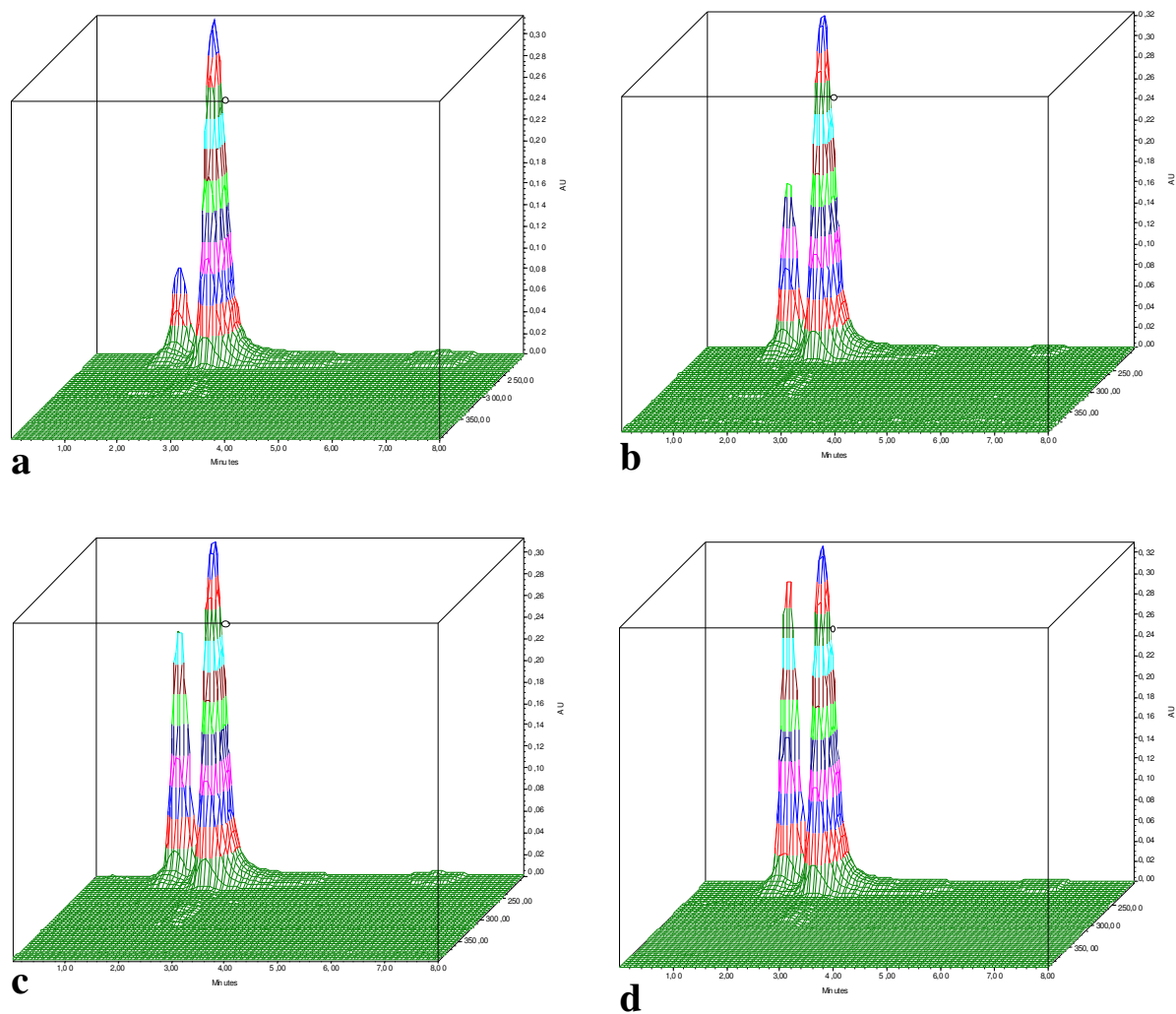


Figure 5.21: Three-dimensional plots of differently concentrated mannitol lyophilisate formulations with 100 µg ZOL dissolved in water: 5 mg mannitol (a), 10 mg mannitol (b), 15 mg mannitol (c) and 20 mg mannitol (d).

5.6 Cytotoxicity test

By dissolving ZOL directly in water a Calu-3 cell viability of less than 2% could be evaluated within the first test series. The data are shown in Figure 5.22 and demonstrated low cell viability in a ZOL concentration range of 4.14–1060 $\mu\text{g/mL}$.

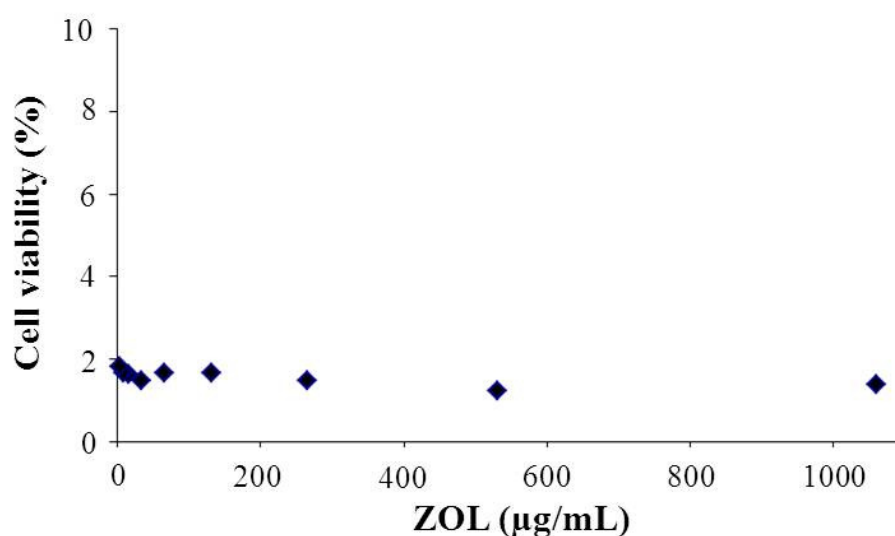


Figure 5.22: Cell viability (%) of different concentrated ZOL solutions directly dissolved in water ($n = 4$; error bars = standard deviation).

In the second test, the osmolarity was adjusted to 290–300 mosmol. The resulting pH values of the prepared ZOL solutions are shown in Figure 5.23 a. An exponential decrease in pH was demonstrated for increasing ZOL concentrations. The lowest concentrated ZOL solution of 3.88 $\mu\text{g/mL}$ resulted in a pH of 5.59 ± 0.10 . For example, a pH value of 3.06 ± 0.06 was determined for a 993 $\mu\text{g/mL}$ concentrated ZOL solution. The cell viability of the different ZOL solutions is shown in Figure 5.23 b. Under test conditions, the ZOL concentration covered a cell viability range from $99.67 \pm 11.06\%$ for the lowest ZOL concentration of 3.88 $\mu\text{g/mL}$ to $2.31 \pm 0.47\%$ for the highest concentrated ZOL solution of 993 $\mu\text{g/mL}$. Up to a concentration of 31.03 $\mu\text{g/mL}$ and a pH

value of 4.70 ± 0.06 the cell viability was approximately 100%. The $62.06 \mu\text{g/mL}$ concentrated ZOL solution resulted in a cell viability of $97.25 \pm 9.88\%$. At a concentration of $124.12 \mu\text{g/mL}$ and a pH of 3.99 ± 0.07 the cell viability decreased to $76.35 \pm 10.44\%$. A cell viability of $58.79 \pm 8.50\%$ and $6.65 \pm 5.68\%$ respectively, was evaluated for the $248.25 \mu\text{g/mL}$ (pH of 3.66 ± 0.12) and $496.48 \mu\text{g/mL}$ (pH of 3.34 ± 0.08) concentrated ZOL solutions.

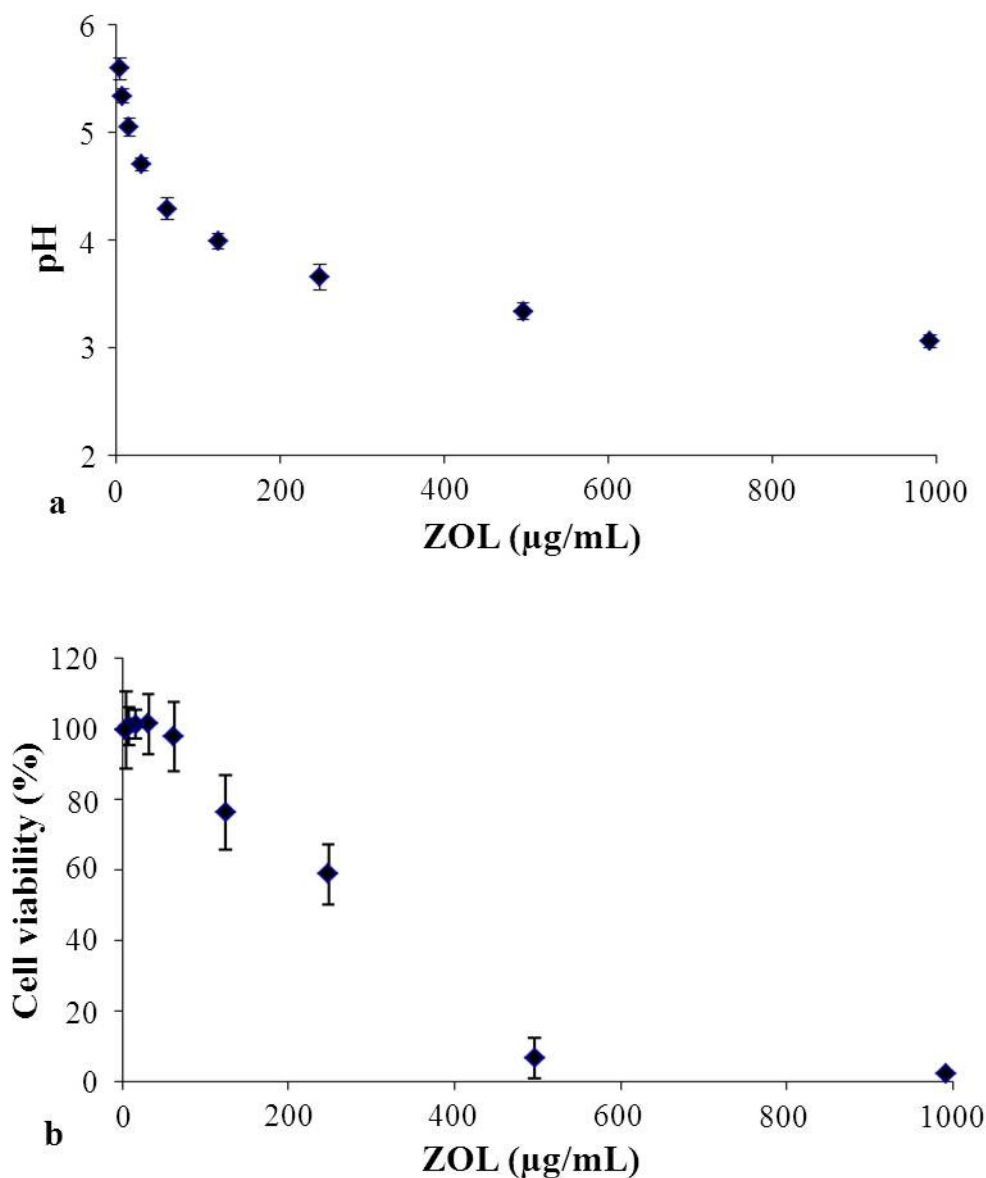


Figure 5.23: pH values of different iso-osmolar ZOL concentrations (a) and cell viability (%) of iso-osmolar ZOL solutions (b) ($n = 4$; error bars = standard deviation).

In the third test series, pH values and osmolarity were adjusted. The data for cell viability of different concentrated ZOL solutions are shown in Figure 5.24. The data demonstrated a cell viability of more than 85% over all tested ZOL concentrations in a range of 3.66–936 $\mu\text{g}/\text{mL}$. Up to a ZOL concentration of 117 $\mu\text{g}/\text{mL}$ cell viability was higher than 95%. The cell viability slightly decreased to $87.14 \pm 18.65\%$ at a concentration of 234 $\mu\text{g}/\text{mL}$ and to $86.60 \pm 11.82\%$ for the 936 $\mu\text{g}/\text{mL}$ ZOL solution.

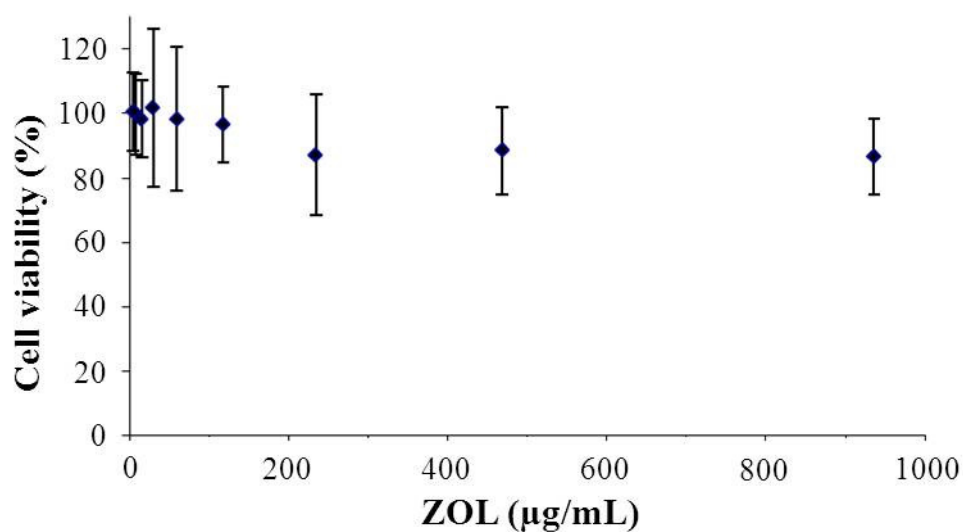


Figure 5.24: Cell viability (%) of iso-osmolar ZOL solutions with an adjusted pH value of 6.8 ($n = 4$; error bars = standard deviation).

To evaluate the toxicity of HydroSet[®] plugs used for the *in vivo* animal study, release samples of verum and placebo plugs were tested without adjusting the pH value. The data for the tested dissolution media after three hours and five days are shown in Figure 5.25. Both implant types and both releasing time points demonstrated cell viability higher than 90%. After three hours releasing time, the verum plug resulted in a cell viability of $98.94 \pm 19.27\%$ and the placebo formulation showed $93.32 \pm 15.55\%$ cell viability. For the five days time point, the verum formulation had a cell viability of $90.24 \pm 12.55\%$ and the placebo formulation of $95.26 \pm 14.95\%$.

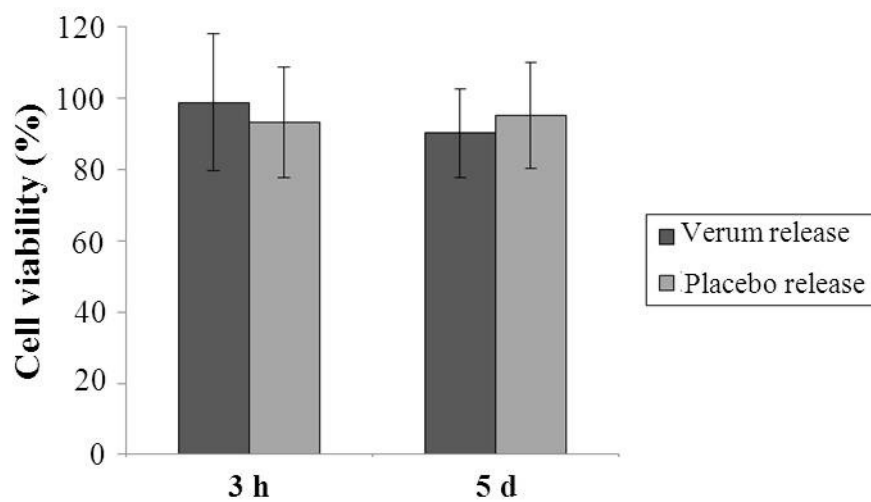


Figure 5.25: Cell viability of release samples from HydroSet[®] plugs (n = 4; error bars = standard deviation).

5.7 Characterisation of modified HydroSet[®] formulations

5.7.1 Semi-quantitative wetting of HydroSet[®] powder

The results of semi-quantitative wetting process are shown as photographs in Figure 5.26. HydroSet[®] powder has to be mixed with at least 25% additional water to make sure that the powder is fully wetted (Figure 5.26 c). Even 20% additional water is not enough to surround the powder completely (Figure 5.26 b). This formulation showed powder clusters. With a higher amount of additional water the viscosity of the suspension decreased (Figure 5.26 d).

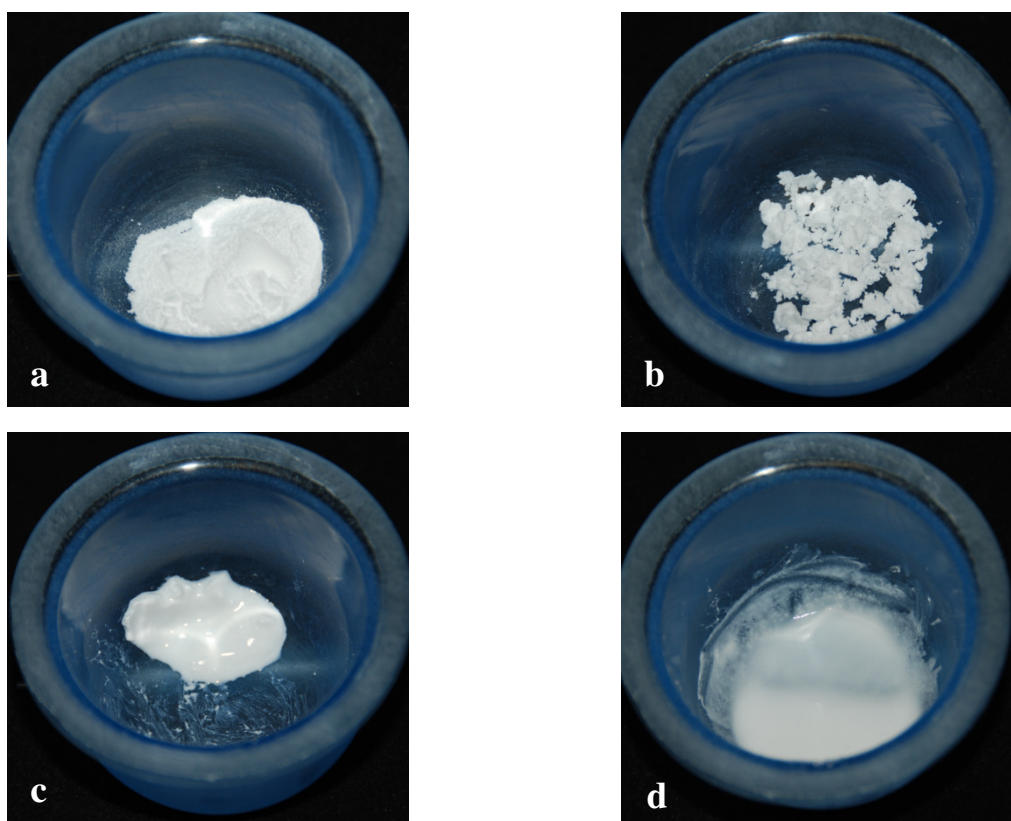


Figure 5.26: HydroSet[®] powder mixed with different amounts of water: pure (a), 20% (b), 25% (c), and 40% (d).

5.7.2 Cement hardness

The influence of additional water or ZOL solution to the HydroSet[®] hardening process was evaluated by means of hardness measurements. The hardness measurement results are shown in Figure 5.27.

The hardness of normal HydroSet[®] cement at the different time points is shown in Figure 5.27 a. A maximum force of 1.4 N was evaluated after 3 minutes. The force increased with time. After 18 minutes a maximum force of 23.47 N was measured. A similar profile was evaluated for the HydroSet[®] cement with 50 μ L additional ZOL solution (Figure 5.27 b). The maximum force after 18 minutes was 26.54 N. A different profile could be measured for HydroSet[®] cement with 30% additional water (Figure 5.27 c). A major effect on cement hardness was seen. The maximum force after 18 minutes resulted in 2.14 N. The results of hardness measurements of the ZOL loaded and dried HydroSet[®] powder are shown in Figure 5.27 d. This powder demonstrated a maximum force of 0.26 N over the whole time period.

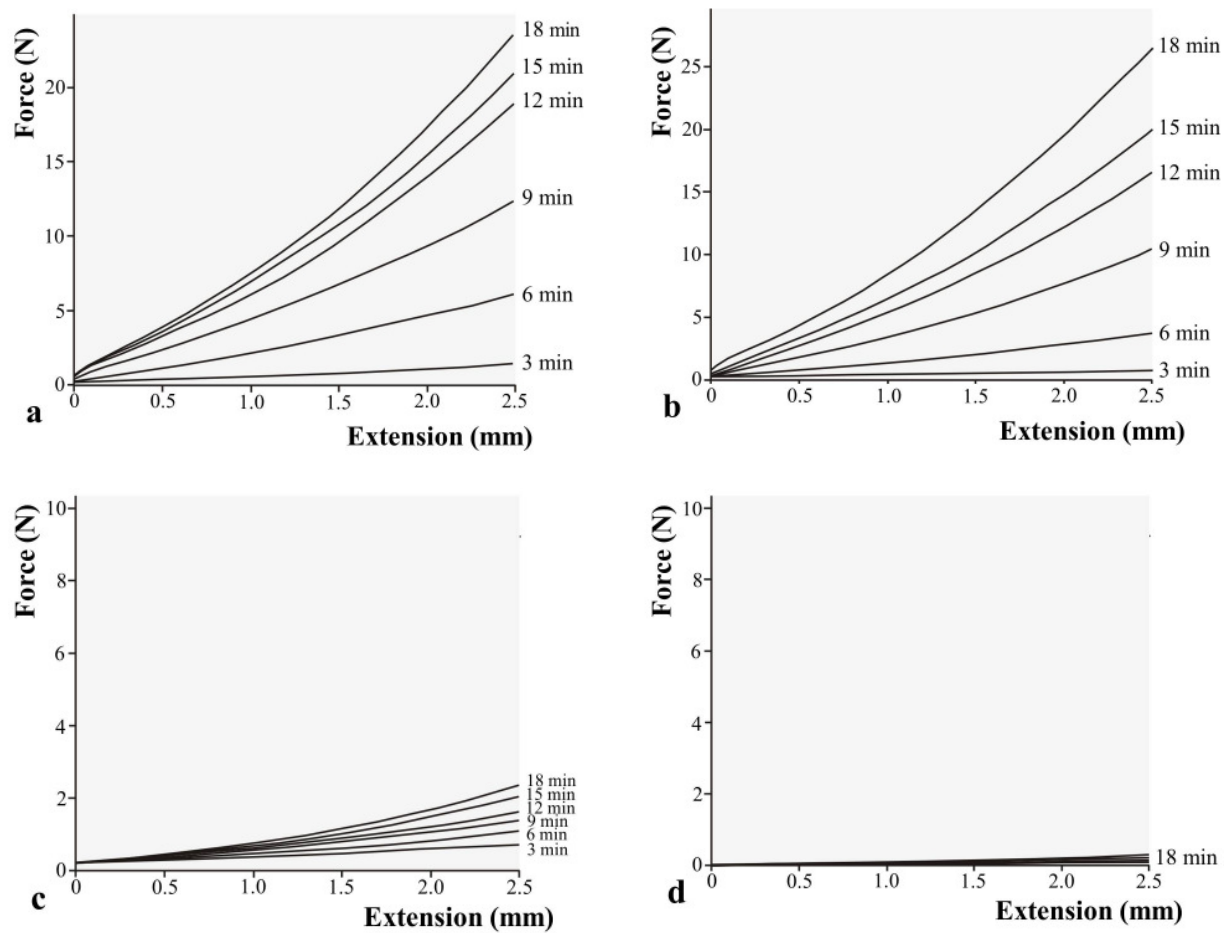


Figure 5.27: Hardness measurements of normal HydroSet[®] cement (a), HydroSet[®] with 50 µL ZOL solution (b), HydroSet[®] with 30% additional water (c) and ZOL loaded and dried HydroSet[®] (d).

5.7.3 Solubility of ZOL in HydroSet[®] hardening solution

The semi-quantitative solubility of ZOL in 500 μ L HydroSet[®] hardening solution was determined to be in a range of 5.90–7.71 mg/500 μ L (11.8–15.4 mg/mL) as calculated from the values in Table 5.2.

Table 5.2: *Semi-quantitative solubility data of ZOL in HydroSet[®] hardening solution.*

total ZOL amount (mg)	solubility (500 μ L)
2.64	yes
4.16	yes
5.90	yes
7.71	no

5.8 *In vivo* animal study

5.8.1 Sterility of HydroSet[®] bone cement plugs

All test media and negative controls (media without sample) revealed no growth. The HydroSet[®] implants confirmed to the test for sterility according to the PhEur.

5.8.2 Crushing strength

The results of crushing strengths of dry and wet HydroSet[®] verum and placebo plugs are shown in Figure 5.28. Dry HydroSet[®] verum plugs had a crushing strength of 41.0 ± 3.6 N and dry placebo plugs demonstrated a slightly higher strength of 45.7 ± 2.5 N. For the wet verum plug, 20.7 ± 3.1 N was measured. The wet placebo implant resulted in 24.7 ± 2.5 N.

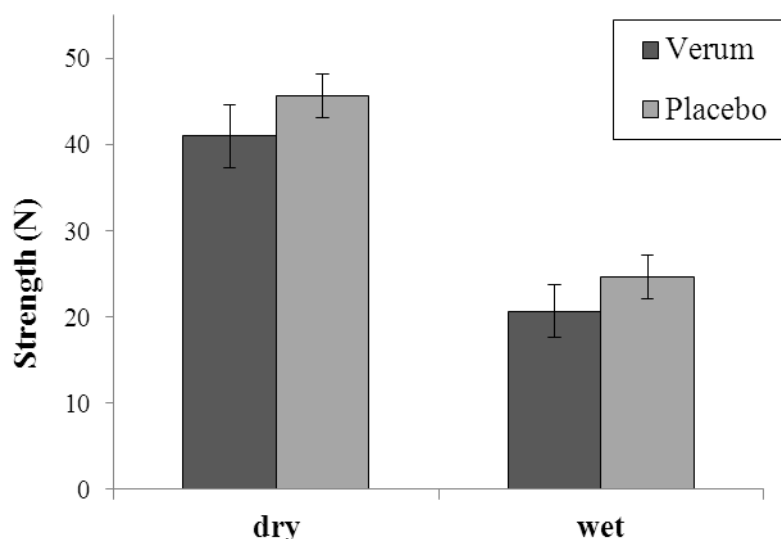


Figure 5.28: *Crushing strengths of dry and wet HydroSet[®] verum and placebo plugs (n = 3; error bars = standard deviation).*

5.8.3 Surgeries and bone harvesting

No inflammatory reactions (no sign of infection) and no wound healing disturbances were observed macroscopically at the time of sacrifice. No problems were seen in the animals, all survived and none showed any signs of illness. All implants remained in place for the one week group. After three weeks, all rats appeared healthy, none showed any sign of pain or infection and all had normal skin. One implant had the head dislocated, but the sample could be utilised for qPCR analysis.

5.8.4 SEM analysis of implants

The visualisation of moulded implant surfaces of the bone cement plugs by SEM presented rough structures and a porous texture with open pores and channels in micrometer range (Figure 5.29).

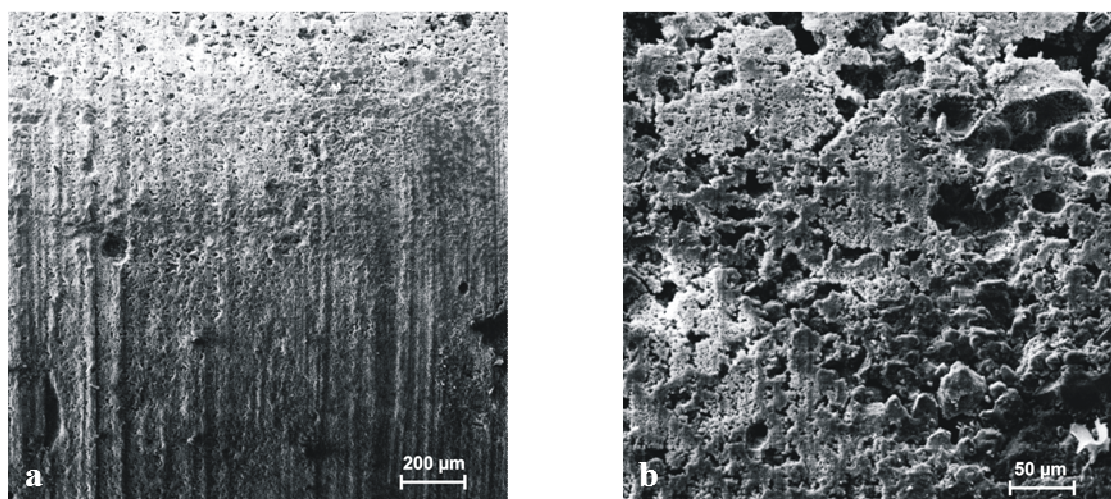


Figure 5.29: SEM images of the plug surface in different magnifications.

5.8.5 Quantitative PCR analysis

The expression of 18S ribosomal RNA subunits at the plug surface may be used as an indicator for the total number of cells in the bone sample adherent to the plug surface. The gene expression analysis in peri-implant bone surrounding the placebo plug showed significantly higher expression of 18S RNA both after one week ($p < 0.001$) and after three weeks ($p = 0.028$) compared to verum plug samples (Figure 4 a). A greater amount of cells were detected in placebo samples as indicated by higher expression of 18S RNA (Figure 5.30 a). Another reference gene widely used in qPCR analysis is glyceraldehyde-3-phosphate dehydrogenase (GAPDH). Significantly decreased levels for verum plug was shown for the reference gene GAPDH both after one week ($p = 0.003$) and after three weeks ($p = 0.021$) (Figure 5.30 b).

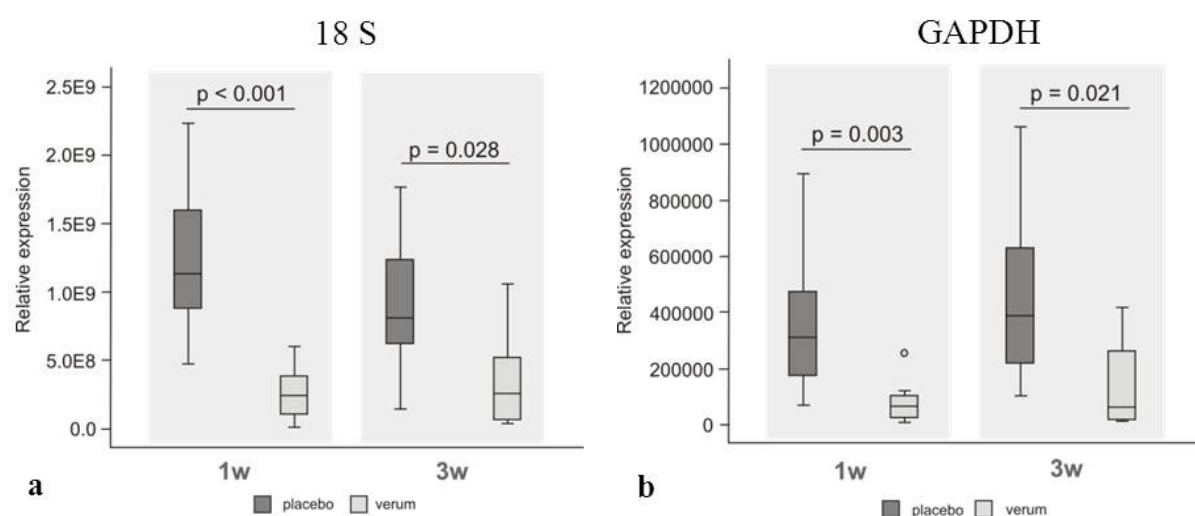


Figure 5.30: The 18S (a) and GAPDH (b) ribosomal RNA expression.

The gene expression levels at implants retrieved from verum and placebo plugs were compared based on the normalized data. No significant differences of selected genes were found between placebo and verum plugs at each time-point when normalized to 18S RNA (Figure 5.31).

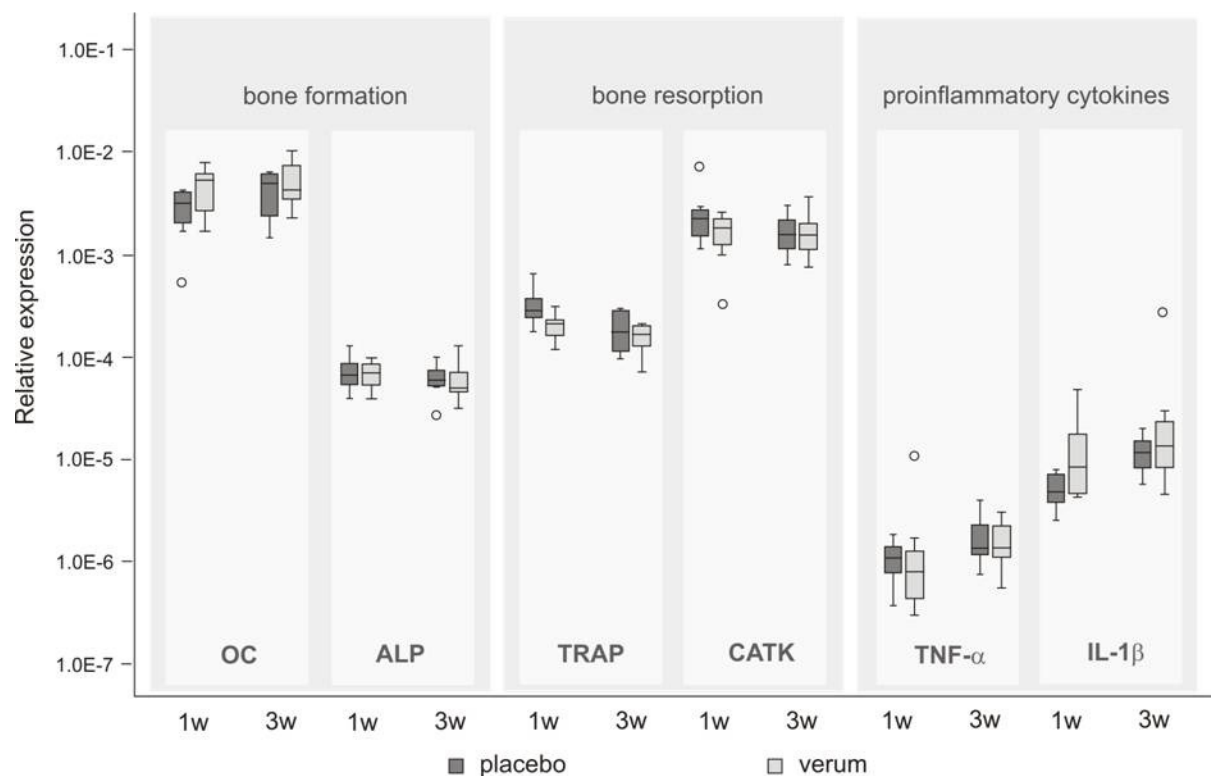


Figure 5.31: Gene expression in rat bone. The total (normalized) relative expression levels of bone formation, bone resorption and proinflammatory markers (log-scale).

5.8.6 Histological analysis

In Figure 5.32, a light optical micrograph of a placebo bone cement plug is presented which shows tissue-implant interface and implant position in rat bone. Qualitative evaluation of histological sections revealed that all plugs were appropriately positioned in the tibial metaphysis.

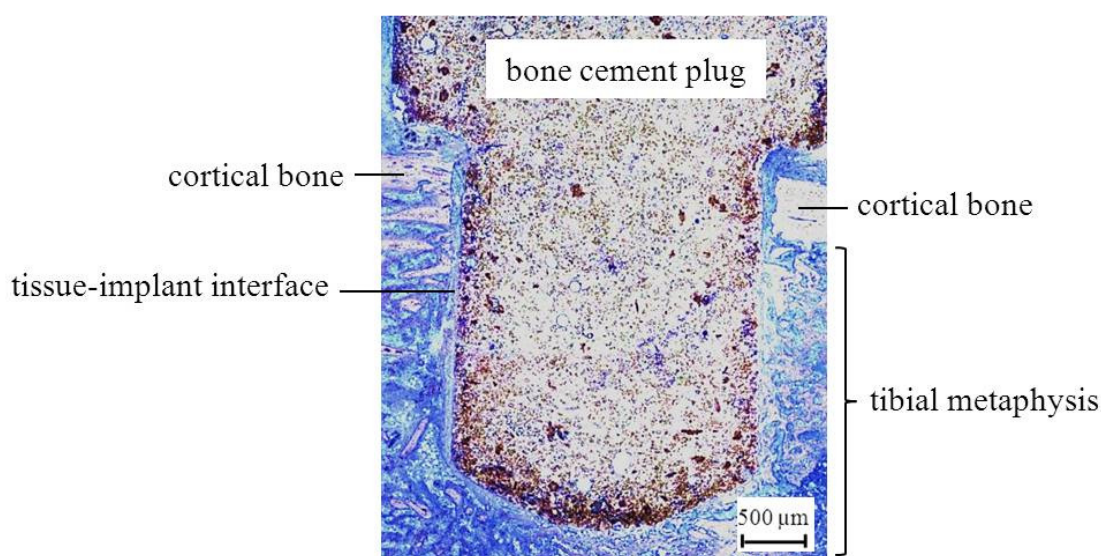


Figure 5.32: Light optical micrograph of an implanted placebo bone cement plug after one week.

Figure 5.33 illustrates a detailed insight into the tissue-implant interface of placebo and verum plugs after one week and how to differentiate old and new bone (Figure 5.33 c). Bone tissue surrounded both implant types and was frequently seen in direct contact with the implant surfaces (Figure 5.33 a and b). No qualitative differences were found between the two types of implants. No adverse tissue reactions were seen in both, verum and placebo implant groups, providing proof for being biocompatible.

No differences regarding bone area and bone-implant contact were observed after one week using qualitative comparison of histological sections of both implant types (Figure 5.33 a and b).

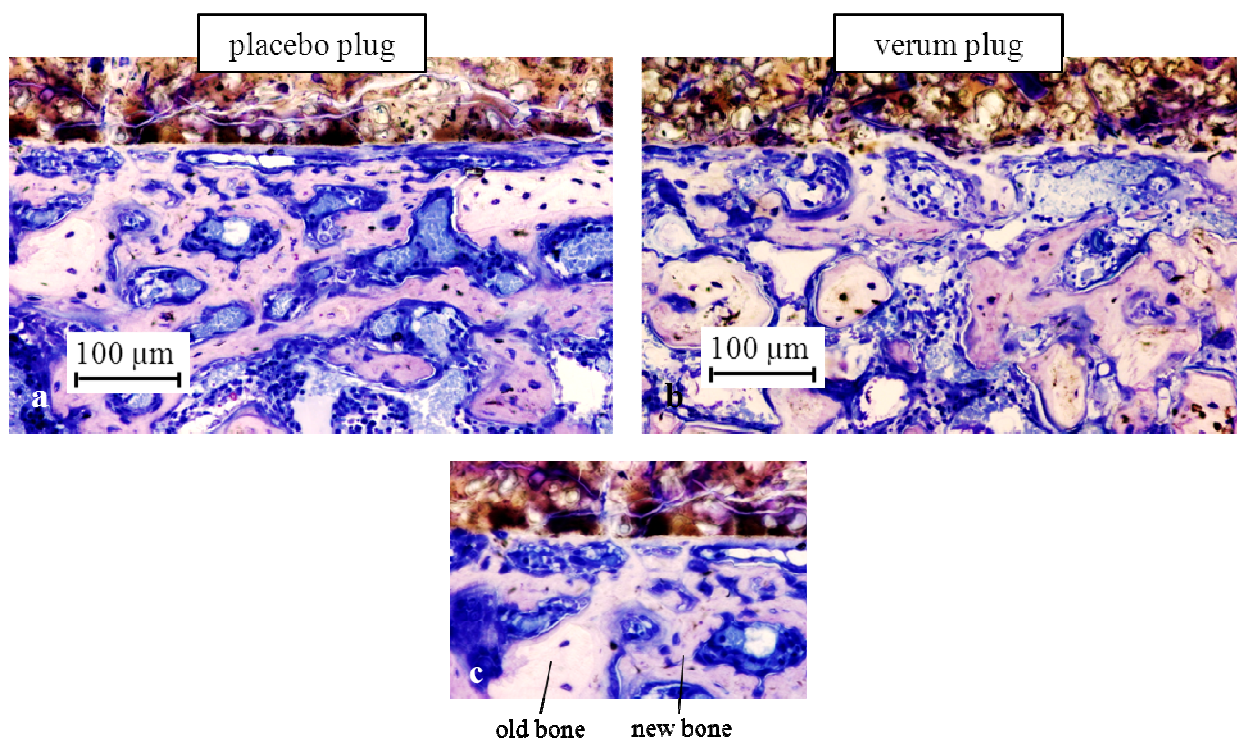


Figure 5.33: Light optical micrographs of a placebo (a) and a verum plug (b) after one week and how to differentiate old and new bone (c).

A qualitative difference in the amount of bone area was detected by comparing verum and placebo plugs after three weeks (Figure 5.34). At the direct tissue-implant interface more bone could be seen at verum plugs (Figure 5.34 a compared to b).

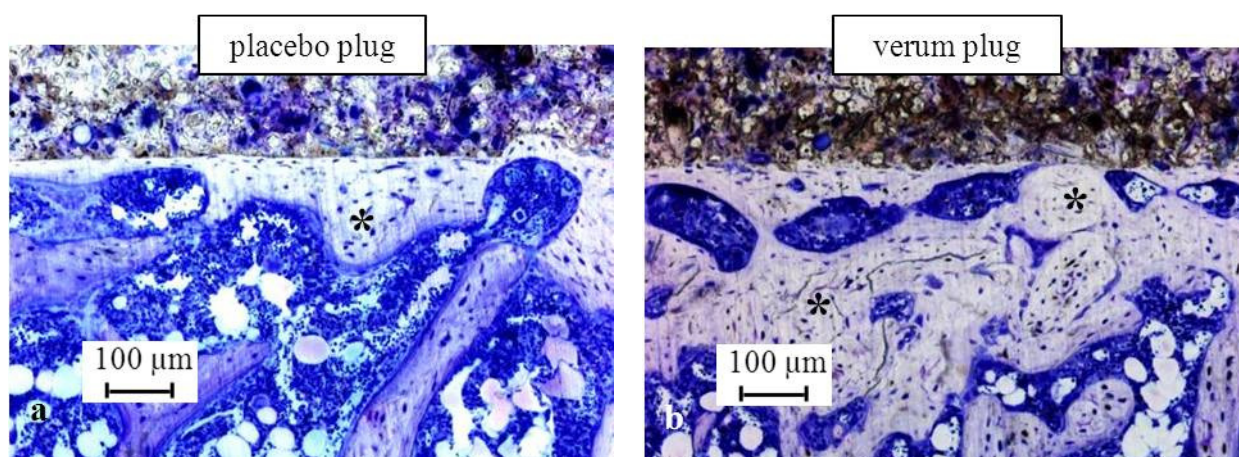


Figure 5.34: Light optical micrographs of placebo (a) and verum plug (b) after three weeks (new bone ()).*

For more objective evaluation, an additional semi-quantitative histopathological analysis was performed [163]. The results are summarized in Table 5.3 and Table 5.4.

Adjacent to placebo (one and three weeks) and verum plugs (one week), a slight grade of macrophages and osteoclast-like cells was observed. Close to the verum plugs (three weeks), no macrophages and a slight grade of healthy osteoclast-like cells could be documented. After one week, a slight to moderate (placebo) and a slight grade (verum) of fibroplasia was formed around the implants. The signs of fibroplasia could not be identified after three weeks for both implant types. None of the samples showed fibrin infiltration, osteolysis or degradation. Around both implant types a moderate (one week) and a marked grade (three weeks) of osteointegration and osteoconduction with mineralized bone was observed. All samples indicated marked osteoblastic activity with a moderate level of bone density. No signs of bone remodelling were evaluated at the implants after one week. However, slight signs of remodelling were detected for both implant types after three weeks. Generally, no material degradation occurred. Only for placebo plugs (three weeks), a slight sign of material degradation could be seen.

As a conclusion, no abnormal signs of inflammation or cytotoxicity could be evaluated around the plugs after one and three weeks. To a certain level, osteoclasts were observed in both groups and time intervals. Smaller amounts of macrophages were detected around the verum implant at three weeks.

Table 5.3: Semi-quantitative histopathological analysis of different cell types and their response (errors = standard deviation).

Time point	Implant type	Polymorphonuclear cells Lymphocytes Plasma cells Necrosis Fatty infiltrate Osteolysis Cells or tissue degradation Fibrin Encapsulation	Macrophages	Giant cells/ osteoclastic cells	Fibroplasia	Fibrosis	Osteoclastic cells
1w	Placebo	0.0 ± 0.0	1.0 ± 0.0	0.0 ± 0.0	1.3 ± 0.5	0.0 ± 0.0	0.8 ± 0.4
	Verum	0.0 ± 0.0	1.0 ± 0.0	0.1 ± 0.3	1.0 ± 0.0	0.3 ± 0.5	0.9 ± 0.3
3w	Placebo	0.0 ± 0.0	0.8 ± 0.4	0.3 ± 0.5	0.0 ± 0.0	0.0 ± 0.0	0.9 ± 0.3
	Verum	0.0 ± 0.0	0.0 ± 0.0	0.0 ± 0.0	0.0 ± 0.0	0.0 ± 0.0	1.0 ± 0.0

Index: 0 = absent, 1 = slight, 2 = moderate, 3 = marked, 4 = severe

Table 5.4: Semi-quantitative histopathological analysis of different performance parameter (errors = standard deviation).

Time point	Implant type	Osteo-integration	Woven bone	Osteoblastic cells	Osteo-conduction	Bone density	Neovessels	Bone marrow	Material degradation	Signs of bone remodelling
1w	Placebo	2.0 ± 0.0	2.0 ± 0.0	2.9 ± 0.3	2.0 ± 0.0	2.0 ± 0.0	3.0 ± 0.0	2.0 ± 0.0	0.0 ± 0.0	0.0 ± 0.0
	Verum	2.0 ± 0.0	2.0 ± 0.0	3.0 ± 0.0	2.0 ± 0.0	2.0 ± 0.0	3.0 ± 0.0	2.0 ± 0.0	0.0 ± 0.0	0.0 ± 0.0
3w	Placebo	3.0 ± 0.0	0.0 ± 0.0	2.7 ± 0.5	3.0 ± 0.0	1.8 ± 0.4	3.0 ± 0.0	2.0 ± 0.0	0.7 ± 0.5	1.0 ± 0.0
	Verum	3.0 ± 0.0	0.0 ± 0.0	3.0 ± 0.0	3.0 ± 0.0	2.0 ± 0.0	3.0 ± 0.0	2.0 ± 0.0	0.1 ± 0.3	1.0 ± 0.0

Index: 0 = absent, 1 = slight, 2 = moderate, 3 = marked, 4 = severe

5.8.7 Histomorphometry

A histomorphometrical analysis was performed to gain objective data of total bone area (BA) and bone-implant contact (BIC) for both implant types.

In Figure 5.35 a, the total BIC of placebo and verum plugs after one and three weeks implantation is shown. A total BIC of 41.18% after one week was evaluated for the placebo plug and 42.61% for the verum plug which indicated no significant differences (Figure 5.35 a). After three weeks a significant increase of BIC was detected for both implant types, but with a stronger correlation for the verum group. The BIC after three weeks resulted in 62.02% for the placebo plugs and 69.69% for the verum plugs. Comparing placebo and verum plugs after three weeks of implantation significantly increased values were measured for verum plugs ($p = 0.029$).

In addition to total BIC, the total bone area of the two implant types and time points were evaluated. The data for bone area comparing areas closer (0-250 μm) and at a distance (250-500 μm) to the plug length are shown in Table 5.5. Comparable amounts of bone area were found close to the implant (0-250 μm) and at a distance (250-500 μm) around both implant types after one week. After three weeks, more bone area was found close (0-250 μm) to both, verum and placebo plugs. Additionally, there was more bone area at 0-250 μm and 250-500 μm distances from the verum plug length in comparison to the placebo plug after three weeks (Table 5.5).

Table 5.5: Bone area (%) comparing areas closer (0-250 μm) and at a distance (250-500 μm) to the plug length (errors = standard deviation).

		BA at 0-250 μm distance (%)	BA at 250-500 μm distance (%)
1w	placebo	50.90 \pm 6.46	51.45 \pm 8.05
	verum	51.44 \pm 10.16	52.93 \pm 8.30
3w	placebo	46.26 \pm 6.84	38.98 \pm 10.51
	verum	72.27 \pm 6.38	60.12 \pm 5.61

In Figure 5.35 b, the total bone area of placebo and verum plugs after one and three weeks implantation is shown. A total bone area of 51.18% after one week was evaluated for the placebo plug and 52.19% for the verum formulation which indicated no significant differences (Figure 5.35 b). After three weeks, the total bone area was significantly decreased ($p = 0.019$) to 42.62% for the placebo formulation and significantly increased ($p < 0.001$) to 66.19% for the verum group. Highly significant differences were observed for total bone area when comparing placebo and verum group after three weeks ($p < 0.001$).

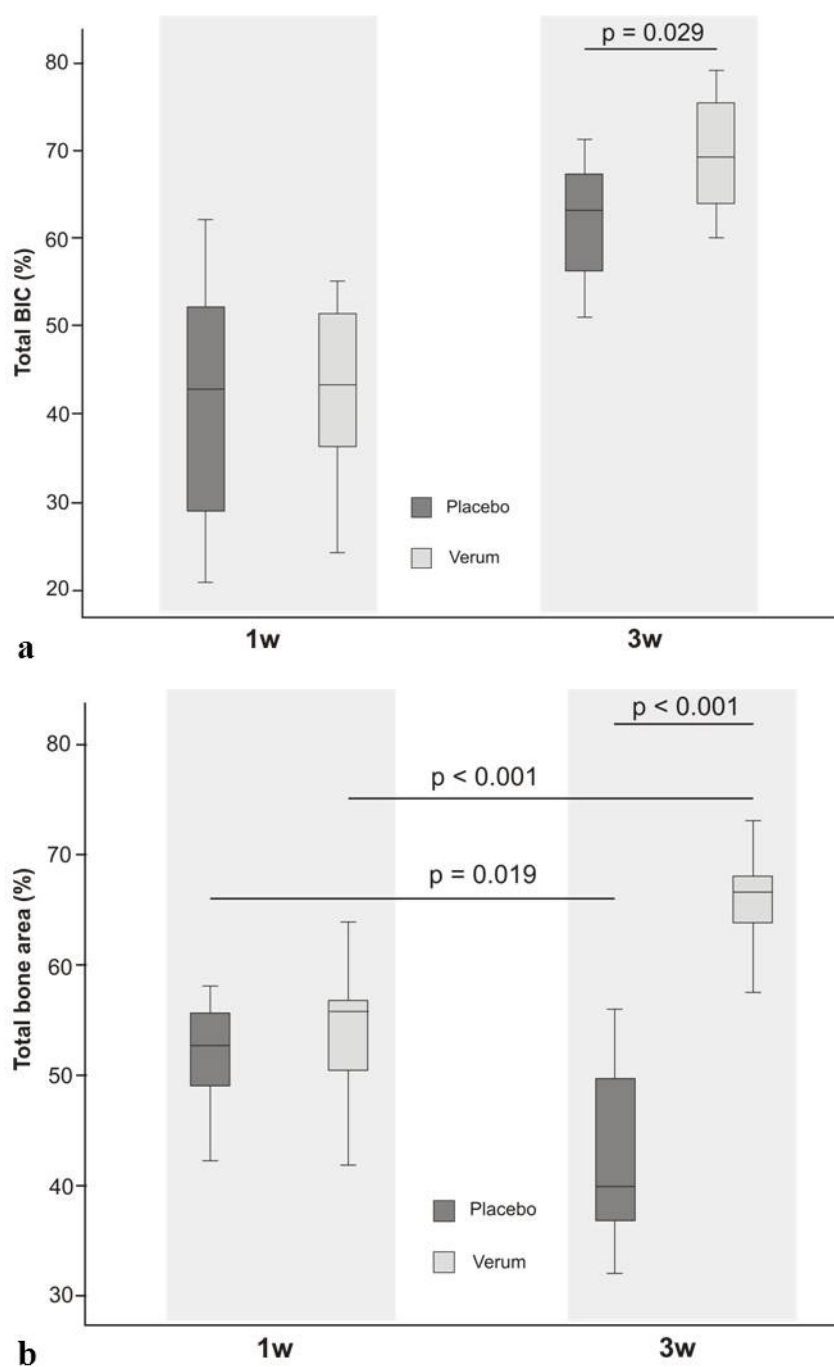


Figure 5.35: Histomorphometric evaluation of total bone implant contact (%) (a) and total bone area (%) (b) out of placebo compared to verum plugs after one and three weeks after implantation.

6 Discussion

The development of drug-loaded medical devices is challenging and based on a careful and comprehensive basic research. The objective of the present thesis was to develop calcium phosphate based drug delivery systems for local application of zoledronic acid (ZOL). For this kind of development many requirements have to be fulfilled. Firstly, the potential ability of a calcium phosphate to be an adequate drug carrier has to be verified. Appropriate analytics for ZOL detection and an adequate drug loading technique have to be established. Furthermore, the system has to release suitable doses of the drug without being cytotoxic. These must also ensure that the original intended use of the medical device is maintained. Finally, an *in vivo* animal model for the selected bone cement implants has to be developed and a study conducted which is capable of generating data for drug-loaded devices that will enable basic conclusions to be drawn. All the above mentioned analyses were described by a variety of methods and the results will now be critically reviewed.

6.1 Physico-chemical characterisation

The first objective of the present thesis was to evaluate the feasibility of different calcium phosphate based bioceramics to be drug carriers. Several parameters can influence both, drug loading and release properties. An adequate investigation and analysis of different physico-chemical properties of each bone substitute material was required in order to evaluate their suitability to be part of an innovative local drug delivery system. The choice of bone substitute materials represents three common forms of materials: solid, granular and an injectable paste that sets *in situ*. They were characterized by using a number of investigative methods such as light microscopy, scanning electron microscopy, true density, surface area measurement, dynamic vapour sorption, and pH value determination.

Light microscopy and SEM were seen to be adequate and practical methods to assess qualitative properties in the present study. The materials investigated varied in porosity, pore structure, pore- and crystal size which was an interesting basis for identifying a sufficient ZOL carrier. The true density of the different materials was slightly higher than that of normal human cortical bone and substantially higher than trabecular or osteoporotic bone density [173]. Surface area measurements were an indicator for the potential amount of drug adsorption onto the surface of the materials. A high surface area resulted in a higher drug adsorption onto the material surfaces. This relation might be beneficial if the use as a drug carrier is intended. A reduced surface area of the used materials is probably induced by sintering of micro- and macropores during the manufacturing process. All used bone substitutes offered specific surface areas less than $1 \text{ m}^2/\text{g}$ without an interconnective pore system. This is of the same order as for other hydroxyapatite ceramics [174-177]. In comparison to natural bone mineral the measured surface areas are much lower. Natural bone mineral has a specific surface area of about $87\text{-}100 \text{ m}^2/\text{g}$ [178, 179]. The specific surface area of synthetic, non-sintered hydroxyapatite materials are reported to be in a range of $17\text{-}82 \text{ m}^2/\text{g}$ [178, 179]. In addition, the specific surface area is important for the ingrowth of new bone. On the one hand, a small surface area is a disadvantage for the incorporation of drugs by adsorption; on the other hand, natural variability of porosity, density, surface structures and chemical compositions can be avoided by using sintered bone substitute materials. Although the specific surface area was less $1 \text{ m}^2/\text{g}$ without an interconnecting pore system, the results suggested enough diffusion pathways for ZOL adsorption and release. Small micropores could even be exploited for controlling drug release which is an important parameter for a use of a bone substitute as a drug carrier. Such ceramic materials are highly crystalline and indicate a substantially slower remodelling than natural bone [21, 180]. These characteristics might be beneficial for the development of prolonged ZOL

release systems. Water sorption kinetics of LagFix[®] cylinder and BoneSave[®] material showed low water uptake. A dipping process in an aqueous environment should not have any impact on material changes of both bone substitute materials. HydroSet[®] powder had a water uptake of up to 3% and a mass increase at 90% RH which could be caused by material changes. These data led to the conclusion that drug incorporation by dipping in an aqueous solution might have an influence to the physical and hardening properties of HydroSet[®] powder. Ionic release, leading to an alkaline milieu, can explain possible interaction between ZOL and the bone substitute materials. Bone ceramics can increase pH values [180] which was also observed for the materials tested. BoneSave[®] reacted as a base even after several neutralisations. This fact could influence adsorption, homogeneity of drug loading, solubility and stability of the drug. Sharpe et al. reported on influenced protein adsorption through changes of pH values [181]. Such findings are not reported for ZOL and could not be confirmed during the present investigations. In summary, physico-chemical properties of the ceramics demonstrated that they are appropriate for use in drug delivery applications.

6.2 Analytics of ZOL

An appropriate analytics for the detection of ZOL had to be established. For this purpose, a HPLC method was developed. An ion-pair method was adapted to an already published method for ZOL detection by HPLC [182]. Such an isocratic ion-pair HPLC method is generally suitable for ZOL detection, especially for stability tests [183]. ZOL contains two phospho acid groups. Their polarity is too strong to retain on non polar stationary phase such as RP-18 column. As a consequence of the poor interaction with the column, the retention time of ZOL was short. Therefore, an ion exchange liquid chromatographic method was required for the analysis [182]. The addition of tetrabutylammonium hydrogen sulphate as ion-pair for ZOL enhanced the hydrophobicity in the mobile phase and enabled the detection of ZOL.

During *in vitro* release studies, HPLC measurements in later test samples were mainly limited by the detection limit of ZOL. Data for release rates less than the LOD could not be quantified and are not shown. The amount of aqueous ZOL solution, also when released from a calcium phosphate carrier, can be detected with the established HPLC method. Due to high standard deviations of very low concentrated drug solutions, it was not possible to quantify values less than the evaluated LOD which is a limitation. In comparison, other bisphosphonates with free amino groups (such as alendronate, palmidronate) can be labelled pre- or post-column with a fluorochrome to allow HPLC analysis with fluorescence detection being highly sensitive [184, 185]. ZOL could not easily be derivatized and UV absorbance was too weak for sensitive detection in column eluates. Sensitivity of chelate formations with aluminium-morin or iron resulted in weak signals. A liquid chromatography method coupled with mass spectrometry (LC/MS/MS) might be more sensitive, but requires a lot of effort to establish [186]. It was attempted to establish a LC-MS analytic for ZOL but this led to irreproducible data and could not be used. The analytical work on ZOL revealed

a number of difficulties. An alternative method for a more sensitive LOD of ZOL might be radioactive labelling of ZOL [187]; however, this would very likely induce changes in drug molecular weight and consequently might cause different affinity to and drug release from the bioceramics under investigation.

Accordingly, the HPLC method established was concluded to be the method of choice and led to reproducible results.

6.3 Drug load

Another objective was to develop a straight forward approach for combining ZOL with bone substitute materials using short-term dipping technique. This approach could be promising for a clinical application in terms of loading bone substitutes directly prior or during surgery with a defined drug content. Another goal was to evaluate the materials with respect to their ZOL loading capacity in a time and concentration dependent manner.

The loading procedure must ensure that an appropriate target load and drug release from the ceramic materials is obtained. Some studies are published dealing with the combination of ceramics with ZOL. Prior to discussing the influence of drug dipping concentrations and dipping times, it is essential to look at the target load and release of ZOL for an enhanced bone formation and reduced bone resorption *in vivo*. The target drug release seems to be in the low μg -range as ZOL is a highly potent bisphosphonate moiety [154, 155, 188-190]. Some investigators have shown that osteoblast proliferation is induced by ZOL at a concentration of 0.5×10^{-3} mmol and greater, and that osteoblast survival was significantly decreased at 0.05 mmol of ZOL [191, 192]. Seo et al. demonstrated that ZOL reduces unwanted bone resorption in intercalary bone allografts. The optimal soaking concentration for the allografts was 0.03 mmol ZOL with a significant increase in bone mass density [189]. Tanzer et al. reported bone augmentation around and within porous implants with local ZOL elution of a formulation with 0.05 mg ZOL [193]. Additionally, there are investigations that

demonstrate enhanced local bone formation for up to one year after surgery by direct elution of ZOL from porous implants [194]. Other studies only show such an effect for up to twelve weeks post-surgery [155, 193]. At the present time, there is no exact ZOL target release rate, or dose for an optimal effect known to date. Finding the most effective ZOL dosage for a bone substitute material would have to be performed in an *in vivo* dose assessment study and can not be evaluated *in vitro*. Peter et al. reported on increased mechanical implant fixation by local delivery of ZOL. The drug was added to a hydroxyapatite coating by dipping in differently concentrated ZOL solutions. The dipping concentrations used in this study were adapted from these investigations [155]. The present investigation creates a basis for the development of new drug delivery carriers, which can easily be loaded with relevant ZOL doses in a controlled manner by defined dipping technique. As demonstrated, an appropriate target ZOL load could be obtained after a dipping time of 5 minutes. The ZOL load of the materials is a function of the surface area, exemplarily shown for the BoneSave[®] material. The surface area and ZOL incorporation could be increased by milling. Experiments with the differently sized fractions and drug concentrations indicated a critical surface area for a full ZOL adsorption by dipping at defined conditions. An almost complete drug adsorption could be achieved by dipping the materials in 5 mL 2.25×10^{-5} and 2.25×10^{-6} molar ZOL solution, respectively. The different materials had different loading capacities for ZOL. The drug loading depended on the material shape, the sample weight and surface area. The results demonstrated the feasibility of controlled loading of the different shaped bone substitutes by short-term dipping. Controlled drug loading of small HydroSet[®] particles ($x_{50} = 21 \pm 0.4 \mu\text{m}$) was feasible over dipping time and concentration of drug solution. In conclusion, an appropriate and controlled drug load can be achieved by both, dipping time and drug concentration. The drug loading experiments demonstrated the feasibility of controlled, reproducible and homogeneous incorporation of ZOL into all materials. A short-term dipping

technique could be promising for a clinical application in terms of loading bone substitutes directly prior or during surgery with defined drug content as also suggested by Aberg et al. [188].

6.4 Drug release

Another aim was to assess the bone substitutes as release systems for ZOL through an *in vitro* approach.

In addition to assuring a target drug load, drug release rates are equally important and are an indicator for ZOL affinity to each material. The *in vitro* drug release kinetics of the materials were found to be similar, but differed in total release amounts. During release studies, the release of ZOL from the materials was measured for the first 30 minutes. The release rates at later test occasions were mainly limited by the detection limit of ZOL with the used HPLC. Data for release rates less than the LOD could not be quantified and are not shown. For later release time points very low ZOL release rates were concluded due to high affinity to the materials and, accordingly, not fully released drug from the materials. The optimal test of release rates and drug efficacy would require an *in vivo* investigation to determine beneficial biological effects. A major issue with *in vitro* drug release kinetics is the correlation to an *in vivo* environment. Conventional drug delivery methods allow the detection of released drug amount, but not drug location or adsorption of released drug to the surrounding bone tissue. The correlation of released drug amount by detection with conventional drug release methods to drug release *in vivo* is not feasible. To evaluate drug load and release rates from powder formulations a special technique was developed. A difficulty of drug release tests from powder formulations was the full removal of ZOL solution after the loading procedure. This fact could explain the high release rates for early time points. The BoneSave[®] 63-90 μm fraction demonstrated the highest ZOL load by short-term dipping compared to the other investigated bioceramics which demonstrated a

high affinity of ZOL to the BoneSave[®] material. Compared to the other BoneSave[®] fractions, the 63-90 μm fraction showed the highest ZOL release *in vitro* which is explained by the larger surface area and better release pathways for ZOL from milled material. With all other BoneSave[®] fractions, the release of ZOL in the *in vitro* investigations was less. The ZOL release per surface area showed a similar range for all used BoneSave[®] materials. This demonstrated that the affinity of ZOL to the material is based on material properties. A higher affinity of ZOL to BoneSave[®] materials compared to HydroSet[®] powder was shown by a higher ZOL release per surface area from HydroSet[®] powder compared to BoneSave[®] material. The low release rates of LagFix[®] cylinder in the first 30 minutes *in vitro* could be explained by the small surface area. The high drug loads and adequate release rates of HydroSet[®] powder suggested that it is feasible to develop a potent drug loaded medical device with acceptable ZOL release rates. However, the correlation of released drug amount *in vitro* to drug release *in vivo* is not feasible. Accordingly, the next step should be to gain *in vivo* confirmation of the efficacy of locally delivered ZOL from a HydroSet[®] carrier.

The development of a drug delivery system is not limited to the use of cement. The *in vitro* findings of ZOL adsorption in relevant doses and the demonstrated release profile from HydroSet[®] powder could also be a promising basis for the development of an efficient pre-shaped calcium phosphate drug carrier. A study could be designed to prove the concept of drug delivery by applying a drug impregnated, moulded HydroSet[®] cement formulation into a cancellous bone defect.

6.5 Stability

A further objective was to determine the stability of ZOL under different storage conditions and to identify a method for enhanced drug stability.

Stability is defined by the time over which a drug retains its integrity in terms of quantity and chemical identity. It can be affected by environmental factors such as temperature, pH, humidity, light, and air [195]. Unfortunately, due to analytical difficulties, ZOL could not be detected in a pH-dependent stability experiment. One of the most important factors that can influence the degradation rate of drugs or stability is temperature [196]. Temperature is a factor that is difficult to control during transport and storage unless a controlled supply chain is utilised. For drug loading experiments in the present thesis, the different bone substitutes were dipped in an aqueous ZOL solution. Therefore, it was important to know how stable an aqueous ZOL solution was during storage at different temperatures and what influence the storage material had. Any degradation and hydrolysis products were detected by evaluation of HPLC peak areas and three-dimensional scans. It should be noted that the presented stability study did not consider sterility and only evaluated chemical stability of ZOL solutions.

Stability data demonstrated temperature dependency during storage and loss of ZOL activity in an aqueous solution when stored in glass vials. ZOL instability was detected particularly at higher temperatures. Under experimental conditions, ZOL seemed to react to something which could not be visualized with the three-dimensional HPLC scans. No additional peaks could be identified in the corresponding scans. Due to this result, it was considered necessary to evaluate other opportunities to ensure adequate drug stability when loading bone substitutes with ZOL.

The stability under different storage conditions demonstrated no major loss of ZOL in an aqueous solution when stored in a plastic vial under a range of different temperatures. The results indicated that ZOL seemed to be more stable

in plastic vials compared to glass vials. It was concluded that glass had an impact on ZOL stability. Bisphosphonates have chelating properties which are reported to be similar to those of EDTA [197]. ZOL might chelate cations out of glass to form complexes. According to current knowledge, no studies are published dealing with the storage issues associated with ZOL. Nakamura et al. reported about the stability of minodronate whose structure is related to ZOL. The group supported the hypothesis that minodronic acid and aluminium ions apparently leached from glass of ampoules build a complex that precipitates [198-200].

In case of an intraoperative loading of bone substitutes, it is important to prepare a ZOL solution immediately. Unfortunately, it is not possible to dissolve crystalline ZOL powder by adding water in an acceptable time period due to a very low intrinsic dissolution of ZOL. The challenge was to develop a dry ZOL formulation with a sufficient stability. It was necessary to look for pharmaceutical technologies being applicable for both, stabilizing ZOL and dissolving the drug immediately. A lyophilisation technique was demonstrated to be suitable for stabilization of ZOL. Lyophilisation is a process in which even thermolabile drugs can be successfully formulated almost without any loss of drug activity [201]. The resulting product has a very porous structure and excellent rehydration properties. Furthermore, the process is suitable for the preparation of sterile products [202]. To ensure adequate stability, most drugs need an additional excipient during the lyophilisation process. Conventional excipients are often divided into matrix former and stabilizers. A common matrix former substance is mannitol [203]. Sucrose and trehalose are often used as stabilizer substances [204, 205]. All presented formulations demonstrated sufficient drug stability of more than 98% during storage time of 180 days. However, only mannitol lyophilisates showed a stable network without collapsing. There may be options to use a mannitol-based lyophilisate for the preparation of an aqueous ZOL solution which can then be used for dipping

bone substitutes. The ZOL lyophilisates demonstrated promising stability and dissolved immediately in water. Presumably, the state of ZOL in the freeze-dried formulations was amorphous but this was not further analysed.

In conclusion, storage of ZOL in glass tubes could have an impact on the drug stability. For adequate storage stability, no glass vials or glass fibres should be used because of interaction between ZOL and glass. Generally, for sufficient stability during storage, especially for liquid formulations, attention must be paid to a chelate formation of ZOL with polyvalent ions. To find a suitable storage container for liquid ZOL formulations would be challenging.

6.6 *In vitro* cytotoxicity

Cytotoxicity tests were performed to gain information about dose-dependent cytotoxic effects of ZOL and if any cytotoxic effects could be expected by using verum and placebo implants for the *in vivo* study.

The MTT assay is a useful and sensitive test for the determination of the acute toxicity of excipients in an *in vitro* system based on Calu-3 cells [161]. Cellular viability depends on medium conditions such as pH value and osmolarity as well as it is a substance characteristic. The influence of these parameters could be demonstrated by the present results. In the first test, ZOL was dissolved in water without adjusting pH and osmolarity. Non adjusted osmolarity of the samples would explain the toxic effect on the cells. It is known that the maximum viability of the Calu-3 cell line used for the present investigations, is maintained at a pH of 6-7 and an osmolarity of 290-390 mosmol [161]. A pH dependency on Calu-3 cell viability could be seen in the second test series with iso-osmolar ZOL solutions. ZOL reacts acidic in aqueous solutions. However, a toxic effect to cell viability could not be seen up to a ZOL concentration of 60 µg/mL and a pH value of more than 4.3. The third test series with high cell viabilities confirmed the expectation of a pH and osmolarity dependency of Calu-3 cells.

Some *in vitro* data showed toxic effects on cells exposed to bisphosphonates

[206]. Zwolak et al. demonstrated that ZOL decreased the number of viable cells in a dose-dependent manner when released from a bone cement formulation [140]. They used concentrations in a range of 100 μg up to 1000 μg per 1.5 cm^3 bone cement and concluded the inhibition of *in vitro* growth of cell lines from giant cell tumor of bone, myeloma, and renal cell carcinoma. A dose-dependent decrease of cell viability could not be found within the present cytotoxicity results for ZOL samples in which pH and osmolarity was adjusted.

An additional major objective of the *in vitro* cytotoxicity test was to find out if the ZOL concentration of verum implants for the animal study show any toxicity to Calu-3 cells. The HydroSet[®] verum plugs used for the *in vivo* study, were loaded with 50 μg ZOL. The present investigation showed that the HydroSet[®] bone cement without ZOL as well as drug-loaded bone cement did not affect the number of viable Calu-3 cells. As a conclusion out of the *in vitro* cytotoxicity tests, no toxic effect for verum and placebo plugs were expected for the upcoming *in vivo* study.

6.7 Characterisation of modified HydroSet[®] formulations

A characterisation of modified cement formulations had to be performed to design an applicable implant for an animal model.

The *in vitro* findings of ZOL adsorption in appropriate doses and the shown release profile from HydroSet[®] powder were a promising base for the development of an efficient pre-shaped drug-loaded calcium phosphate bone cement carrier. Thus, a feasibility study was initiated intended to gain first *in vivo* experience about the efficacy of locally applied ZOL out of a HydroSet[®] carrier. The approach was to ensure the original intended use of HydroSet[®] powder as self-setting cement.

In this part, the impact of a loading technique on cement properties had to be evaluated. The question of how to load HydroSet[®] powder without changing the normal setting reaction had to be answered. The presented semi-quantitative data out of the wetting experiments demonstrated that HydroSet[®] powder had to be mixed with at least 25% additional water in order to make sure that the powder was fully surrounded with water. To ensure a homogenous drug distribution, the powder particles had to be fully surrounded with an aqueous ZOL solution. The data from cement hardness measurements demonstrated that no hardening process occurred when 30% water was added to the HydroSet[®] powder. In conclusion, it would not be possible to add HydroSet[®] powder to an aqueous ZOL solution and then mix the suspension with the HydroSet[®] hardening solution without influencing the hardness of the cement. Furthermore, there was also no hardening when mixing an already ZOL-loaded and dried HydroSet[®] powder with the corresponding hardening solution. Hence, it was not possible to have a normal hardening process when loading HydroSet[®] powder in an aqueous ZOL solution with a dipping technique. It was possible to drug load HydroSet[®] powder by adding small volumes of a highly concentrated ZOL solution to the mixture of powder and hardening solution without influencing

the normal setting reaction. Generally, the results were in line with expectations. Additional water retarded the hardening process which resulted in softer cement formulation. Even DVS data supported the conclusion that drug incorporation by dipping in an aqueous solution might have an influence on the physical and hardening properties of HydroSet[®] powder and on the setting reaction. However, an alternative ZOL loading technique for HydroSet[®] cement had to be developed. In best case, ZOL had to be added to the system without additional water. The solubility of ZOL in the HydroSet[®] hardening solution could be sufficient to directly dissolve ZOL in the hardening solution without influencing the hardening properties of HydroSet[®] cement. The HydroSet[®] hardening solution is highly loaded with salts and it was therefore necessary to clarify whether enough ZOL can be dissolved. A semi-quantitative solubility of more than 10 mg/mL was sufficient for the manufacturing of HydroSet[®] verum plugs for an *in vivo* study.

In conclusion, the results demonstrated that no hardening process will occur when mixing dry HydroSet[®] powder (which is already loaded by dipping in an aqueous ZOL solution) and the HydroSet[®] hardening solution. A sufficient solubility of ZOL in the hardening solution provided an appropriate cement loading without a major impact on to cement setting reaction and the resulting hardness. For the manufacturing of ZOL-loaded HydroSet[®] plugs, the drug could be directly dissolved in the HydroSet[®] hardening solution.

6.8 *In vivo* animal study

The final objective of this thesis was to test the short-term *in vivo* efficacy of a ZOL loaded bone cement plug. After establishing a sufficient implant with an acceptable crushing strength, HydroSet[®] verum and placebo plugs were manufactured and tested *in vivo*. For this purpose, a bone defect model in the proximal tibia of rats was used. An *in vivo* study was conducted to gain experience on how to influence bone-implant contact, bone regeneration, and bone area around the implant in cancellous bone. The interpretation of a drug loading and releasing concept using a preshaped bone cement plug was supported by performing quantitative polymerase chain reaction (qPCR) and histological analysis.

The *in vivo* study illustrated an enhanced bone area and bone-implant contact for verum plugs after three weeks and suggested that ZOL was effectively released. Generally, hydroxyapatite or tricalcium phosphate coatings and bone substitute materials are widely used to improve the fixation of metallic implants to bone during the first weeks or months [20, 207, 208]. Previous investigations have demonstrated the feasibility of developing effective local drug delivery systems based on ceramic substances [22]. Several studies have shown an improved fixation and bone density of implants locally delivering bisphosphonates in bone, especially in rat bone [155, 157, 158, 193, 209-214]. Rat models have been used widely and can be considered a standard for testing the biological response of bone to implant materials in combination with bisphosphonates. In literature, most authors focus on describing the effect of bisphosphonates on the early bone formation and bone resorption in rats within the first three weeks [155, 157, 158, 210]. Therefore, it is appropriate to compare the present results with other investigations. A drawback of the rat model is the fact that the bone metabolism covering healing and remodelling is quite different from that described in humans [215]. Furthermore, the effects in osteoporotic bone

structures might be completely different and were not part of the present research. The ceramic structure of the manufactured hydroxyapatite cement plugs showed physico-chemical properties to be a candidate for controlled drug delivery purposes due to porosity, pore structure and variations in pore size, -shape and -distribution. The exact mechanism of ZOL release from hydroxyapatite bone cement plug has not yet been described. Generally, the release of drugs from calcium phosphate based drug delivery devices depend on the microstructure, the drug solubility, the type of bond between drug and matrix and the potential degradation mechanism of the matrix [20]. The plug degradation was not quantified, but a substantial degradation of the hydroxyapatite up to three weeks could not be detected. In conclusion, the plug represented a non-degradable matrix during the investigated time period. Caused by a non-degradable hydroxyapatite matrix, a ZOL release by diffusion across a concentration gradient to the surrounding microenvironment through pore structures of the moulded bone cement plug was supposed. Within the *in vivo* study, it was not possible to comment on the released ZOL amount to the surrounding tissue which is a limitation. Due to a high affinity of ZOL to hydroxyapatite, no adequate recovery method could be developed to quantify remaining drug content in verum plugs after explantation. However, the investigations presented the described biological effects of released ZOL out of a bone cement plug compared to a placebo plug.

The two main categories of bisphosphonates are non-nitrogen-containing and nitrogen-containing bisphosphonates [133]. Non-nitrogen-containing bisphosphonates are metabolized rapidly, whereas nitrogen-containing bisphosphonates are much more potent and are not metabolized [216]. Lin reported that bisphosphonates which are released from bone can be attached by an osteoclast, and are obviously not destroyed inside the osteoclast, but survive intact [206]. If the drug will be released intact after cell death, it might be beneficial to develop prolonged releasing ZOL formulations. A prolonged

release could ensure that a sufficient ZOL amount remains active locally at the required implantation site over a long and defined period of time. Dhert et al. demonstrated that the dominating biological process in the early postoperative period (three and seven days) is osteoclastic resorption of the interface bone, regardless of the implant type (calcium-phosphate coated or non-coated titanium implants). Two weeks after implantation bone along the implant surfaces had been resorbed [63]. The results of the present study gave information about the response of cortical and cancellous bone to a drug-loaded and non-loaded bone cement plug surface after one and three weeks postoperatively. The histomorphometrical evaluation was considered to be more reliable compared to histology and PCR analysis. The histomorphometric results demonstrated an early bone resorption process at our placebo group from one to three weeks which was indicated by a significant decrease in total bone area. Brånemark et al. found a decrease in the maximum torque of threaded implants compared to the direct postoperative situation in a study on cortical implant healing in rats after three weeks. This corresponds with the results of Dhert describing a decrease in bone-implant contact and thus confirms the presence of a critical postoperative period in terms of implant stability [217]. These results can be confirmed by the recent findings in the placebo group. After implantation, bone resorption may lead to a temporary reduction in bone-implant stability. Andersson et al. demonstrated a significantly increased mechanical implant fixation by immobilizing ZOL to a fibrinogen coated stainless steel implant after two and six weeks of implantation [209]. Such effects are also shown up to eight weeks postoperatively [211]. Histomorphometrical results received out of the verum group, demonstrated a significant increase in total bone area from one to three weeks, confirming the findings in the literature [129, 155, 158, 210, 211, 218]. Wermelin et al. described a long-term increase in mechanical pull-out of the bisphosphonate which is probably explained by a long-lasting influence on the local balance between bone resorption and formation [211]. Such long-term

effects were not part of the presented study, but are in the scope for further investigations.

The target drug release seems to be in a low μg -range as ZOL is a highly potent bisphosphonate moiety [154, 155, 188-190]. Main effects which are reported for ZOL were an induced osteoblast proliferation, a reduced bone resorption, an increase in bone mass density, and an enhanced local bone formation [189, 191-194]. In conclusion, to date, there is no target ZOL release rate for an optimal effect known and the optimal dose is still not defined. In the present study, the ZOL amount used in combination with the described hydroxyapatite cement could be beneficial to increase bone-implant contact and bone area. Local and adequate ZOL release could reduce early bone resorption and increase net bone formation to avoid early biological failures, which are reported after implantation. Biologically, the early time points after implantation are critical for implant stability [219, 220]. The findings of significant differences in total bone-implant contact and total bone area after three weeks for the verum group supported an inhibition of early bone resorption by a ZOL loaded bone cement plug.

Another topic in the present investigations was the ZOL effect at some distance from the plugs. Increased bone density at some distance from implants has also been described in the literature [157, 193]. Studies with ZOL coated implants showed that ZOL had a significant effect on bone remodelling for a distance of up to 400 μm [221]. Peter et al. reported about an increased bone density at 200 μm distance from hydroxyapatite coated implants with adherent bisphosphonate [155]. The effects of hydroxyapatite coated cylindrical implants on pull-out force showed that the density of bone in the 20 μm nearest to the implant was important for enhanced mechanical fixation [155]. The results of the present study demonstrated significantly higher total bone area at 0–250 μm distance from the verum plug length in comparison to the placebo plug after three weeks and confirmed in general, the findings in the literature

[155, 157, 193, 221].

Another important aspect was the toxicity of the released ZOL. In the literature it is described that ZOL may decrease the number of viable tumor cells in a dose-dependent manner [140]. In contrast, the results of the presented cytotoxicity test did not confirm a decreased number of viable cells for verum plugs. In the present *in vivo* study, a procedure for the analysis of gene expression of plug adherent cells in bone was used. The qPCR explored the differences in relative gene expression between verum and placebo plugs. During qPCR investigations, a significant higher level of 18S ribosomal RNA expression was determined in the placebo plugs after one and three weeks of implantation. A decreased cell number for the verum samples was indicated by lower 18S RNA expression. An explanation for the decreased viable cells could be the pharmacological action of ZOL in the mevalonate pathway which is involved in many key functions leading to the production of sterols such as cholesterol. These substances are essential for membrane formation [222, 223]. However, the amount of ZOL used in the present study is very low and thus, the risk of toxic effects on other cell types is suggested to be low which was also confirmed by *in vitro* cytotoxicity tests. Systemic effects or effects millimetres away from the implant are thought to be minimal. The gene used for normalization was 18S ribosomal RNA. GAPDH has frequently been considered as a constitutive reference gene and used to normalize changes in specific gene expression. GAPDH has shown to be up-regulated in many cancers and down-regulated by chemotherapeutic drugs like the bisphosphonate ZOL. Valenti et al. showed that GAPDH is inaccurate for normalizing mRNA levels in studies investigating the effect of bisphosphonates on gene expression and it should be avoided [224]. Considering the present results for GAPDH, the applied ZOL led to the same conclusion and was therefore not used as a gene for normalization. Nevertheless, no significant differences in gene expression of bone formation, bone response markers and proinflammatory cytokines in the 18S RNA

normalized data were found. Omar et al. demonstrated that implant surface properties influence protein-cell morphology, cell recruitment and gene expression at the immediate implant surface during the first 24 hours after implant insertion in bone. It was concluded that material surface properties rapidly modulate the expression of receptors which are crucial for the inflammatory and regenerative processes at implant surfaces *in vivo* [225]. With respect to significant differences of histomorphometrical results for verum plugs after three weeks, it is concluded that the chosen time points of the presented study were not adequate to demonstrate differences of biochemical markers with qPCR analysis. To determine differences in biochemical markers it might be necessary to analyse during the first 24 hours.

In conclusion, the results of the rat study suggest that locally administrated ZOL improves bone-implant contact and bone area in rats after three weeks. This also gave further insight into the short term beneficial effects of ZOL in enhancing bone-implant contact, bone regeneration and bone density in cancellous rat bone. However, the number of animals limited the statistical power of the study to detect possible differences between the groups. Furthermore, the dosage equivalence is still not known and further studies are needed to investigate the long-term and dose-dependent effects of locally induced ZOL on bone cement integration. Nevertheless, the ZOL-loaded HydroSet[®] bone cement formulation decreased the time period for resorption and provided a functional drug loading and release concept that resulted in enhanced bone formation. ZOL influenced the complex bone healing processes by reducing early bone resorption close to the implant surface whilst at the same time promoting bone formation.

7 Conclusion

The findings of the present thesis support the use of calcium phosphate-based bone substitute materials as effective and functional delivery systems for ZOL. The physico-chemical properties allow drug loading of solid, granular and injectable bioceramics with zoledronic acid (ZOL) and provide a better understanding of ZOL and calcium phosphate interactions. ZOL is shown to be adsorbed onto bone substitutes in a time and concentration dependent manner under defined conditions. Sufficient *in vitro* release rates, without cytotoxicity, enable development of a feasible and potent drug loaded medical device. The short-term dipping technique may be applicable for use in certain clinical applications allowing intraoperative loading with ZOL of bone substitutes. For reliable storage stability of ZOL, no glass vials or glass fibres can be used because of interaction between ZOL and glass. Furthermore, the *in vitro* findings were a promising basis for the development of an efficient pre-shaped calcium phosphate bone cement plug. This implant demonstrated the effectiveness of a local ZOL delivery concept intended to increase total bone-implant contact and bone area *in vivo*. Using a rat model, ZOL, presented in a hydroxyapatite bone cement plug significantly affected the bone regeneration process by reducing the effects of early bone resorption. The results, achieved in a tibial bone defect model, provided evidence that ZOL, locally administered from a calcium phosphate plug enhanced bone formation at the implantation site at an early stage. The results create a basis for further development of new drug delivery systems with controlled drug load and prolonged release. Overall, the bioceramics evaluated can be used as carrier systems for ZOL. However, further studies are needed to investigate dose-dependent and long-term effects of locally delivered ZOL on the *in vivo* performance of bone regeneration.

8 Abstract (summary)

Calcium phosphate-like bone substitute materials have a long history of successful orthopaedic applications such as bone void filling and augmentation. Based on the clinical indications, these materials may be loaded with active agents by adsorption offering a perspective for providing innovative drug delivery systems. The highly effective antiporotic, nitrogen-containing, bisphosphonate zoledronic acid (ZOL) demonstrated a strong affinity to calcium phosphates. It has been shown to significantly impact anabolic and catabolic pathways in bone remodelling towards reduction of osteoclast activity. The effects of locally applied ZOL on the early bone formation are of scientific and therapeutic interest, but still not fully understood. The local application of ZOL on implants is considered to support implant stabilisation by reducing early bone resorption. Support of early bone formation and reduction of bone resorption can be expected after implantation of bioceramics releasing ZOL.

The aim of the present thesis was to develop a feasible method for combining ZOL with bone substitutes by use of a dipping technique. The properties of three different materials (sintered body, granules and powder) were investigated to evaluate their potential as drug carriers for ZOL. This included the use of a range of physico-chemical methods such as light microscopy, scanning electron microscopy (SEM), true density, surface area measurement, dynamic vapour sorption (DVS), and pH value determination. In addition to the physico-chemical characterisation, the bone substitutes were evaluated for their ZOL loading capacity (time and concentration). Also, the materials were assessed as release systems in an *in vitro* study. Furthermore, ZOL stability under different storage conditions, cytotoxicity of ZOL with a cell line and a characterisation of modified cement formulations were performed to design a suitable implant for an animal model. In an *in vivo* study, ZOL was released from a drug-loaded preshaped calcium phosphate bone cement plug, which was implanted into a

bone defect in the proximal tibia of rats. The aim was to gain experience about the short term effects of ZOL on bone implant contact, bone regeneration and bone area. In a short term investigation, one and three weeks post operationem, tissue reactions as well as bone regeneration capabilities at the implant site were investigated by means of histological and imaging analysis. Furthermore, tissue samples, harvested at placebo and verum plug sites were used to analyse the gene expression of selected bone-specific markers. Levels of osteocalcin (OC), alkaline phosphatase (ALP), cathepsin K (CATK), tartrate-resistant acid phosphatase (TRAP), interleukin-1 β (IL-1 β) and tumor necrosis factor- α (TNF α) were determined by using quantitative polymerase chain reaction (qPCR). Data were normalized against 18S and GAPDH ribosomal subunits.

The results of the present thesis indicated differences between the bone substitute materials used and their potential use as a local drug delivery system in terms of physico-chemical properties, drug adsorption and release profiles. The *in vitro* investigations demonstrated a controlled ZOL load in a range of 0.04 – 1.86 $\mu\text{g}/\text{mg}$ material and a release of 0.02 – 0.18 $\mu\text{g}/\text{mg}$ within 30 minutes. The findings of the *in vivo* study showed that in the placebo interface a higher amount of cells could be detected as indicated by higher expression of small subunit ribosomal RNA (18S). Nevertheless, comparing the normalized data of the selected gene expression levels, no significant differences were detected. Histopathological analysis revealed no adverse tissue effects and provided evidence of biocompatibility for both implant types. The histomorphometric results showed a significantly higher bone to implant contact and bone area for ZOL loaded bone cement plug at three weeks after implantation. The study showed some significant differences in the biological tissue response to loaded and non-loaded bone cement plugs. In this model, ZOL was demonstrated to be effective in impacting the bone regeneration process towards reduction of early bone resorption and enhanced bone formation.

9 Summary (German version)

Calciumphosphat-basierte Knochenersatzmaterialien werden seit langem erfolgreich in der Orthopädie zur Füllung von Knochendefekten und zum Knochenaufbau eingesetzt. Diese Materialien könnten, je nach klinischer Indikation, durch Adsorption mit Arzneistoffen beladen werden, was eine Perspektive für innovative arzneistofffreisetzende Systeme darstellt. Das hochpotente, antiporotisch wirkende, stickstoffhaltige Bisphosphonat Zoledronsäure (ZOL) weist eine hohe Affinität zu Calciumphosphaten auf. Der Arzneistoff hat bereits einen signifikanten Einfluss auf anabole und katabole Stoffwechselfvorgänge während des Knochenumbaus hin zu einer reduzierten Osteoklastenaktivität gezeigt. Die Effekte von lokal applizierter ZOL auf die frühe Knochenneubildung sind von wissenschaftlichem und therapeutischem Interesse, bisher aber noch nicht vollständig verstanden. Eine gezielte, lokale Applikation von ZOL mit Hilfe eines Calciumphosphatträgers könnte zu einer verminderten Knochenresorption und einer erhöhten Knochenneubildung führen, wodurch ein Implantat gerade in einer frühen Heilungsphase stabilisiert werden könnte.

Das Ziel der vorliegenden Dissertation war es, eine einfach durchzuführende Beladungstechnik von Knochenersatzmaterialien mit ZOL zu entwickeln. Die Eigenschaften von drei verschiedenen Knochenersatzmaterialien wurden mit Hilfe einer Vielzahl von physiko-chemischen Methoden wie z.B. Lichtmikroskopie, Rasterelektronenmikroskopie, Dichtebestimmungen, Oberflächenbestimmungen, dynamischer Wassersorption und pH-Wert Bestimmungen charakterisiert, um die Möglichkeiten eines potenziellen Arzneistoffträgers zu ermitteln. Neben der physiko-chemischen Charakterisierung wurden die ZOL Beladungskapazitäten der verschiedenen Materialien zeit- und konzentrationsabhängig ermittelt. Zusätzlich wurden die *in vitro* Freisetzungskinetiken der beladenen Materialien bestimmt. Des Weiteren wurde die ZOL Stabilität unter verschiedenen Lagerungsbedingungen,

die Zytotoxizität auf eine Zelllinie und die Charakterisierung von modifizierten Zementformulierungen experimentell getestet, um ein geeignetes Implantat für einen Tierversuch zu entwickeln. In einer *in vivo* Studie wurde ZOL aus einem vorgeformten, arzneistoffbeladenen Calciumphosphat-Knochenzementimplantat freigesetzt, welches in die proximale Rattentibia implantiert wurde. Das Ziel war es, Kenntnis über die kurzzeitigen Effekte von ZOL in Bezug auf die Knochenimplantatkontaktfläche, die Knochenregeneration und die Knochenfläche zu erlangen. Innerhalb des Untersuchungszeitraumes von ein und drei Wochen nach Operation wurden sowohl Gewebereaktionen als auch Knochenregenerationsmöglichkeiten mit Hilfe von histologischen und bildgebenden Analysen untersucht. Ergänzend wurden Gewebeproben, die von Placebo- und Verumimplantaten entnommen wurden, einer Genexpressionsanalyse von ausgewählten knochenspezifischen Markern unterzogen. Die Konzentrationen von Osteocalcin (OC), Alkaliphosphatase (ALP), Kathepsin K (CATK), Tartrat-resistenter saurer Phosphatase (TRAP), Interleukin-1 β und Tumornekrosefaktor α wurden über ein quantitatives Polymerasekettenreaktionsverfahren (qPCR) bestimmt. Die Daten wurden gegen 18S und GAPDH ribosomale Untereinheiten normalisiert.

Die Ergebnisse der physiko-chemischen Untersuchungen, der Arzneistoffadsorption und der Freisetzungskinetiken der vorliegenden Arbeit zeigten Unterschiede der verwendeten Knochenersatzmaterialien im Gebrauch als lokales, arzneistofffreisetzendes System. Die *in vitro* Untersuchungen präsentierten die Möglichkeit einer kontrollierten ZOL Beladung in einem Bereich von 0,04 – 1,86 $\mu\text{g}/\text{mg}$ der jeweiligen Materialien und eine Freisetzung von 0,02 – 0,18 $\mu\text{g}/\text{mg}$ innerhalb von 30 Minuten. Die Ergebnisse der *in vivo* Studie zeigten, dass eine vermehrte Zellzahl an der Placebokontaktfläche ermittelt werden konnte, was aus einer höheren Expression der 18S RNA Untereinheit geschlussfolgert wurde. Beim Vergleich der normalisierten Daten der Genexpression konnten keine signifikanten Unterschiede ermittelt werden.

Eine histopathologische Auswertung ergab, dass keine nachteiligen Gewebereaktionen für beide Implantattypen nachgewiesen werden konnten, was die Vermutung einer guten Biokompatibilität unterstützt. Die histomorphometrischen Ergebnisse demonstrierten eine signifikant erhöhte Knochen-Implantat-Kontaktfläche und Knochenfläche für die ZOL-beladenen Implantate nach drei Wochen. Zusammengefasst konnten mit Hilfe der durchgeführten Tierstudie signifikante Unterschiede in der biologischen Gewebeantwort von ZOL-beladenen Knochenzementimplantaten gezeigt werden. In dem verwendeten Modell beeinflusste ZOL den Knochenregenerationsprozess hin zu einer Verringerung der frühen Knochenresorption und einer erhöhten Knochenneubildung.

10 Attachments

10.1 List of abbreviations

Ø	Diameter
°C	Degree celsius
µg	Microgram (10^{-6} gram)
µL	Microliter (10^{-6} liter)
ALP	Alkaline phosphatase
ATCC	American type culture collection
AU	Adsorption units
BA	Bone area
BET	Sorption isotherm equation according Brunauer, Emmet and Teller
BIC	Bone implant contact
BMD	Bone mineral density
BMP	Bone morphogenetic protein
BMU	Basic multicellular units
CaP	Calcium phosphate
CASO	Fluid soybean casein digest medium
CATK	Cathepsin K
cDNA	Complementary deoxyribonucleic acid
d	Days
DMF	Dimethylformamide
DVS	Dynamic vapour sorption
EDTA	Ethylenediaminetetraacetic acid
FGF	Fibroblast growth factor
FPP	Farnesyl diphosphate
FPPS	Farnesyl diphosphate synthase
g	Gram
GAPDH	Glyceraldehyde-3-phosphate dehydrogenase
GGP	Geranylgeranyl diphosphate
Gla	Gamma-carboxyglutamic acid residue

GTPases	Hydrolase enzyme
h	Hours
HBSS	Hanks buffered salt solution
HEPES	2-(4-(2-Hydroxyethyl)-1-piperaziny)-ethansulfon acid
HMG-CoA	Hydroxy-methylglutaryl-coenzym A
HPLC	High pressure liquid chromatography
IGF	Insulin-like growth factor
IL	Interleukin
ISO	International Organization for Standardization
L	Liter
LC	Liquid chromatography
LOD	Limit of detection
LOQ	Limit of quantification
mA	Milliampere (10^{-3} ampere)
MEM	Minimal essential medium
MeOH	Methanol
mg	Milligram (10^{-3} gram)
min	Minute
mL	Milliliter (10^{-3} liter)
mm	Millimeter (10^{-3} meter)
mmol	Millimol (10^{-3} mol)
MS	Mass spectrometry
MTT	3-(4,5-Dimethylthiazol-2-yl)-2,5-diphenyl-tetrazoliumbromide
N	Newton
n	Number of samples
NaH ₂ PO ₄	sodium hydrogen phosphate buffer
ng	Nanometer (10^{-9} gram)
nm	Nanometer (10^{-9} meter)
OC	Osteocalcin
OPG	Osteoprotegerin
Pa	Pascal
PDGF	Plateled-derived growth factor
PE	Polyethylene

pH	Potentia Hydrogenii
PhEur	Pharmacopoeia Europaea
PTH	Parathyroid hormone
PVP	Polyvinylpyrrolidon
qPCR	Quantitative polymerase chain reaction
RANKL	Rezeptor activator of nuclear factor-kappa B ligand
rH	Relative humidity
RNA	Ribonucleic acid
RP	Reversed phase
S	Svedberg units
SD	Standard deviation
SDS	Sodium dodecyl sulphate
SEM	Scanning electron microscopy
SERM	Selective estrogen receptor modulators
SI	Slope
TGF	Transforming growth factor
THF	Tetrahydrofuran
Thio	Thioglycollate
TNF- α	Tumor necrosis factor alpha
TRAP	Tartrate-resistant acid phosphatase
v/v	Volume per volume
w	Week
X ₅₀	50% quantile of particle size distribution
ZOL	Zoledronic acid

10.2 List of utilized substances

Table 10.1: List of utilized substances.

Substance	Supplier
BoneSave [®] granules	Stryker Howmedica Osteonics, Limerick, Ireland
Ethicon	Johnson & Johnson, Brussels, Belgium
Hanks buffered salt solution	Biochrom AG, Berlin, Germany
HEPES-buffer	Biochrom AG, Berlin, Germany
HydroSet [®]	Stryker Leibinger GmbH, Freiburg, Germany
Isoflurane	Schering-Plough, Uxbridge, England
LagFix [®] cylinder	Stryker Trauma GmbH, Schönkirchen, Germany
Mannitol	Roquette Frères, Lestrem, France
Methanol	J.T. Baker, Deventer, Holland
Polysorbate 80	Goldschmidt, Essen, Germany
RNA Later solution	Quiagen GmbH, Hilden, Germany
Sodium chloride	Merck, Darmstadt, Germany
Sodium chloride peptone broth	Merck, Darmstadt, Germany
Sodium hydrogene phosphate	Merck, Darmstadt, Germany
Sodium pentobarbital	ATL Apoteket Production & Laboratories, Kungens Kurva, Sweden
Soybean-casein digest medium	Merck, Darmstadt, Germany
Sucrose	Merck, Darmstadt, Germany
Temgesic	Reckitt & Coleman, Hull, Great Britain
Tetrabutylammonium hydrogen sulfate	Sigma-Aldrich Chemie GmbH, Steinheim
Trehalose-dihydrate	Fluka AG, Buchs, Switzerland
Water (aqua. bidest.)	In-house equipment (FinnAqua 75-E-4, FinnAqua, Finland)
Zoledronic acid	Alexis Biochemicals, Lausen, Switzerland

10.3 Raw data of qPCR analysis

Table 10.2: Raw data of 18S RNA and GAPDH correlation.

	Verum		Placebo	
	1w	3w	1w	3w
18S	117273569.30	37015521.84	2236023093.00	139408568.40
	6693600.31	332446061.00	1764986360.00	1764326342.00
	596082645.10	88905676.33	842889824.70	667138181.90
	95350739.10	196303740.20	1226821242.00	702665356.30
	173819927.20	1057634539.00	1431081145.00	1125148723.00
	416003633.90	305775533.50	1035928209.00	575362415.10
	308048741.30	34485814.62	910376929.10	919245721.90
	350243560.20	702274856.50	471627829.80	1337805248.00
GAPDH	34558.40	13989.10	572580.80	97019.30
	6117.20	199120.00	313138.80	735142.90
	115541.40	22317.00	210368.70	517080.40
	24332.70	56239.60	891790.10	273990.20
	25693.50	415992.70	364035.10	406030.10
	82659.70	326403.80	297649.30	151584.90
	81068.30	21913.10	128391.90	363401.40
	251029.10	74031.60	63857.30	1059891.30

Table 10.3: Not normalized raw data of the gene panel.

	Verum		Placebo	
	1w	3w	1w	3w
18S	157813228.30	58119920.99	3032660988.00	174343645.20
	20329699.88	382952887.20	2224234279.00	1821454110.00
	727610485.60	135874926.90	1056068934.00	656974764.30
	134461553.10	209959329.50	1691404720.00	630236336.40
	323295525.50	1032210436.00	1864648708.00	1104304367.00
	551758088.90	300847691.10	1412885862.00	560870885.10
	520787899.20	60362186.65	1184212691.00	1129118277.00
	537107721.40	259124153.50	661001033.50	1301223802.00
OC	855457.82	579739.56	9803111.05	400128.64
	51907.91	2840977.78	9772757.06	11872841.06
	3851797.10	313138.76	2654959.28	966191.97
	833310.77	823359.72	902534.60	3046615.90
	902534.60	3589814.91	5845202.66	7044542.06
	3259102.46	2202647.18	5770171.47	2827742.69
	877127.15	209603.51	2031354.72	2725239.88
	4235133.23	1154569.72	2821638.98	8295502.41

ALP	10198.99	7582.42	269499.74	9045.73
	1344.78	18691.79	180630.68	186826.03
	72725.45	4355.47	42450.43	17700.81
	6185.44	9204.91	115832.31	38263.94
	27231.67	50827.08	125044.76	67894.90
	42260.65	15426.77	186188.64	37946.69
	20662.66	5724.05	66028.32	60574.32
	46687.79	14221.91	37555.07	110340.04
TRAP	18944.42	11807.49	977197.44	24213.69
	4996.34	82359.35	660948.95	553628.15
	229886.42	9810.53	188445.01	68174.70
	29723.89	38870.89	424653.98	142614.28
	56796.79	219972.64	511656.24	305138.65
	116901.74	35083.07	940700.48	72689.51
	82223.94	9203.58	290790.04	113389.56
	116918.59	38075.52	298251.38	397028.78
CATK	157105.26	78417.29	7702431.41	247248.94
	6507.06	1387035.48	4669970.40	3153433.43
	1312801.57	130179.23	1429344.30	888404.58
	215169.15	305138.65	2985002.95	1624700.63
	821037.44	2476451.39	4549215.46	3248576.24
	1091754.45	479243.17	4115598.23	550858.42
	1286859.67	44673.32	1342101.03	852089.27
	917378.32	423557.13	4695721.19	2396809.09
TNF-α	113.35	77.72	3817.48	132.64
	215.36	553.14	3212.36	5453.74
	1225.07	371.90	1862.63	1125.80
	132.22	260.39	1278.58	780.91
	95.93	1849.27	1781.17	4371.85
	239.64	918.65	1101.35	811.24
	219.94	56.31	1395.32	1274.43
	451.66	148.07	233.30	1493.57
IL-1β	7484.80	681.63	11525.89	1480.70
	188.17	7003.24	17525.36	10187.52
	9214.01	36812.30	7741.70	11015.59
	3299.46	3256.37	10396.21	12283.56
	1467.00	10583.15	7077.98	14329.09
	4294.37	8968.63	5398.82	7026.53
	2219.95	272.15	8171.73	11412.17
	2444.85	1768.13	1690.87	10236.26

Table 10.4: Raw data of the gene panel normalized to 18S RNA.

	Verum		Placebo	
	1w	3w	1w	3w
OC	0.005420698	0.010083768	0.003231812	0.002293641
	0.002566629	0.007418609	0.004413333	0.006509623
	0.005297034	0.002307459	0.002522346	0.001472122
	0.006204541	0.003991150	0.000532948	0.004850184
	0.002788257	0.003485678	0.003141338	0.006397310
	0.005907003	0.007300641	0.004084719	0.005056177
	0.001684231	0.003451587	0.001715363	0.002462069
	0.007916256	0.004533806	0.004272429	0.006329575
ALP	0.000064627	0.000129803	0.000088912	0.000052112
	0.000066308	0.000048630	0.000081852	0.000101978
	0.000099976	0.000031831	0.000040185	0.000027116
	0.000046077	0.000044269	0.000068463	0.000060831
	0.000083953	0.000048950	0.000067319	0.000061323
	0.000076615	0.000051294	0.000131686	0.000067607
	0.000039692	0.000094678	0.000055757	0.000055413
	0.000088018	0.000055847	0.000056832	0.000085073
TRAP	0.000120043	0.000202609	0.000321848	0.000138408
	0.000247544	0.000214746	0.000299603	0.000304887
	0.000315557	0.000071893	0.000180053	0.000103976
	0.000219985	0.000185135	0.000251193	0.000226882
	0.000175927	0.000213253	0.000273490	0.000276830
	0.000211854	0.000116626	0.000664743	0.000129733
	0.000157806	0.000154281	0.000245556	0.000100007
	0.000219408	0.000146939	0.000443146	0.000306063
CATK	0.000995514	0.001349690	0.002539826	0.001419776
	0.000324597	0.003646029	0.002120276	0.001727190
	0.001817572	0.000957490	0.001345175	0.001356281
	0.001599964	0.001473321	0.001769756	0.002581986
	0.002564441	0.002394028	0.002421206	0.002946833
	0.001978031	0.001597294	0.002905622	0.000982330
	0.002473122	0.000750765	0.001133328	0.000774644
	0.001724940	0.001643372	0.007240932	0.001838278
TNF-α	0.000000718	0.000001307	0.000001260	0.000000756
	0.000010760	0.000001432	0.000001457	0.000002998
	0.000001665	0.000002749	0.000001808	0.000001714
	0.000000980	0.000001299	0.000000756	0.000001233
	0.000000298	0.000001794	0.000000960	0.000003969
	0.000000440	0.000003054	0.000000779	0.000001451
	0.000000423	0.000000942	0.000001178	0.000001174
	0.000000856	0.000000556	0.000000366	0.000001145

IL-1β	0.000047428	0.000011872	0.000003798	0.000008481
	0.000009125	0.000018260	0.000007943	0.000005611
	0.000012657	0.000271640	0.000007356	0.000016795
	0.000024522	0.000015627	0.000006148	0.000019542
	0.000004533	0.000010244	0.000003815	0.000013035
	0.000007769	0.000029819	0.000003824	0.000012588
	0.000004253	0.000004588	0.000006901	0.000010343
	0.000004599	0.000006851	0.000002560	0.000007872

10.4 Raw data of histomorphometrical analysis

Table 10.5: Raw data of total bone-implant contact (BIC) and total bone area (BA)

	Verum		Placebo	
	1w	3w	1w	3w
total BIC	41.92	62.38	58.86	56.21
	43.21	76.39	49.88	54.05
	51.43	78.94	62.22	67.21
	55.16	74.01	31.32	50.95
	28.42	63.86	42.72	67.49
	36.15	75.57	28.70	62.99
	53.72	60.00	52.03	71.28
	49.48	67.76	20.69	67.00
	23.97	67.10	24.22	59.72
			63.28	
total BA	41.85	67.04	56.65	56.14
	56.77	57.57	54.15	38.32
	56.28	62.17	42.90	44.09
	57.22	67.39	51.07	36.90
	51.35	64.09	55.31	38.62
	55.85	72.11	52.30	52.09
	50.47	63.87	57.67	32.10
	63.92	68.20	48.65	41.49
	35.97	66.24	41.88	36.58
	73.27		49.90	

10.5 Histological evaluation system

Table 10.6: Histological evaluation system for cell type and response.

Cell type/Response	Score				
	0	1	2	3	4
Polymorphonuclear cells (Heterophils)	0	Rare, 1-5/phf ^a	5-10/phf	Heavy infiltrate	Packed
Lymphocytes	0	Rare, 1-5/phf ^a	5-10/phf	Heavy infiltrate	Packed
Plasma cells	0	Rare, 1-5/phf ^a	5-10/phf	Heavy infiltrate	Packed
Macrophages	0	Rare, 1-5/phf ^a	5-10/phf	Heavy infiltrate	Packed
Giant cells / osteoclastic cells	0	Rare, 1-2/phf ^a	3-5/phf	Heavy infiltrate	Sheets
Necrosis	0	Slight	Moderate	Marked	Severe
Infection signs	0	Slight	Moderate	Marked	Severe
Fibrinous exudate (fibrin)	0	Slight	Moderate	Marked	Severe
Tissue degeneration	0	Slight	Moderate	Marked	Severe

^a phf= per high powered (400x) field

Table 10.7: Histological evaluation system for performance response.

Performance	Score				
	0	1	2	3	4
Neovascularization	0	Minimal capillary proliferation focal, 1-3 buds	Groups of 4-7 capillaries with supporting fibroblastic structures	Broad band of capillaries with supporting structures	Extensive band of capillaries with supporting fibroblastic structures
Fibrocytes/ fibroconnective tissue, fibrosis/encapsulation	0	Narrow band	Moderately thick band	Thick band	Extensive band
Fatty infiltrate/ Bone marrow	0	Minimal amount of fat associated with fibrosis	Several layers of fat and fibrosis	Elongated and broad accumulation of fat cells around the implant site	Extensive fat completely surrounding the implant
Osteolysis	0	Slight extent of bone resorption	Moderate extent of bone resorption	Marked extent of bone resorption	Severe extent of bone resorption
Newly formed bone	0	Slight extent of bone formation	Moderate extent of bone formation	Marked extent of bone formation	Severe extent of bone formation

Osteointegration	≈ 0% of bone to implant contact	1 – 25%	26% - 50%	51% - 75%	76% - 100%
Osteoblastic cells	0	Slight = equivalent to normal bone	Moderate, >normal bone	Marked, >> normal bone	Very marked
Bone density*	0	Slight = equivalent to normal bone	Moderate, >normal bone	Marked, >> normal bone	Severe, extended corticalization or packed bone
Osteoconduction	≈ 0% bone ingrowth/ on growth	1 – 25%	20% - 50%	51% - 76%	76% - 100%
Material degradation [▲]	0	Slight	Moderate	Marked	Severe (100% degraded)
Implant migration (peripheral dissemination/diffusion)	0	Slight	Moderate	Marked	Severe (100% disseminated)
Bone remodelling*	0 (primary woven bone)	Slight (initial signs of remodelling)	Moderate	Marked	Severe (up to corticalization)

[▲] compared to previous time point

* compared to distant normal bone density

11 Figure captions

Figure 2.1:	Schematic drawing of bone structure modified from Rahn [40].	5
Figure 2.2:	Overview of the main bone composition.	6
Figure 2.3:	Bone remodelling process by a BMU described by Canalis et al. [60].	9
Figure 2.4:	Overlapping stages of secondary fracture healing: hematoma formation (a), fibrocartilaginous callus formation (b), bony callus formation (c) and bone remodelling (d).	13
Figure 2.5:	Trabecular bone architecture of normal (a) and osteoporotic cancellous bone (b) described by Moritz et al. [131].	21
Figure 2.6:	Simplified pharmacological action of ZOL in the mevalonate pathway.	24
Figure 4.1:	Three-dimensional HPLC plot of ZOL dissolved in water.	33
Figure 4.2:	Experimental setup for the determination of cement hardness.	44
Figure 4.3:	Geometric shape of the HydroSet [®] plug (a), the corresponding two-piece moulding systems for manufacturing (b) and packaging of sterile implants (c).	47
Figure 4.4:	Principle of crushing strength test for HydroSet [®] bone cement plug.	48
Figure 4.5:	Schematic drawing of sterility test principle.	49
Figure 4.6:	Drilling procedure: 2.1 mm \varnothing dental drill (cortex opening) (a), 2.5 mm \varnothing dental drill (b), bone defect (c), final implant position (d), wound closure (e) and after surgery (f).	51
Figure 4.7:	Plug before dissection (a), medial aspect of the tibia before trephine drilling (b), trephine drilled sample for qPCR (c) and sample for histology (d).	53

Figure 4.8:	Schematic drawing of histomorphometric evaluation areas.	56
Figure 4.9:	Information from a box- and whisker plot.	57
Figure 5.1:	Light microscopy of LagFix [®] cylinder (a), HydroSet [®] powder (b) and different sizes of granules: BoneSave [®] 2-4 mm (c), BoneSave [®] 63-90 μm (d), BoneSave [®] 90-355 μm (e) and BoneSave [®] 355-500 μm (f).	59
Figure 5.2:	Scanning electron microscopy (SEM) of LagFix [®] cylinder (a), BoneSave [®] granules (b) and HydroSet [®] powder (c).	60
Figure 5.3:	Particle size distribution of HydroSet [®] powder.	62
Figure 5.4:	DVS kinetics of LagFix [®] cylinder (a), BoneSave [®] granules (b) and HydroSet [®] powder (c).	63
Figure 5.5:	pH value of bone substitute materials after different time periods (n = 3; error bars = standard deviation).	64
Figure 5.6:	Three-dimensional plots of different concentrated ZOL solutions: 8.44 $\mu\text{g}/\text{mL}$ (a), 4.22 $\mu\text{g}/\text{mL}$ (b), 2.11 $\mu\text{g}/\text{mL}$ (c), 1.05 $\mu\text{g}/\text{mL}$ (d).	65
Figure 5.7:	Time dependent ZOL load ($\mu\text{g}/\text{mg}$) onto bone substitutes after dipping in 5 mL of a 2.25×10^{-4} molar ZOL solution (n = 3; error bars = standard deviation). Selected statistically significant differences between the material types are labeled in the diagram by a line and the corresponding p-value (n = 9).	67
Figure 5.8:	Time and concentration dependent ZOL adsorption ($\mu\text{g}/\text{mg}$) to HydroSet [®] powder after dipping in 5 mL aqueous solution of different ZOL concentrations (n = 3; error bars = standard deviation).	68
Figure 5.9:	Loading efficiency ($\mu\text{g}/\text{mg}$) versus surface area (cm^2) of 300 mg BoneSave [®] fractions (n = 3; error bars = standard deviation).	69

-
- Figure 5.10: Time and concentration dependent ZOL adsorption (μg) to a placebo plug after dipping in 5 mL aqueous solution of different ZOL concentrations ($n = 3$; error bars = standard deviation). 70
- Figure 5.11: Cumulative ZOL release ($\mu\text{g}/\text{mg}$) from HydroSet[®] powder, BoneSave[®] 63-90 μm , BoneSave[®] 355-500 μm , BoneSave[®] 2-4 mm, and LagFix[®] cylinder ($n = 3$; error bars = standard deviation). Selected statistically significant differences between the release profiles of the material types are labeled in the diagram by a line and the corresponding p-value ($n = 9$). 72
- Figure 5.12: Cumulative ZOL release per surface area ($\mu\text{g}/\text{cm}^2$) from HydroSet[®] powder, BoneSave[®] 63-90 μm , BoneSave[®] 355-500 μm , and BoneSave[®] 2-4 mm ($n = 3$; error bars = standard deviation). 73
- Figure 5.13: Temperature profile of ZOL stability ($n = 3$; error bars = standard deviation). 75
- Figure 5.14: Three-dimensional evaluation of time-dependent ZOL stability at a storage temperature of 60°C. 76
- Figure 5.15: ZOL stability stored in glass and plastic at different temperatures ($n = 3$; error bars = standard deviation). 77
- Figure 5.16: 2.25×10^{-4} mol/L concentrated ZOL solution stored in a plastic vial (a) and a glass vial (b) 78
- Figure 5.17: Three-dimensional plots of a 2.25×10^{-4} mol/L concentrated ZOL solution stored for one day at 40°C in plastic (a) and glass (b). 79
- Figure 5.18: Light microscopy picture of a lyophilisate containing 20 mg mannitol and 100 μg ZOL. 80
- Figure 5.19: Photograph of different lyophilisates containing 100 μg
-

	ZOL and 5 mg (1), 10 mg (2), 15 mg (3), 20 mg (4) mannitol, 15 mg trehalose (5) or 15 mg sucrose (6).	80
Figure 5.20:	Stability of different ZOL lyophilisates (n = 3; error bars = standard deviation).	81
Figure 5.21:	Three-dimensional plots of differently concentrated mannitol lyophilisate formulations with 100 µg ZOL dissolved in water: 5 mg mannitol (a), 10 mg mannitol (b), 15 mg mannitol (c) and 20 mg mannitol (d).	82
Figure 5.22:	Cell viability (%) of different concentrated ZOL solutions directly dissolved in water (n = 4; error bars = standard deviation).	83
Figure 5.23:	pH values of different iso-osmolar ZOL concentrations (a) and cell viability (%) of iso-osmolar ZOL solutions (b) (n = 4; error bars = standard deviation).	84
Figure 5.24:	Cell viability (%) of iso-osmolar ZOL solutions with an adjusted pH value of 6.8 (n = 4; error bars = standard deviation).	85
Figure 5.25:	Cell viability of release samples from HydroSet [®] plugs (n = 4; error bars = standard deviation).	86
Figure 5.26:	HydroSet [®] powder mixed with different amounts of water: pure (a), 20% (b), 25% (c), and 40% (d).	87
Figure 5.27:	Hardness measurements of normal HydroSet [®] cement (a), HydroSet [®] with 50 µL ZOL solution (b), HydroSet [®] with 30% additional water (c) and ZOL loaded and dried HydroSet [®] (d).	89
Figure 5.28:	Crushing strengths of dry and wet HydroSet [®] verum and placebo plugs (n = 3; error bars = standard deviation).	91
Figure 5.29:	SEM images of the plug surface in different magnifications.	92
Figure 5.30:	The 18S (a) and GAPDH (b) ribosomal RNA expression.	93

-
- Figure 5.31: Gene expression in rat bone. The total (normalized) relative expression levels of bone formation, bone resorption and proinflammatory markers (log-scale). 94
- Figure 5.32: Light optical micrograph of an implanted placebo bone cement plug after one week. 95
- Figure 5.33: Light optical micrographs of a placebo (a) and a verum plug (b) after one week and how to differentiate old and new bone (c). 96
- Figure 5.34: Light optical micrographs of placebo (a) and verum plug (b) after three weeks (new bone (*)). 96
- Figure 5.35: Histomorphometric evaluation of total bone implant contact (%) (a) and total bone area (%) (b) out of placebo compared to verum plugs after one and three weeks after implantation. 101

12 Table captions

Table 2.1:	Chemical structures of major bisphosphonates and their relative potency to inhibit bone resorption in rats modified from Fleisch [132].	23
Table 5.1:	True density and specific surface area of different bone substitute materials (n = 3; errors = standard deviation).	61
Table 5.2:	Semi-quantitative solubility data of ZOL in HydroSet [®] hardening solution.	90
Table 5.3:	Semi-quantitative histopathological analysis of different cell types and their response (errors = standard deviation).	98
Table 5.4:	Semi-quantitative histopathological analysis of different performance parameter (errors = standard deviation).	98
Table 5.5:	Bone area (%) comparing areas closer (0-250 μm) and at a distance (250-500 μm) to the plug length (errors = standard deviation).	100
Table 10.1:	List of utilized substances.	131
Table 10.2:	Raw data of 18S RNA and GAPDH correlation.	132
Table 10.3:	Not normalized raw data of the gene panel.	132
Table 10.4:	Raw data of the gene panel normalized to 18S RNA.	134
Table 10.5:	Raw data of total bone-implant contact (BIC) and total bone area (BA)	135
Table 10.6:	Histological evaluation system for cell type and response.	136
Table 10.7:	Histological evaluation system for performance response.	136

13 References

1. Kauvar DS and Wade CE. The epidemiology and modern management of traumatic hemorrhage: US and international perspectives. *Crit Care* 9 Suppl 5 (2005) 1-9.
2. Kauvar DS, Lefering R and Wade CE. Impact of hemorrhage on trauma outcome: an overview of epidemiology, clinical presentations, and therapeutic considerations. *J Trauma* 60 (2006) 3-11.
3. Frost HM. The biology of fracture healing. An overview for clinicians. Part II. Clinical orthopaedics and related research (1989) 294-309.
4. Nauth A, Miclau T, Li R and Schemitsch EH. Gene therapy for fracture healing. *J Orthop Trauma* 24 Suppl 1 (2010) 17-24.
5. Bochlogyros PN. Non-union of fractures of the mandible. *J Maxillofac Surg* 13 (1985) 189-193.
6. Sen MK and Miclau T. Autologous iliac crest bone graft: should it still be the gold standard for treating nonunions? *Injury* 38 Suppl 1 (2007) 75-80.
7. Larsson S. Calcium phosphates: what is the evidence? *J Orthop Trauma* 24 Suppl 1 (2010) 41-45.
8. Kurashina K, Kurita H, Hirano M, Kotani A, Klein CP and de Groot K. In vivo study of calcium phosphate cements: implantation of an alpha-tricalcium phosphate/dicalcium phosphate dibasic/tetracalcium phosphate monoxide cement paste. *Biomaterials* 18 (1997) 539-543.
9. Apelt D, Theiss F, El-Warrak AO, Zlinszky K, Bettschart-Wolfisberger R, Böhner M, Matter S, Auer JA and von Rechenberg B. In vivo behavior of three different injectable hydraulic calcium phosphate cements. *Biomaterials* 25 (2004) 1439-1451.
10. Friedman CD, Costantino PD, Takagi S and Chow LC. BoneSource hydroxyapatite cement: a novel biomaterial for craniofacial skeletal tissue engineering and reconstruction. *J Biomed Mater Res* 43 (1998) 428-432.
11. Larsson S and Bauer TW. Use of injectable calcium phosphate cement for fracture fixation: a review. *Clinical orthopaedics and related research* (2002) 23-32.
12. Ooms EM, Wolke JG, van de Heuvel MT, Jeschke B and Jansen JA. Histological evaluation of the bone response to calcium phosphate cement implanted in cortical bone. *Biomaterials* 24 (2003) 989-1000.
13. Seeman E. Invited Review: Pathogenesis of osteoporosis. *J Appl Physiol* 95 (2003) 2142-2151.
14. Johnell O and Kanis JA. An estimate of the worldwide prevalence and disability associated with osteoporotic fractures. *Osteoporos Int* 17 (2006) 1726-1733.
15. Barrios C, Brostrom LA, Stark A and Walheim G. Healing complications after internal fixation of trochanteric hip fractures: the prognostic value of

-
- osteoporosis. *J Orthop Trauma* 7 (1993) 438-442.
 16. Cornell CN. Internal fracture fixation in patients with osteoporosis. *J Am Acad Orthop Surg* 11 (2003) 109-119.
 17. Rodan GA and Reszka AA. Osteoporosis and bisphosphonates. *The Journal of bone and joint surgery* 85-A Suppl 3 (2003) 8-12.
 18. Hjerten S, Levin O and Tiselius A. Protein chromatography on calcium phosphate columns. *Arch Biochem Biophys* 65 (1956) 132-155.
 19. Urist MR, Huo YK, Brownell AG, Hohl WM, Buyske J, Lietze A, Tempst P, Hunkapiller M and DeLange RJ. Purification of bovine bone morphogenetic protein by hydroxyapatite chromatography. *Proc Natl Acad Sci U S A* 81 (1984) 371-375.
 20. Ginebra MP, Traykova T and Planell JA. Calcium phosphate cements as bone drug delivery systems: a review. *J Control Release* 113 (2006) 102-110.
 21. Joschek S, Nies B, Krotz R and Göpferich A. Chemical and physicochemical characterization of porous hydroxyapatite ceramics made of natural bone. *Biomaterials* 21 (2000) 1645-1658.
 22. Paul W and Sharma CP. Ceramic drug delivery: a perspective. *Journal of biomaterials applications* 17 (2003) 253-264.
 23. Josse S, Faucheux C, Soueidan A, Grimandi G, Massiot D, Alonso B, Janvier P, Laib S, Pilet P, Gauthier O, Daculsi G, Guicheux JJ, Bujoli B and Bouler JM. Novel biomaterials for bisphosphonate delivery. *Biomaterials* 26 (2005) 2073-2080.
 24. Moroni A, Faldini C, Hoang-Kim A, Pegreff F and Giannini S. Alendronate improves screw fixation in osteoporotic bone. *The Journal of bone and joint surgery* 89 (2007) 96-101.
 25. Aspenberg P, Wermelin K, Tengwall P and Fahlgren A. Additive effects of PTH and bisphosphonates on the bone healing response to metaphyseal implants in rats. *Acta orthopaedica* 79 (2008) 111-115.
 26. Hilding M and Aspenberg P. Local peroperative treatment with a bisphosphonate improves the fixation of total knee prostheses: a randomized, double-blind radiostereometric study of 50 patients. *Acta orthopaedica* 78 (2007) 795-799.
 27. Arkfeld DG and Rubenstein E. Quest for the Holy Grail to cure arthritis and osteoporosis: emphasis on bone drug delivery systems. *Advanced drug delivery reviews* 57 (2005) 939-944.
 28. Gao Y, Zou S, Liu X, Bao C and Hu J. The effect of surface immobilized bisphosphonates on the fixation of hydroxyapatite-coated titanium implants in ovariectomized rats. *Biomaterials* 30 (2009) 1790-1796.
 29. Saghieh S, Khoury NJ, Tawil A, Masrouha KZ, Musallam KM, Khalaf K, Dosh L, Jaouhari RR, Birjawi G and El-Hajj-Fuleihan G. The impact of zoledronic acid on regenerate and native bone after consolidation and removal of the external fixator: An animal model study. *Bone* (2009)
 30. Eriksen EF, Eghbali-Fatourehchi GZ and Khosla S. Remodeling and

- vascular spaces in bone. *J Bone Miner Res* 22 (2007) 1-6.
31. Martin TJ and Seeman E. Bone remodelling: its local regulation and the emergence of bone fragility. *Best Pract Res Clin Endocrinol Metab* 22 (2008) 701-722.
 32. Fazzalari NL. Bone remodeling: A review of the bone microenvironment perspective for fragility fracture (osteoporosis) of the hip. *Seminars in cell & developmental biology* 19 (2008) 467-472.
 33. Sjostedt A, Zetterberg C, Hansson T, Hult E and Ekstrom L. Bone mineral content and fixation strength of femoral neck fractures. A cadaver study. *Acta orthopaedica Scandinavica* 65 (1994) 161-165.
 34. Buckwalter JA, Glimcher MJ, Cooper RR and Recker R. Bone biology. I: Structure, blood supply, cells, matrix, and mineralization. *Instr Course Lect* 45 (1996) 371-386.
 35. Omar O, Suska F, Lenneras M, Zoric N, Svensson S, Hall J, Emanuelsson L, Nannmark U and Thomsen P. The Influence of Bone Type on the Gene Expression in Normal Bone and at the Bone-Implant Interface: Experiments in Animal Model. *Clinical implant dentistry and related research* 13 (2009) 146-156.
 36. McKibbin B. The biology of fracture healing in long bones. *J Bone Joint Surg Br* 60-B (1978) 150-162.
 37. Riggs BL, Melton LJ, Robb RA, Camp JJ, Atkinson EJ, McDaniel L, Amin S, Rouleau PA and Khosla S. A population-based assessment of rates of bone loss at multiple skeletal sites: evidence for substantial trabecular bone loss in young adult women and men. *J Bone Miner Res* 23 (2008) 205-214.
 38. Zysset PK. A review of morphology-elasticity relationships in human trabecular bone: theories and experiments. *Journal of biomechanics* 36 (2003) 1469-1485.
 39. Rubin C, Turner AS, Muller R, Mittra E, McLeod K, Lin W and Qin YX. Quantity and quality of trabecular bone in the femur are enhanced by a strongly anabolic, noninvasive mechanical intervention. *J Bone Miner Res* 17 (2002) 349-357.
 40. Rahn BA. Knochengewebe. Staubesand J Benninghoff *Anatomie Bd 1*, 14. Aufl, Urban und Schwarzenberg, München Wien Baltimore (1985)
 41. Buckwalter JA, Glimcher MJ, Cooper RR and Recker R. Bone biology. II: Formation, form, modeling, remodeling, and regulation of cell function. *Instr Course Lect* 45 (1996) 387-399.
 42. van den Bos T, Steinfort J and Beertsen W. Effect of bound phosphoproteins and other organic phosphates on alkaline phosphatase-induced mineralization of collagenous matrices in vitro. *Bone and mineral* 23 (1993) 81-93.
 43. Seeman E and Delmas PD. Bone quality--the material and structural basis of bone strength and fragility. *N Engl J Med* 354 (2006) 2250-2261.
 44. Reinstorf A, Ruhnow M, Gelinsky M, Pompe W, Hempel U, Wenzel KW

- and Simon P. Phosphoserine--a convenient compound for modification of calcium phosphate bone cement collagen composites. *Journal of materials science* 15 (2004) 451-455.
45. Ralston SH and Martin TJ. Advances in the molecular pharmacology and therapeutics of bone disease and International Symposium on Paget's Disease July 10-14, 2007 St. Catherine's College, Oxford, UK. *Bone* 41 (2007) 1059-1062.
 46. Boskey AL and Posner AS. Bone structure, composition, and mineralization. *Orthop Clin North Am* 15 (1984) 597-612.
 47. Takahashi N, Udagawa N, Kobayashi Y and Suda T. Generation of osteoclasts in vitro, and assay of osteoclast activity. *Methods Mol Med* 135 (2007) 285-301.
 48. Chambers TJ. The pathobiology of the osteoclast. *J Clin Pathol* 38 (1985) 241-252.
 49. Kanczler JM and Oreffo RO. Osteogenesis and angiogenesis: the potential for engineering bone. *European cells & materials* 15 (2008) 100-114.
 50. Vaananen K. Mechanism of osteoclast mediated bone resorption--rationale for the design of new therapeutics. *Advanced drug delivery reviews* 57 (2005) 959-971.
 51. Kim H, Lee JH and Suh H. Interaction of mesenchymal stem cells and osteoblasts for in vitro osteogenesis. *Yonsei Med J* 44 (2003) 187-197.
 52. Im GI, Qureshi SA, Kenney J, Rubash HE and Shanbhag AS. Osteoblast proliferation and maturation by bisphosphonates. *Biomaterials* 25 (2004) 4105-4115.
 53. Tsiridis E, Upadhyay N and Giannoudis P. Molecular aspects of fracture healing: which are the important molecules? *Injury* 38 Suppl 1 (2007) 11-25.
 54. Cox G, Einhorn TA, Tzioupis C and Giannoudis PV. Bone-turnover markers in fracture healing. *J Bone Joint Surg Br* 92 (2010) 329-334.
 55. Parfitt AM. Targeted and nontargeted bone remodeling: relationship to basic multicellular unit origination and progression. *Bone* 30 (2002) 5-7.
 56. Huiskes R, Ruimerman R, van Lenthe GH and Janssen JD. Effects of mechanical forces on maintenance and adaptation of form in trabecular bone. *Nature* 405 (2000) 704-706.
 57. Knothe Tate ML. "Whither flows the fluid in bone?" An osteocyte's perspective. *Journal of biomechanics* 36 (2003) 1409-1424.
 58. Abendroth K and Abendroth B. [Pathophysiology and epidemiology of osteoporosis]. *Z Arztl Fortbild (Jena)* 89 (1995) 5-11.
 59. Manolagas SC. Birth and death of bone cells: basic regulatory mechanisms and implications for the pathogenesis and treatment of osteoporosis. *Endocrine reviews* 21 (2000) 115-137.
 60. Canalis E, Giustina A and Bilezikian JP. Mechanisms of anabolic therapies for osteoporosis. *N Engl J Med* 357 (2007) 905-916.
 61. Phillips AM. Overview of the fracture healing cascade. *Injury* 36 Suppl 3

- (2005) 5-7.
62. Einhorn TA. The cell and molecular biology of fracture healing. *Clinical orthopaedics and related research* (1998) 7-21.
 63. Dhert WJ, Thomsen P, Blomgren AK, Esposito M, Ericson LE and Verbout AJ. Integration of press-fit implants in cortical bone: a study on interface kinetics. *J Biomed Mater Res* 41 (1998) 574-583.
 64. Einhorn TA. The science of fracture healing. *J Orthop Trauma* 19 (2005) 4-6.
 65. Yamaji T, Ando K, Wolf S, Augat P and Claes L. The effect of micromovement on callus formation. *J Orthop Sci* 6 (2001) 571-575.
 66. Landry PS, Marino AA, Sadasivan KK and Albright JA. Bone injury response. An animal model for testing theories of regulation. *Clinical orthopaedics and related research* (1996) 260-273.
 67. Simon AM, Manigrasso MB and O'Connor JP. Cyclo-oxygenase 2 function is essential for bone fracture healing. *J Bone Miner Res* 17 (2002) 963-976.
 68. Brighton CT and Hunt RM. Early histological and ultrastructural changes in medullary fracture callus. *The Journal of bone and joint surgery* 73 (1991) 832-847.
 69. Einhorn TA, Majeska RJ, Rush EB, Levine PM and Horowitz MC. The expression of cytokine activity by fracture callus. *J Bone Miner Res* 10 (1995) 1272-1281.
 70. Kon T, Cho TJ, Aizawa T, Yamazaki M, Nooh N, Graves D, Gerstenfeld LC and Einhorn TA. Expression of osteoprotegerin, receptor activator of NF-kappaB ligand (osteoprotegerin ligand) and related proinflammatory cytokines during fracture healing. *J Bone Miner Res* 16 (2001) 1004-1014.
 71. Lind M, Schumacker B, Soballe K, Keller J, Melsen F and Bunger C. Transforming growth factor-beta enhances fracture healing in rabbit tibiae. *Acta orthopaedica Scandinavica* 64 (1993) 553-556.
 72. Trippel SB. Potential role of insulinlike growth factors in fracture healing. *Clinical orthopaedics and related research* (1998) 301-313.
 73. Lind M. Growth factor stimulation of bone healing. Effects on osteoblasts, osteomies, and implants fixation. *Acta Orthop Scand Suppl* 283 (1998) 2-37.
 74. Canalis E, McCarthy TL and Centrella M. Effects of platelet-derived growth factor on bone formation in vitro. *J Cell Physiol* 140 (1989) 530-537.
 75. Lee FY, Choi YW, Behrens FF, DeFouw DO and Einhorn TA. Programmed removal of chondrocytes during endochondral fracture healing. *J Orthop Res* 16 (1998) 144-150.
 76. Bolander ME. Regulation of fracture repair by growth factors. *Proc Soc Exp Biol Med* 200 (1992) 165-170.
 77. Puleo DA and Nanci A. Understanding and controlling the bone-implant

- interface. *Biomaterials* 20 (1999) 2311-2321.
78. Demers LM. Clinical usefulness of markers of bone degradation and formation. *Scand J Clin Lab Invest Suppl* 227 (1997) 12-20.
 79. Gabbay JS, Heller J, Spoon DB, Mooney M, Acarturk O, Askari M, Wasson KL and Bradley JP. Noggin underexpression and runx-2 overexpression in a craniosynostosis rabbit model. *Ann Plast Surg* 56 (2006) 306-311.
 80. Honsawek S, Powers RM and Wolfinbarger L. Extractable bone morphogenetic protein and correlation with induced new bone formation in an in vivo assay in the athymic mouse model. *Cell Tissue Bank* 6 (2005) 13-23.
 81. McKee MD, Farach-Carson MC, Butler WT, Hauschka PV and Nanci A. Ultrastructural immunolocalization of noncollagenous (osteopontin and osteocalcin) and plasma (albumin and alpha 2HS-glycoprotein) proteins in rat bone. *J Bone Miner Res* 8 (1993) 485-496.
 82. Pufe T, Scholz-Ahrens KE, Franke AT, Petersen W, Mentlein R, Varoga D, Tillmann B, Schrezenmeir J and Gluer CC. The role of vascular endothelial growth factor in glucocorticoid-induced bone loss: evaluation in a minipig model. *Bone* 33 (2003) 869-876.
 83. Wildemann B, Kadow-Romacker A, Pruss A, Haas NP and Schmidmaier G. Quantification of growth factors in allogenic bone grafts extracted with three different methods. *Cell Tissue Bank* 8 (2007) 107-114.
 84. Zhang J, Lu Y, Dai J, Yao Z, Kitazawa R, Kitazawa S, Zhao X, Hall DE, Pienta KJ and Keller ET. In vivo real-time imaging of TGF-beta-induced transcriptional activation of the RANK ligand gene promoter in intraosseous prostate cancer. *Prostate* 59 (2004) 360-369.
 85. Dimitriou R, Tsiridis E and Giannoudis PV. Current concepts of molecular aspects of bone healing. *Injury* 36 (2005) 1392-1404.
 86. Seibel MJ. Molecular markers of bone turnover: biochemical, technical and analytical aspects. *Osteoporos Int* 11 Suppl 6 (2000) 18-29.
 87. Hammett-Stabler CA. The use of biochemical markers in osteoporosis. *Clin Lab Med* 24 (2004) 175-197.
 88. Li X, Quigg RJ, Zhou J, Ryaby JT and Wang H. Early signals for fracture healing. *J Cell Biochem* 95 (2005) 189-205.
 89. Gerdhem P, Ivaska KK, Alatalo SL, Halleen JM, Hellman J, Isaksson A, Pettersson K, Vaananen HK, Akesson K and Obrant KJ. Biochemical markers of bone metabolism and prediction of fracture in elderly women. *J Bone Miner Res* 19 (2004) 386-393.
 90. Meier C, Nguyen TV, Center JR, Seibel MJ and Eisman JA. Bone resorption and osteoporotic fractures in elderly men: the dubbo osteoporosis epidemiology study. *J Bone Miner Res* 20 (2005) 579-587.
 91. Seibel MJ, Lang M and Geilenkeuser WJ. Interlaboratory variation of biochemical markers of bone turnover. *Clin Chem* 47 (2001) 1443-1450.
 92. Bu R, Borysenko CW, Li Y, Cao L, Sabokbar A and Blair HC.

- Expression and function of TNF-family proteins and receptors in human osteoblasts. *Bone* 33 (2003) 760-770.
93. Locksley RM, Killeen N and Lenardo MJ. The TNF and TNF receptor superfamilies: integrating mammalian biology. *Cell* 104 (2001) 487-501.
 94. Katagiri T and Takahashi N. Regulatory mechanisms of osteoblast and osteoclast differentiation. *Oral Dis* 8 (2002) 147-159.
 95. Won C, Park HJ and Shin HC. Interleukin-1 beta facilitates afferent sensory transmission in the primary somatosensory cortex of anesthetized rats. *Neurosci Lett* 201 (1995) 255-258.
 96. Murakami S, Lefebvre V and de Crombrughe B. Potent inhibition of the master chondrogenic factor Sox9 gene by interleukin-1 and tumor necrosis factor-alpha. *The Journal of biological chemistry* 275 (2000) 3687-3692.
 97. Cheung CK, Panesar NS, Haines C, Masarei J and Swaminathan R. Immunoassay of a tartrate-resistant acid phosphatase in serum. *Clin Chem* 41 (1995) 679-686.
 98. Rissanen JP, Suominen MI, Peng Z and Halleen JM. Secreted tartrate-resistant acid phosphatase 5b is a Marker of osteoclast number in human osteoclast cultures and the rat ovariectomy model. *Calcif Tissue Int* 82 (2008) 108-115.
 99. Andersson GN, Ek-Rylander B, Hammarstrom LE, Lindskog S and Toverud SU. Immunocytochemical localization of a tartrate-resistant and vanadate-sensitive acid nucleotide tri- and diphosphatase. *J Histochem Cytochem* 34 (1986) 293-298.
 100. Perez-Amodio S, Beertsen W and Everts V. (Pre-)osteoclasts induce retraction of osteoblasts before their fusion to osteoclasts. *J Bone Miner Res* 19 (2004) 1722-1731.
 101. Littlewood-Evans A, Kokubo T, Ishibashi O, Inaoka T, Wlodarski B, Gallagher JA and Bilbe G. Localization of cathepsin K in human osteoclasts by in situ hybridization and immunohistochemistry. *Bone* 20 (1997) 81-86.
 102. Garnero P, Borel O, Byrjalsen I, Ferreras M, Drake FH, McQueney MS, Foged NT, Delmas PD and Delaisse JM. The collagenolytic activity of cathepsin K is unique among mammalian proteinases. *The Journal of biological chemistry* 273 (1998) 32347-32352.
 103. Calvo MS, Eyre DR and Gundberg CM. Molecular basis and clinical application of biological markers of bone turnover. *Endocrine reviews* 17 (1996) 333-368.
 104. Stoffel K, Engler H, Kuster M and Riesen W. Changes in biochemical markers after lower limb fractures. *Clin Chem* 53 (2007) 131-134.
 105. Veitch SW, Findlay SC, Hamer AJ, Blumsohn A, Eastell R and Ingle BM. Changes in bone mass and bone turnover following tibial shaft fracture. *Osteoporos Int* 17 (2006) 364-372.
 106. Hauschka PV, Lian JB, Cole DE and Gundberg CM. Osteocalcin and

- matrix Gla protein: vitamin K-dependent proteins in bone. *Physiol Rev* 69 (1989) 990-1047.
107. Hoang QQ, Sicheri F, Howard AJ and Yang DS. Bone recognition mechanism of porcine osteocalcin from crystal structure. *Nature* 425 (2003) 977-980.
 108. Brown JP, Delmas PD, Malaval L, Edouard C, Chapuy MC and Meunier PJ. Serum bone Gla-protein: a specific marker for bone formation in postmenopausal osteoporosis. *Lancet* 1 (1984) 1091-1093.
 109. Hessle L, Johnson KA, Anderson HC, Narisawa S, Sali A, Goding JW, Terkeltaub R and Millan JL. Tissue-nonspecific alkaline phosphatase and plasma cell membrane glycoprotein-1 are central antagonistic regulators of bone mineralization. *Proc Natl Acad Sci U S A* 99 (2002) 9445-9449.
 110. Crofton PM, Stirling HF and Kelnar CJ. Bone alkaline phosphatase and height velocity in short normal children undergoing growth-promoting treatments: longitudinal study. *Clin Chem* 41 (1995) 672-678.
 111. Kuroda S, Viridi AS, Dai Y, Shott S and Sumner DR. Patterns and localization of gene expression during intramembranous bone regeneration in the rat femoral marrow ablation model. *Calcif Tissue Int* 77 (2005) 212-225.
 112. Bauer TW and Muschler GF. Bone graft materials. An overview of the basic science. *Clinical orthopaedics and related research* (2000) 10-27.
 113. Matsuda A, Furuzono T, Walsh D, Kishida A and Tanaka J. Surface modification of a porous hydroxyapatite to promote bonded polymer coatings. *Journal of materials science* 14 (2003) 973-978.
 114. Osborn JF and Newesely H. The material science of calcium phosphate ceramics. *Biomaterials* 1 (1980) 108-111.
 115. Driessens FC. Physiology of hard tissues in comparison with the solubility of synthetic calcium phosphates. *Ann N Y Acad Sci* 523 (1988) 131-136.
 116. Guo D, Xu K and Han Y. The in situ synthesis of biphasic calcium phosphate scaffolds with controllable compositions, structures, and adjustable properties. *Journal of biomedical materials research* 88 (2009) 43-52.
 117. Schmitz JP and Hollinger JO. The critical size defect as an experimental model for craniomandibulofacial nonunions. *Clinical orthopaedics and related research* (1986) 299-308.
 118. Larsson S. Calcium phosphates: what is the evidence? *J Orthop Trauma* 24 Suppl 1 S41-45.
 119. <http://www.graftys.com/en/news/detail/graftys-initiates-clinical-trial.6.html>.
 120. Gates BJ, Sonnett TE, Duvall CA and Dobbins EK. Review of osteoporosis pharmacotherapy for geriatric patients. *Am J Geriatr Pharmacother* 7 (2009) 293-323.
 121. Adachi JD. The correlation of bone mineral density and biochemical

-
- markers to fracture risk. *Calcif Tissue Int* 59 Suppl 1 (1996) 16-19.
122. Hochberg MC, Greenspan S, Wasnich RD, Miller P, Thompson DE and Ross PD. Changes in bone density and turnover explain the reductions in incidence of nonvertebral fractures that occur during treatment with antiresorptive agents. *J Clin Endocrinol Metab* 87 (2002) 1586-1592.
 123. Namkung-Matthai H, Appleyard R, Jansen J, Hao Lin J, Maastricht S, Swain M, Mason RS, Murrell GA, Diwan AD and Diamond T. Osteoporosis influences the early period of fracture healing in a rat osteoporotic model. *Bone* 28 (2001) 80-86.
 124. Hochberg MC, Ross PD, Black D, Cummings SR, Genant HK, Nevitt MC, Barrett-Connor E, Musliner T and Thompson D. Larger increases in bone mineral density during alendronate therapy are associated with a lower risk of new vertebral fractures in women with postmenopausal osteoporosis. Fracture Intervention Trial Research Group. *Arthritis Rheum* 42 (1999) 1246-1254.
 125. Nevitt MC, Ross PD, Palermo L, Musliner T, Genant HK and Thompson DE. Association of prevalent vertebral fractures, bone density, and alendronate treatment with incident vertebral fractures: effect of number and spinal location of fractures. The Fracture Intervention Trial Research Group. *Bone* 25 (1999) 613-619.
 126. John Camm A. Review of the cardiovascular safety of zoledronic acid and other bisphosphonates for the treatment of osteoporosis. *Clin Ther* 32 (2010) 426-436.
 127. Akesson K. New approaches to pharmacological treatment of osteoporosis. *Bull World Health Organ* 81 (2003) 657-664.
 128. Robioneck PB. Einfluss der ultraschallgestützten Implantatfixation auf das Knochenremodelling im experimentellen Osteotomiemodell am Femurcondylus des Kaninchens. Inauguraldissertation Gießen (2010)
 129. Peter B, Gauthier O, Laib S, Bujoli B, Guicheux J, Janvier P, van Lenthe GH, Muller R, Zambelli PY, Bouler JM and Pioletti DP. Local delivery of bisphosphonate from coated orthopedic implants increases implants mechanical stability in osteoporotic rats. *Journal of biomedical materials research* 76 (2006) 133-143.
 130. Larsson S and Procter P. Optimising implant anchorage (augmentation) during fixation of osteoporotic fractures: Is there a role for bone-graft substitutes? *Injury* (2011)
 131. Moritz N, Alm JJ, Lankinen P, Mäkinen TJ, Mattila K and Aro HT. Quality of intertrochanteric cancellous bone as predictor of femoral stem RSA migration in cementless total hip arthroplasty. *Journal of biomechanics* 44 (2010) 221-227.
 132. Fleisch H. Bisphosphonates: mechanisms of action. *Endocrine reviews* 19 (1998) 80-100.
 133. Green JR. Bisphosphonates: preclinical review. *The oncologist* 9 Suppl 4 (2004) 3-13.
-

134. Reinholz GG, Getz B, Pederson L, Sanders ES, Subramaniam M, Ingle JN and Spelsberg TC. Bisphosphonates directly regulate cell proliferation, differentiation, and gene expression in human osteoblasts. *Cancer research* 60 (2000) 6001-6007.
135. Polyzos SA, Anastasilakis AD, Efstathiadou Z, Kita M, Litsas I, Avramidis A, Arsos G, Moralidis E, Gerou S, Pavlidou V, Papatheodorou A and Terpos E. The effect of zoledronic acid on serum dickkopf-1, osteoprotegerin, and RANKL in patients with Paget's disease of bone. *Hormone and metabolic research = Hormon- und Stoffwechselforschung = Hormones et métabolisme* 41 (2009) 846-850.
136. Tenenbaum HC, Torontali M and Sukhu B. Effects of bisphosphonates and inorganic pyrophosphate on osteogenesis in vitro. *Bone* 13 (1992) 249-255.
137. Denissen H, van Beek E, Lowik C, Papapoulos S and van den Hooff A. Ceramic hydroxyapatite implants for the release of bisphosphonate. *Bone and mineral* 25 (1994) 123-134.
138. Russell RG, Croucher PI and Rogers MJ. Bisphosphonates: pharmacology, mechanisms of action and clinical uses. *Osteoporos Int* 9 Suppl 2 (1999) 66-80.
139. Astrand J, Harding AK, Aspenberg P and Tagil M. Systemic zoledronate treatment both prevents resorption of allograft bone and increases the retention of new formed bone during revascularization and remodelling. A bone chamber study in rats. *BMC musculoskeletal disorders* 7 (2006) 63.
140. Zwolak P, Manivel JC, Jasinski P, Kirstein MN, Dudek AZ, Fisher J and Cheng EY. Cytotoxic effect of zoledronic acid-loaded bone cement on giant cell tumor, multiple myeloma, and renal cell carcinoma cell lines. *The Journal of bone and joint surgery* 92 (2010) 162-168.
141. Zhang D, Udagawa N, Nakamura I, Murakami H, Saito S, Yamasaki K, Shibasaki Y, Morii N, Narumiya S, Takahashi N and et al. The small GTP-binding protein, rho p21, is involved in bone resorption by regulating cytoskeletal organization in osteoclasts. *J Cell Sci* 108 (Pt 6) (1995) 2285-2292.
142. Lyles KW, Colon-Emeric CS, Magaziner JS, Adachi JD, Pieper CF, Mautalen C, Hyldstrup L, Recknor C, Nordsletten L, Moore KA, Lavecchia C, Zhang J, Mesenbrink P, Hodgson PK, Abrams K, Orloff JJ, Horowitz Z, Eriksen EF and Boonen S. Zoledronic acid and clinical fractures and mortality after hip fracture. *N Engl J Med* 357 (2007) 1799-1809.
143. Black DM, Delmas PD, Eastell R, Reid IR, Boonen S, Cauley JA, Cosman F, Lakatos P, Leung PC, Man Z, Mautalen C, Mesenbrink P, Hu H, Caminis J, Tong K, Rosario-Jansen T, Krasnow J, Hue TF, Sellmeyer D, Eriksen EF and Cummings SR. Once-yearly zoledronic acid for treatment of postmenopausal osteoporosis. *N Engl J Med* 356 (2007)

- 1809-1822.
144. Khosla S, Burr D, Cauley J, Dempster DW, Ebeling PR, Felsenberg D, Gagel RF, Gilsanz V, Guise T, Koka S, McCauley LK, McGowan J, McKee MD, Mohla S, Pendrys DG, Raisz LG, Ruggiero SL, Shafer DM, Shum L, Silverman SL, Van Poznak CH, Watts N, Woo SB and Shane E. Bisphosphonate-associated osteonecrosis of the jaw: report of a task force of the American Society for Bone and Mineral Research. *J Bone Miner Res* 22 (2007) 1479-1491.
 145. Vahtsevanos K, Kyrgidis A, Verrou E, Katodritou E, Triaridis S, Andreadis CG, Boukovinas I, Koloutsos GE, Teleioudis Z, Kitikidou K, Paraskevopoulos P, Zervas K and Antoniadis K. Longitudinal cohort study of risk factors in cancer patients of bisphosphonate-related osteonecrosis of the jaw. *J Clin Oncol* 27 (2009) 5356-5362.
 146. Wutzl A, Biedermann E, Wanschitz F, Seemann R, Klug C, Baumann A, Watzinger F, Schicho K, Ewers R and Millesi G. Treatment results of bisphosphonate-related osteonecrosis of the jaws. *Head Neck* 30 (2008) 1224-1230.
 147. Compston J. Treatments for osteoporosis - looking beyond the HORIZON. *N Engl J Med* 356 (2007) 1878-1880.
 148. Schilcher J, Michaelsson K and Aspenberg P. Bisphosphonate use and atypical fractures of the femoral shaft. *N Engl J Med* 364 1728-1737.
 149. Porter JR, Ruckh TT and Popat KC. Bone tissue engineering: a review in bone biomimetics and drug delivery strategies. *Biotechnology progress* 25 (2009) 1539-1560.
 150. Ziv G. Drug selection and use in mastitis: systemic vs local therapy. *J Am Vet Med Assoc* 176 (1980) 1109-1115.
 151. de Araujo DR, Pinto Lde M, Braga Ade F and de Paula E. Drug-delivery systems for local anesthetics: therapeutic applications. *Rev Bras Anesthesiol* 53 (2003) 663-671.
 152. Friend DR and Pangburn S. Site-specific drug delivery. *Med Res Rev* 7 (1987) 53-106.
 153. Utreja P, Jain S and Tiwary AK. Novel drug delivery systems for sustained and targeted delivery of anti- cancer drugs: current status and future prospects. *Curr Drug Deliv* 7 (2010) 152-161.
 154. Aspenberg P. Bisphosphonates and implants: an overview. *Acta orthopaedica* 80 (2009) 119-123.
 155. Peter B, Pioletti DP, Laib S, Bujoli B, Pilet P, Janvier P, Guicheux J, Zambelli PY, Bouler JM and Gauthier O. Calcium phosphate drug delivery system: influence of local zoledronate release on bone implant osteointegration. *Bone* 36 (2005) 52-60.
 156. Greiner S, Kadow-Romacker A, Lubberstedt M, Schmidmaier G and Wildemann B. The effect of zoledronic acid incorporated in a poly(D,L-lactide) implant coating on osteoblasts in vitro. *Journal of biomedical materials research* 80 (2007) 769-775.

157. Wermelin K, Suska F, Tengvall P, Thomsen P and Aspenberg P. Stainless steel screws coated with bisphosphonates gave stronger fixation and more surrounding bone. *Histomorphometry in rats*. *Bone* 42 (2008) 365-371.
158. Tengvall P, Skoglund B, Askendal A and Aspenberg P. Surface immobilized bisphosphonate improves stainless-steel screw fixation in rats. *Biomaterials* 25 (2004) 2133-2138.
159. Karakus S, Kucukguzel I and Kucukguzel SG. Development and validation of a rapid RP-HPLC method for the determination of cetirizine or fexofenadine with pseudoephedrine in binary pharmaceutical dosage forms. *Journal of pharmaceutical and biomedical analysis* 46 (2008) 295-302.
160. Rothen-Rutishauser B, Blank F, Muhlfeld C and Gehr P. In vitro models of the human epithelial airway barrier to study the toxic potential of particulate matter. *Expert Opin Drug Metab Toxicol* 4 (2008) 1075-1089.
161. Scherliess R. The MTT assay as tool to evaluate and compare excipient toxicity in vitro on respiratory epithelial cells. *International journal of pharmaceuticals* 411 (2011) 98-105.
162. Thomsen P and Eriksson A. Study report: Bisphosphonate enhanced HydroSet - Effects on the early postoperative bone formation. (2011)
163. Alves A, Boutrand JP and Clermont G. Study report: Local tissue effects and performance of a drug eluting bone cement after 1 and 3 weeks implantation in rat tibial metaphysis - Histopathological and histomorphometrical analysis. (2011)
164. Omar O, Svensson S, Zoric N, Lenneras M, Suska F, Wigren S, Hall J, Nannmark U and Thomsen P. In vivo gene expression in response to anodically oxidized versus machined titanium implants. *Journal of biomedical materials research* 92 (2009) 1552-1566.
165. Donath K and Breuner G. A method for the study of undecalcified bones and teeth with attached soft tissues. The Sage-Schliff (sawing and grinding) technique. *J Oral Pathol* 11 (1982) 318-326.
166. Pfaffl MW. A new mathematical model for relative quantification in real-time RT-PCR. *Nucleic acids research* 29 (2001) e45.
167. Zubery Y, Goldlust A, Alves A and Nir E. Ossification of a novel cross-linked porcine collagen barrier in guided bone regeneration in dogs. *Journal of periodontology* 78 (2007) 112-121.
168. von Doernberg MC, von Rechenberg B, Bohner M, Grunenfelder S, van Lenthe GH, Muller R, Gasser B, Mathys R, Baroud G and Auer J. In vivo behavior of calcium phosphate scaffolds with four different pore sizes. *Biomaterials* 27 (2006) 5186-5198.
169. Shapiro SS and Wilk MB. An analysis of variance test for normality (complete samples). *Biometrika* 52 (3-4) (1965) 591-611.
170. Wilcoxon F. Individual comparisons of grouped data by ranking methods. *J Econ Entomol* 39 (1946) 269.
171. Mann HB and Whitney DR. On a test of whether one of two random

- variables is stochastically larger than the other. *Annals of Mathematical Statistics* 18 (1) (1947) 50-60.
172. Metropolis N and Ulam S. The Monte Carlo method. *J Am Stat Assoc* 44 (1949) 335-341.
173. Sikavitsas VI, Temenoff JS and Mikos AG. Biomaterials and bone mechanotransduction. *Biomaterials* 22 (2001) 2581-2593.
174. Frentzen M, Osborn JF and Nolden R. [Use of porous hydroxyapatite in systematic periodontal treatment. A 2-year clinical study]. *Dtsch Zahnarztl Z* 43 (1988) 713-718.
175. Frentzen M, Osborn JF and Nolden R. [Clinical example of porous hydroxyapatite ceramic in setting of systematic periodontal treatment (III)]. *Quintessenz* 38 (1987) 1857-1866.
176. Frentzen M, Osborn JF and Nolden R. [Clinical example of porous hydroxyapatite ceramic in setting of systematic periodontal treatment (II)]. *Quintessenz* 38 (1987) 1671-1679, 1682.
177. Frentzen M, Osborn JF and Nolden R. [Clinical example of porous hydroxyapatite ceramic in setting of systematic periodontal treatment (I)]. *Quintessenz* 38 (1987) 1509-1519.
178. Misra DN, Bowen RL and Mattamal GJ. Surface area of dental enamel, bone, and hydroxyapatite: chemisorption from solution. *Calcif Tissue Res* 26 (1978) 139-142.
179. Wood NV, Jr. Specific Surfaces of Bone, Apatite, Enamel, and Dentine. *Science* 105 (1947) 531-532.
180. Saalfeld U, Meenen NM, Jures TT and Saalfeld H. Solubility behaviour of synthetic hydroxyapatites in aqueous solution: influence of amorphous constituents on pH value. *Biomaterials* 15 (1994) 905-908.
181. Sharpe JR, Sammons RL and Marquis PM. Effect of pH on protein adsorption to hydroxyapatite and tricalcium phosphate ceramics. *Biomaterials* 18 (1997) 471-476.
182. Zhang X, Jiang Y and Xu Z. [Separation of zoledronic acid and its related substances by ion-pair reversed-phase high performance liquid chromatography]. *Se pu = Chinese journal of chromatography / Zhongguo hua xue hui* 22 (2004) 428-430.
183. Rao BM, Srinivasu MK, Rani Ch P, kumar SS, Kumar PR, Chandrasekhar KB and Veerender M. A validated stability indicating ion-pair RP-LC method for zoledronic acid. *Journal of pharmaceutical and biomedical analysis* 39 (2005) 781-790.
184. Kline WF and Matuszewski BK. Improved determination of the bisphosphonate alendronate in human plasma and urine by automated precolumn derivatization and high-performance liquid chromatography with fluorescence and electrochemical detection. *Journal of chromatography* 583 (1992) 183-193.
185. Flesch G, Tominaga N and Degen P. Improved determination of the bisphosphonate pamidronate disodium in plasma and urine by pre-column

- derivatization with fluorescamine, high-performance liquid chromatography and fluorescence detection. *Journal of chromatography* 568 (1991) 261-266.
186. Zhu LS, Lapko VN, Lee JW, Basir YJ, Kafonek C, Olsen R and Briscoe C. A general approach for the quantitative analysis of bisphosphonates in human serum and urine by high-performance liquid chromatography/tandem mass spectrometry. *Rapid Commun Mass Spectrom* 20 (2006) 3421-3426.
187. Legay F, Gauron S, Deckert F, Gosset G, Pfaar U, Ravera C, Wiegand H and Schran H. Development and validation of a highly sensitive RIA for zoledronic acid, a new potent heterocyclic bisphosphonate, in human serum, plasma and urine. *Journal of pharmaceutical and biomedical analysis* 30 (2002) 897-911.
188. Aberg J, Brohede U, Mihranyan A, Stromme M and Engqvist H. Bisphosphonate incorporation in surgical implant coatings by fast loading and co-precipitation at low drug concentrations. *Journal of materials science* 20 (2009) 2053-2061.
189. Seo SW, Cho SK, Storer SK and Lee FY. Zoledronate reduces unwanted bone resorption in intercalary bone allografts. *Int Orthop* 34 (2009) 599-603.
190. Greiner SH, Wildemann B, Back DA, Alidoust M, Schwabe P, Haas NP and Schmidmaier G. Local application of zoledronic acid incorporated in a poly(D,L-lactide)-coated implant accelerates fracture healing in rats. *Acta orthopaedica* 79 (2008) 717-725.
191. Pan B, To LB, Farrugia AN, Findlay DM, Green J, Gronthos S, Evdokiou A, Lynch K, Atkins GJ and Zannettino AC. The nitrogen-containing bisphosphonate, zoledronic acid, increases mineralisation of human bone-derived cells in vitro. *Bone* 34 (2004) 112-123.
192. Schindeler A and Little DG. Osteoclasts but not osteoblasts are affected by a calcified surface treated with zoledronic acid in vitro. *Biochemical and biophysical research communications* 338 (2005) 710-716.
193. Tanzer M, Karabasz D, Krygier JJ, Cohen R and Bobyn JD. The Otto Aufranc Award: bone augmentation around and within porous implants by local bisphosphonate elution. *Clinical orthopaedics and related research* 441 (2005) 30-39.
194. Bobyn JD, McKenzie K, Karabasz D, Krygier JJ and Tanzer M. Locally delivered bisphosphonate for enhancement of bone formation and implant fixation. *The Journal of bone and joint surgery* 91 Suppl 6 (2009) 23-31.
195. Bott RF and Oliveira WP. Storage conditions for stability testing of pharmaceuticals in hot and humid regions. *Drug Dev Ind Pharm* 33 (2007) 393-401.
196. Mollica JA, Ahuja S and Cohen J. Stability of pharmaceuticals. *Journal of pharmaceutical sciences* 67 (1978) 443-465.
197. Farina AR, Tacconelli A, Teti A, Gulino A and Mackay AR. Tissue

- inhibitor of metalloproteinase-2 protection of matrix metalloproteinase-2 from degradation by plasmin is reversed by divalent cation chelator EDTA and the bisphosphonate alendronate. *Cancer research* 58 (1998) 2957-2960.
198. Nakamura K, Yokohama S and Sonobe T. Failure of stability prediction for minodronic acid injectable by accelerated stability testing. *International journal of pharmaceutics* 241 (2002) 65-71.
 199. Nakamura K, Yokohama S, Katsuma M, Sawada T and Sonobe T. A new stressed test to predict the foreign matter formation of minodronic acid in solution. *International journal of pharmaceutics* 251 (2003) 99-106.
 200. Nakamura K, Tanaka T, Saito K, Yokohama S and Sonobe T. Stabilization of minodronic acid in aqueous solution for parenteral formulation. *International journal of pharmaceutics* 222 (2001) 91-99.
 201. O'Fagain C. Storage and lyophilisation of pure proteins. *Methods Mol Biol* 681 (2010) 179-202.
 202. Abascal K, Ganora L and Yarnell E. The effect of freeze-drying and its implications for botanical medicine: a review. *Phytother Res* 19 (2005) 655-660.
 203. Varshney DB, Kumar S, Shalaev EY, Sundaramurthi P, Kang SW, Gatlin LA and Suryanarayanan R. Glycine crystallization in frozen and freeze-dried systems: effect of pH and buffer concentration. *Pharm Res* 24 (2007) 593-604.
 204. Bakaltcheva I, O'Sullivan AM, Hmel P and Ogbu H. Freeze-dried whole plasma: evaluating sucrose, trehalose, sorbitol, mannitol and glycine as stabilizers. *Thromb Res* 120 (2007) 105-116.
 205. Jovanovic N, Bouchard A, Hofland GW, Witkamp GJ, Crommelin DJ and Jiskoot W. Distinct effects of sucrose and trehalose on protein stability during supercritical fluid drying and freeze-drying. *Eur J Pharm Sci* 27 (2006) 336-345.
 206. Lin JH. Bisphosphonates: a review of their pharmacokinetic properties. *Bone* 18 (1996) 75-85.
 207. Klein CP, Patka P, Wolke JG, de Blicke-Hogervorst JM and de Groot K. Long-term in vivo study of plasma-sprayed coatings on titanium alloys of tetracalcium phosphate, hydroxyapatite and alpha-tricalcium phosphate. *Biomaterials* 15 (1994) 146-150.
 208. Dean JC, Tisdell CL, Goldberg VM, Parr J, Davy D and Stevenson S. Effects of hydroxyapatite tricalcium phosphate coating and intracancellous placement on bone ingrowth in titanium fibermetal implants. *J Arthroplasty* 10 (1995) 830-838.
 209. Andersson T, Agholme F, Aspenberg P and Tengvall P. Surface immobilized zoledronate improves screw fixation in rat bone: a new method for the coating of metal implants. *Journal of materials science* 21 (2010) 3029-3037.
 210. Wermelin K, Aspenberg P, Linderback P and Tengvall P. Bisphosphonate

- coating on titanium screws increases mechanical fixation in rat tibia after two weeks. *Journal of biomedical materials research* 86 (2008) 220-227.
211. Wermelin K, Tengvall P and Aspenberg P. Surface-bound bisphosphonates enhance screw fixation in rats--increasing effect up to 8 weeks after insertion. *Acta orthopaedica* 78 (2007) 385-392.
 212. Yoshinari M, Oda Y, Inoue T, Matsuzaka K and Shimono M. Bone response to calcium phosphate-coated and bisphosphonate-immobilized titanium implants. *Biomaterials* 23 (2002) 2879-2885.
 213. Yoshinari M, Oda Y, Ueki H and Yokose S. Immobilization of bisphosphonates on surface modified titanium. *Biomaterials* 22 (2001) 709-715.
 214. Peter B, Zambelli PY, Guicheux J and Pioletti DP. The effect of bisphosphonates and titanium particles on osteoblasts: an in vitro study. *J Bone Joint Surg Br* 87 (2005) 1157-1163.
 215. Egermann M, Goldhahn J and Schneider E. Animal models for fracture treatment in osteoporosis. *Osteoporos Int* 16 Suppl 2 (2005) S129-138.
 216. Tenenbaum HC, Shelemay A, Girard B, Zohar R and Fritz PC. Bisphosphonates and periodontics: potential applications for regulation of bone mass in the periodontium and other therapeutic/diagnostic uses. *Journal of periodontology* 73 (2002) 813-822.
 217. Branemark R, Ohnells LO, Nilsson P and Thomsen P. Biomechanical characterization of osseointegration during healing: an experimental in vivo study in the rat. *Biomaterials* 18 (1997) 969-978.
 218. Kajiwara H, Yamaza T, Yoshinari M, Goto T, Iyama S, Atsuta I, Kido MA and Tanaka T. The bisphosphonate pamidronate on the surface of titanium stimulates bone formation around tibial implants in rats. *Biomaterials* 26 (2005) 581-587.
 219. Esposito M, Hirsch JM, Lekholm U and Thomsen P. Biological factors contributing to failures of osseointegrated oral implants. (II). Etiopathogenesis. *European journal of oral sciences* 106 (1998) 721-764.
 220. Esposito M, Hirsch JM, Lekholm U and Thomsen P. Biological factors contributing to failures of osseointegrated oral implants. (I). Success criteria and epidemiology. *European journal of oral sciences* 106 (1998) 527-551.
 221. Stadelmann VA, Gauthier O, Terrier A, Bouler JM and Pioletti DP. Implants delivering bisphosphonate locally increase periprosthetic bone density in an osteoporotic sheep model. A pilot study. *European cells & materials* 16 (2008) 10-16.
 222. Zhang FL, Kirschmeier P, Carr D, James L, Bond RW, Wang L, Patton R, Windsor WT, Syto R, Zhang R and Bishop WR. Characterization of Ha-ras, N-ras, Ki-Ras4A, and Ki-Ras4B as in vitro substrates for farnesyl protein transferase and geranylgeranyl protein transferase type I. *The Journal of biological chemistry* 272 (1997) 10232-10239.
 223. Swanson KM and Hohl RJ. Anti-cancer therapy: targeting the mevalonate

- pathway. *Current cancer drug targets* 6 (2006) 15-37.
224. Valenti MT, Bertoldo F, Dalle Carbonare L, Azzarello G, Zenari S, Zanatta M, Balducci E, Vinante O and Lo Cascio V. The effect of bisphosphonates on gene expression: GAPDH as a housekeeping or a new target gene? *BMC cancer* 6 (2006) 49.
225. Omar O, Lenneras M, Svensson S, Suska F, Emanuelsson L, Hall J, Nannmark U and Thomsen P. Integrin and chemokine receptor gene expression in implant-adherent cells during early osseointegration. *Journal of materials science* 21 (2009) 969-980.

Acknowledgement

The presented thesis has been acquired within the scope of cooperation between the Department of Pharmaceutical Technology and Biopharmacy at the CAU in Kiel and Stryker Trauma GmbH in Schönkirchen under the supervision of Prof. Dr. Hartwig Steckel.

I would like to express my gratitude to my supervisor Prof. Dr. Hartwig Steckel for giving me the opportunity to perform my PhD thesis in his department, for his continuous encouragement and belief in my work, and for giving me the freedom to realize my own ideas.

I would sincerely like to express my thanks to Prof. Dr. Rainer Adlung for taking over the co-reference for this work.

At this place I would like to acknowledge Stryker Trauma GmbH for financial support of this thesis. To Dr. Bernd Robioneck I wish to convey my thanks for his encouragement to realize the cooperation and make the project happen. I acknowledge Dr. Jörg Arnoldi for supervising the present thesis as a representative from Stryker, his careful corrections, valuable notes and constructive feedback during the whole time of my PhD programme, Dr. Anders Jönsson for the conduction of the rat surgeries and Claudia Beimel for constructive statistical advice. I am grateful to Prof. Dr. Philip Procter, Dr. Carol Toth, and the whole Medical Science group of Stryker Trauma GmbH for helpful suggestions and stimulating comments.

The whole pharmaceutical technology working group I would like to thank for the kind atmosphere. I gratefully acknowledge Dr. Regina Scherließ for her support during *in vitro* cytotoxicity tests and the whole technical and analytical support from Regina Krehl, Hanna Rohwer, Maren Rohlf, Dirk Böhme, Arne Herzog and Detlef Rödiger. Rüdiger Smal, I would like to thank you for excellent art work, but also for a lot of exciting conversations. I acknowledge Dr. Maren Kuhli, Jan Sörensen, Kirsten Petersen for careful corrections of this thesis, and Dr. Franz Furkert for support during implant manufacturing.

I have to thank the Institute of Biomaterials and Cell Therapy (IBCT) for the conduction, sample preparation and support of the rat study, especially Prof. Dr. Peter Thomsen, Dr. Anders Palmquist and Lena Emanuelsson. Additionally, I would like to thank Maria Lennerås from Tataa Biocenter for performing the PCR analysis, Antoine Alves from Biomatech for histopathological analysis, and Dr. Jonathan Green for his advice about ZOL.

Last, but not least, I thank all those people who have provided me with help and encouragement on this way. To my parents, my brother, my girlfriend Sabrina and circle of friends I wish to express my gratitude and a lot of thanks for their understanding and for so much more than I can't write down here.

Curriculum vitae (CV)

Personal Data

Surname	Sörensen
Name	Torben Christian
Date of Birth	December 23, 1982
Place of Birth	Kiel
Citizenship	German

Education

1989 – 1993	Primary School, Schönkirchen
1993 – 2002	Heinrich-Heine High-School, Heikendorf
06/2002	University Entrance Diploma
04/2003 – 05/2007	Studies of Pharmacy, CAU Kiel
07/2007 – 12/2007	Postgraduate Studies for “Diplom-Pharmazeut” at the Department of Pharmaceutical Technology and Biopharmacy, CAU Kiel
01/2008 – 06/2008	Trainee for Approbation, Belvedere Apotheke in Kiel
07/2008 – 09/2008	Apotheke am Rathaus, Schwentinental
08/2008	Approbation as Pharmacist
Since 10/2008	PhD-student at the Department of Pharmaceutical Technology and Biopharmacy, CAU Kiel

Military Service

07/2002 – 03/2003	Social Service at Johanniter-Unfallhilfe e.V. in Preetz
-------------------	---

Erklärung

Hiermit erkläre ich gemäß § 9 der Promotionsordnung der Mathematisch-Naturwissenschaftliche Fakultät der Christian-Albrechts-Universität zu Kiel, dass ich die vorliegenden Arbeit, abgesehen von der Beratung durch meine Betreuer, selbstständig und ohne fremde Hilfe verfasst habe. Ich habe keine anderen als die angegebenen Quellen oder Hilfsmittel benutzt und die den benutzen Werken wörtlich oder inhaltlich entnommenen Stellen als solche kenntlich gemacht. Die vorliegende Arbeit ist unter Einhaltung guter wissenschaftlicher Praxis entstanden und wurde bei keiner anderen Universität zur Begutachtung eingereicht.

Torben Christian Sörensen